TRANSPORTATION RESEARCH
CIRCULAR
Number E-C257 November 2019

Primer on Bridge Load Testing

The National Academies of
SCIENCES • ENGINEERING • MEDICINE
TRB
TRANSPORTATION RESEARCH BOARD

TRANSPORTATION RESEARCH CIRCULAR E-C257

Primer on Bridge Load Testing

November 2019

Transportation Research Board
500 Fifth Street, NW
Washington, D.C.
www.trb.org

TRANSPORTATION RESEARCH CIRCULAR E-C257
ISSN 0097-8515

The **Transportation Research Board** is one of seven major programs of the National Academies of Sciences, Engineering, and Medicine. The mission of the Transportation Research Board is to provide leadership in transportation innovation and progress through research and information exchange, conducted within a setting that is objective, interdisciplinary, and multimodal.

The Transportation Research Board is distributing this E-Circular to make the information contained herein available for use by individual practitioners in state and local transportation agencies, researchers in academic institutions, and other members of the transportation research community. The information in this E-Circular was taken directly from the submission of the authors. This document is not a report of the National Academies of Sciences, Engineering, and Medicine.

Transportation Research Board
500 Fifth Street, NW
Washington, D.C.
www.trb.org

Preface

The TRB Testing and Evaluation of Transportation Structures committee consists of members from infrastructure owners, practicing engineers, nondestructive testing providers, and researchers. This committee is concerned with condition assessment and evaluation of the performance of transportation structures. The committee addresses the use of testing, monitoring, and nondestructive evaluation methods to assess the load-carrying capacity of structures, detect and quantify defects, and assess condition.

The primary focus of the committee has been the transfer of knowledge to promote practical application of research for evaluation of structures for effective asset management. To encourage rapid adoption of the latest technologies and methods, the committee has been pursuing products that demonstrate the successful application of technologies and methods for the condition assessment and performance evaluation of transportation structures. This E-Circular is a product of these efforts.

Load testing has been one of the recognized methods to evaluate and load rate bridge structures. While advanced calculation methods are available to determine the ultimate capacity of existing structures, timely and accurate in-service data needed for model input and service life prediction is not always forthcoming. Load testing provides a useful alternative for such cases where current calculation methods, for one reason or another, cannot provide satisfactory answers to performance questions on existing bridges. AASHTO's *Manual for Bridge Evaluation* and the 1998 *Manual for Bridge Rating Through Load Testing* have been generally used as a guidance to load testing. This E-Circular provides significant updates to the existing documents to reflect the current state of the practice on bridge load testing, and will cover the preparation, execution, and analysis of load tests, including diagnostic and proof tests. If effectively used, these methods can extend the useful life of existing bridges in a cost-effective fashion.

ACKNOWLEDGMENTS

The standing committee recognizes the following who were the primary authors of this E-Circular: Sreenivas Alampalli, Dan M. Frangopol, Jesse Grimson, David Kosnik, Marvin Halling, Eva O.L. Lantsoght, Jeff S. Weidner, David Y. Yang, and Y. Edward Zhou. The standing committee also recognizes the following members and friends who reviewed the document and provided input: Erin Bell, Christina Freeman, James Long, Brent Phares, Franklin Moon, Duane Otter, and Thomas E. Beitelman.

Contents

CHAPTER 1

Introduction

SREENIVAS ALAMPALLI
New York State Department of Transportation

DAN M. FRANGOPOL
Lehigh University, ATLSS Research Center

JESSE GRIMSON
BDI Bridge Diagnostics, Inc.

MARVIN HALLING
Utah State University

DAVID KOSNIK
CTL Group

EVA O. L. LANTSOGHT
Universidad San Francisco de Quito and Delft University of Technology

Y. EDWARD ZHOU
AECOM

HISTORY OF LOAD TESTING FOR LOAD RATING

Load testing of bridges is a practice that has been used throughout history to assess bridge performance. In times when engineering models were not as accurate and available as today, a critical step in the construction of a bridge was to load test prior to opening or during the opening ceremony of the bridge (*1*). Performing the load test and measuring deflections demonstrated to the public that the bridge was safe. Several bridges such as the steel framework bridge over the Morava River near Ljubitschewo in Serbia, the road bridge near Salez, Switzerland, and a suspension bridge in Maurin, France, collapsed during such load tests (*1*).

Load tests as part of inspection procedures date to at least as far back as applications in Switzerland in 1891. Those early load tests can be considered proof load tests due to the fact that the full design loads were used—the bridge was considered to pass if (*a*) it did not collapse and (*b*) it fulfilled deflection or vibration criteria.

In the 20th century, calculation methods improved and load testing became less important. Some countries, such as France (*2*), Italy (*3, 4*), and Switzerland (*5*), still require load tests prior to opening a new bridge. In other countries, load tests are used for long-span or special bridges or bridges in which novel concepts are applied (*6–8*).

At the beginning of the 21st century in the United States and Europe, numerous bridges built during periods of rapid expansion of road and railroad networks during the Interbellum and

after World War II reached the end of their originally designed service lives. Consequently, increasing time and effort are required to assess and rate existing bridges to ensure the safety of the traveling public (*9*).

While advanced calculation methods to estimate the ultimate capacity of existing structures are widely available (*10–15*), timely and accurate data from existing structures needed as inputs for such models are not always forthcoming. Furthermore, ongoing time-related deterioration of in-service bridges increases the difficulty of evaluation.

Load testing provides a useful alternative for such cases where current calculation methods cannot provide satisfactory answers to performance questions on existing bridges (*16, 17*). Specific examples of recent load test applications that can be consulted for reference include

- Development of field-verified finite element models (*18*);
- Evaluation of material damage (alkali–silica reactivity) on reinforced concrete (RC) bridge performance (*19*);
- Assessment of bridges without design plans (*20–22*);
- Evaluation of strengthening measures (*23–25*);
- Analysis of historic bridges (*26–28*);
- Determination of contributions of additional load-resisting mechanisms, such as arching action (*29*);
- Evaluation of new materials, such as fiber-reinforced polymers (FRPs) (*30–34*);
- Estimation of remaining fatigue life (*35*); and
- Verification of design assumptions for new bridges (*36*).

The preceding, and other examples (*37–42*), have shown load tests to be a useful tool for load rating existing bridges (*37–42*). In several countries, the codes, guidelines, and recommendations with regard to load testing are being developed or updated (*5, 43–49*) and the measurement possibilities are evaluated (*50–54*).

OBJECTIVES OF LOAD TESTS

Depending on the specific objectives of a load test (i.e., the types of data to be obtained to aid in rating a particular structure) different load test programs may be appropriate. In current practice, load tests may fall into two different categories: diagnostic tests conducted with small fractions of the design live loads and proof load tests carried out with live loads corresponding to those specified by applicable design codes.

In diagnostic load tests, the known load applied to the structure facilitates comparison between the analytically predicted bridge response and the actual measured response. This comparison can then be used to develop field-verified analytical models by fine tuning, for example, finite element (FE) model parameters, to improve the accuracy of the model-based rating of the bridge. Once a field-validated model is developed, it is important to remove unreliable mechanisms (e.g., frozen bearings) or mechanisms that should not be considered at the ultimate limit state (e.g., unintended composite action or barrier participation) prior to performing the load rating. If a rating based on an analytical model is not required, the comparison between the analytical and measured response can be used to gain further insight in the structural behavior.

The goal of a proof load test is to evaluate a bridge directly by applying loads corresponding to those modeled by the considered design code (*36*). If the bridge successfully carries the applied loads, it is considered to meet the capacity requirements of the code. Successfully carrying the applied load not only means that no collapse takes place, but also that the proof load should not induce permanent damage on the structure. Proof load testing alleviates the need to extrapolate structural responses to larger load levels. For a final assessment, the engineer still needs to evaluate which mechanisms (present during the test) are reliable to consider long term. Examples include temperature-dependent responses (e.g., frozen soil that provides confinement) and mechanisms such as confinement due to frozen bearings or unintended composite action that have uncertain reliability long term.

APPLICATION OF LOAD TESTS

Certain structure types are better suited to load testing than others. Based on the current load rating and type of bridge, it can be determined if the bridge is suitable for load testing. If the rating factor is well above 1, load testing is typically not necessary (*55*). If the rating factor is close to 0, it is unlikely that a load test will be sufficient to avoid posting. Similarly, if the bridge is nonredundant, such as a simple-span two-girder bridge, there is little chance that the rating would improve much through a load test. The best candidate bridges for load testing are those that have a rating factor close to 1.0 and the type or geometry of the bridge will likely result in additional stiffness through redundancy or alternate load paths that can be relied upon for load rating purposes. For these bridges load testing can typically be used to remove existing posting or can avoid the need for posting. In general, the following types of bridges are suitable for load testing:

- Multigirder bridges for which measuring strain on all girders on a selected position in the longitudinal direction will provide information about the lateral load distribution characteristics, while measuring strain at multiple depths on a single girder will help identify the stiffness contributed by the deck; measuring strain near the supports will help identify the unintended fixity present in the supports;
- Slab bridges, since the transverse load redistribution in slab bridges is typically larger than according to traditional design calculations;
- Existing bridges of which the effect of material degradation on the load-carrying behavior is unknown;
- Bridges that have been damaged (i.e., vehicle impacts);
- Bridges of which structural plans are missing or incomplete; and
- Arch bridges, to determine the performance of the arch under loading. The primary issue for these bridges is the stiffness of the foundations, which may be temperature-dependent.

Certain questions with regard to the behavior and performance of bridges are better suited to load testing than others. In general, load testing can be used to evaluate the following:

- Transverse load distribution;
- Secondary components that add stiffness or change load paths (integral curbs–sidewalks);

- Actual stiffness of the bridge;
- Load paths throughout the bridge;
- Proper functioning of rehabilitation and strengthening measures;
- Effect of intended and unintended composite action between steel girders and concrete deck;
- Effect of the support conditions: Frozen bearings can cause unintentional hogging moments at the support of elements originally designed with hinged supports and provide longitudinal restraint, which may reduce the tensile strains in the sagging moment region. This positive influence should not be relied upon for load rating, and thus should be decoupled from the other mechanisms; and
- Remaining fatigue life.

Moreover, load tests can be used prior to opening new bridges. These results can then be used to compare to load tests on the bridge throughout its service life, and to evaluate deterioration modes such as reduction in stiffness over time.

Bridges with fracture-critical elements and concrete bridges that can fail in a brittle failure mode (e.g, shear and punching) can be analyzed with a diagnostic load test. When proof load testing is necessary, these structures can only be studied under exceptional circumstances and with an extended sensor plan.

OVERVIEW AND SCOPE OF DOCUMENT

This document details the aspects related to the preparation, execution, and analysis of load tests, including both diagnostic and proof tests. Long-span bridges (such as suspension, cable-stayed, or movable bridges) are not considered in this document as standard load testing methods would not apply to these structures; however, load testing of individual components of long-span bridges may be conducted according to the information presented herein.

Chapter 2 summarizes general considerations for load testing. Determination of the load rating factor and preparatory work in terms of the preliminary structural investigations are described. Different types of load tests, and appropriate bridge evaluation scenarios for each, are described, as are safety considerations. A method to determine the benefit–cost analysis of load tests is presented.

Chapter 3 describes procedures common to all load tests. This chapter includes information about load test objectives and the planning and preparatory phases of a load test. Special considerations for different structure types are given. The equipment and personnel requirements for load tests is also reviewed.

Chapter 4 details diagnostic load testing procedures. It includes the planning, execution, and analysis of test results. For the analysis and post-processing, the rating procedures are revised.

Chapter 5 covers proof load tests and includes test execution and analysis of test results. During execution, real-time interpretation of the measurements is required to ensure there are no signs of irreversible damage to the bridge.

Chapter 6 summarizes structural reliability-based analysis methods for load tests. It includes a method for determining the reliability index before, during, and after a load test, a method to determine the remaining service life, and life-cycle considerations.

In **Chapter 7**, detailed examples of a diagnostic load test and a proof load test are presented, as well as shorter summarized case studies. Finally, an overview of literature resources on reported load tests is provided.

REFERENCED STANDARDS AND DOCUMENTS

This document is to be consulted together with the current American Association of State Highway and Transportation Officials (AASHTO) Load and Resistance Factor Design (LRFD) Code (*56*) and the *Manual for Bridge Evaluation* (MBE) (*57*), and, where relevant, the AASHTO Load Factor Design (LFD) Code. The previous version of this document dates back to 1998 (*58*). For concrete buildings, American Concrete Institute (ACI) 437.2-13 (*59*) is available. This code provides detailed acceptance criteria for concrete structures and has clearly prescribed the required loading procedures. The distribution of member forces in concrete bridges can be taken according to ACI 342R-16 (*60*). International standards that can be consulted are the German guidelines (*61*), the Irish guidelines (*62*), the French guidelines (*2*), the British guidelines (*63*), the Polish guidelines (*64*), the Czech and Slovak guidelines (*65*), the Spanish guidelines (*66*, *67*), and the Hungary guidelines (*68*), as well as the practice described in Italy (*3*, *4*), Switzerland (*5*, *69*, *70*), and the Netherlands (*71*).

CHAPTER 2

General Considerations

DAN M. FRANGOPOL
DAVID Y. YANG
Lehigh University, ATLSS Research Center

JESSE GRIMSON
BDI Bridge Diagnostics, Inc.

MARVIN HALLING
Utah State University

DAVID KOSNIK
CTL Group

EVA O. L. LANTSOGHT
Universidad San Francisco de Quito, Delft University of Technology

JEFF S. WEIDNER
University of Texas at El Paso

Y. EDWARD ZHOU
AECOM

INTRODUCTION

This chapter discusses general considerations that are valid for all types of load tests, such as the preliminary structural investigation that needs to be carried out before a load test, and safety considerations. A discussion on the types of load tests, and when it can be useful to load test a bridge is provided.

According to the MBE (*72*) the following general expression for load rating of each component and connection subjected to a single-force effect (i.e., axial force, flexure, or shear) is given as Equation 2.1 (Equation 6A.4.2.1-1 of the MBE).

$$RF = \frac{C - (\gamma_{DC})(DC) - (\gamma_{DW})(DW) \pm (\gamma_P)(P)}{(\gamma_{LL})(LL + IM)} \tag{2.1}$$

with, for the strength limit states:

$$C = \varphi_c \varphi_s \varphi R_n \text{ with } \varphi_c \varphi_s \geq 0.85 \tag{2.2}$$

and for the serviceability limit states:

$$C = f_R \tag{2.3}$$

where

RF = rating factor;
C = capacity;
f_R = allowable stress specified in the LRFD Code (*56*);
R_n = nominal member resistance (as inspected);
DC = dead load effect due to structural components and attachments;
DW = dead load effect due to wearing surface and utilities;
P = permanent loads other than dead loads;
LL = live load effect;
IM = dynamic load allowance;
γ_{DC} = LRFD load factor for structural components and attachments;
γ_{DW} = LRFD load factor for wearing surfaces and utilities;
γ_P = LRFD load factor for permanent loads other than dead load = 1.0;
γ_{LL} = evaluation live load factor;
ϕ_c = condition factor;
ϕ_s = system factor; and
ϕ = LRFD resistance factor.

The governing load factors, depending on the considered type of bridge and limit state, can be consulted in Table 6A.4.2.2-1 of the MBE. The condition factor provides a reduction based on observed deterioration and can be found in Table 6A.4.2.3-1 of the MBE. System factors reflect the level of redundancy of the superstructure system. Less redundant bridges will have lower ratings. The values of the system factors can be found in Table 6A.4.2.4-1 of the MBE.

Load tests are used to more accurately characterize the distribution of live load force effects (*LL*) in Equation 2.1. Load tests to failure can be used to determine the value of the numerator of Equation 2.1. This method is not further discussed in this document, as a destructive test can only be carried out on decommissioned structures in special situations.

Two types of load tests can be distinguished. The diagnostic load tests, which determine the response of a bridge under known applied loads, is the first type. The second type is the proof load tests, which approve the bridge for a certain capacity based on its performance in a load test. Both methods are considered in this document.

An important element in this chapter is the preliminary structural investigation recommended prior to the load test design and execution. It is recommended to consult all reports that are available for the bridge under consideration. If full-calculation reports of previous load ratings are available, these reports should be consulted in more depth than simply the resulting rating factor and the controlling member for each span. For load rating according to conventional methods, the assumptions that were made need to be verified. Assumptions and good documentation become even more critical when FE models and field tests are considered and used for further evaluation.

Documentation is crucially important for load ratings that result in an official decision. The engineering and the assumptions behind the decision should be fully accessible, thoroughly

documented and technically comprehensive. To ensure a solid foundation for the official decision, a quality control–quality assurance (QC-QA) process should be implemented and documented.

PRELIMINARY STRUCTURAL INVESTIGATION

Existing Documentation

Prior to load testing any structure, a preliminary structural investigation should be conducted. The first step is to gather all existing documentation of the bridge. The following documentation, if available, needs to be gathered:

- Structural plans and information about the design of the structure:
  - Design plans,
  - As-built plans,
  - Project specifications and results of material testing on construction materials, and
  - Structural design reports and calculations.
- Inspection reports, including results of destructive and nondestructive tests, carried out on the structure.
- Reports on the existing–conventional load rating of the structure.
- Information on changes to the structure:
  - Rehabilitation plans,
  - Calculation reports of the design of the rehabilitation measures, and
  - Maintenance records.

It is recommended to summarize the main findings of the study of these reports into a short description of the current state of the structure based on the available information.

Preliminary Calculations and Considerations

After collecting and studying the available documentation of the bridge under consideration, a field inspection is recommended. The inspection should be carried out in accordance with the MBE (*57*). Further guidelines can also be found in the *Bridge Inspector's Reference Manual* (*73*). The inspection will give information about estimated section losses and material deterioration, which can be used as input for the preliminary calculations. In particular, the inspection should measure displacements, crack widths, misalignments, and movements at the joints and bearings. Modifications to the dead load such as additional wearing of surface and pavement layers need to be reported.

If a movable bearing cannot move freely anymore, this observation should be noted, and the restraint caused by the blocking of the bearing should be taken into account. To evaluate if a movable bearing is blocked, the temperature during the inspection should be measured (*73*). The bearing should be in its expanded position for temperatures greater than the design (or average) temperature, and in the contracted position for temperatures less than the design (or average) temperature. The design temperature is 68°F unless otherwise noted (*73*). Additionally, evidence of a bearing being frozen includes bending, buckling, improper alignment of the members, or

cracks in the bearing seat. Pitting, section loss, deterioration, and debris build-up can result in the binding up or freezing of a bearing. For further details, reference is made to the *Bridge Inspector's Reference Manual* (*73*).

As part of preliminary calculations, two types of analysis need to be carried out.

1. A load rating (see Equation 2.1) according to the MBE (*57*) complemented with requirements of the owner–operator, such as state-specific live loads or state-specific policies for weight limits (*74*) at load posted structures. Rating method depends on the prevailing specifications and owner's applicable practice [ASD, LFD, or load and resistance factor rating (LRFR)]. The rating can be improved by using a FE model in which other vehicles can be applied.
2. An estimate of the mean capacity of the structure based on measured average material properties and without load and resistance factors.

The tools developed during this stage, spreadsheets and analytical models [such as FE modeling (FEM)], will be used after the load test to update the load rating of the bridge. During the preliminary calculations, the critical structural elements—including connection details and their load capacities—need to be determined. The structure needs to be analyzed to identify additional load-bearing mechanisms that can increase the capacity and the reserve strength should be assessed. The calculations should give an idea of the expected failure mechanism. For structure types where the code provisions do not consider all strength-enhancing mechanisms, these contributions should be estimated when determining the mean capacities. An example is the shear capacity of reinforced-concrete slab bridges under concentrated live loads, where transverse load redistribution results in a higher shear capacity than the beam shear capacities according to the code provisions.

If the condition of the bridge and the materials has been assessed based on destructive or nondestructive testing, the estimated material parameters should be used in the preliminary calculations. For finding the mean capacity of the structure, the average measured values of the material properties are used.

The results of the inspection and the preliminary calculations need to be used to select the type of load test and the method of testing and to define the goals and required information from the load test. As a function of the type of load test and the goals of the experiment, the position(s) and maximum value of the applied load can be determined.

Analytical Model Development

With a load test, the load rating based on an analytical model can be improved with the measurements of the load test. The requirements for the analytical model depend on the purpose of the load test. To determine distribution factors, the analytical method from the AASHTO code (*56*) can provide sufficient information. Additionally, for concrete bridges, information can be found in ACI 342R-16 (*60*), or the method of Guyon-Massonet can be used to estimate the distribution factors. For finding the neutral axis, a hand calculation considering the occurring moment, stresses, and strains can be sufficient.

When the effect of a number of factors on the behavior of the bridge need to be considered, the analytical model can be an FEM. FE modeling can be a useful component of load rating through load testing. It is also a natural segue between simplified load rating procedures

that are common (single-line girder methods) and experimental methods. Refined load rating using FEMs may preclude the bridge owner from having to conduct a field experiment in many cases. Though outside the scope of this document, refined ratings using FEM should be considered prior to field deployment.

Beyond refined load ratings, development of an FEM has other benefits. The process, built upon the documentation and field visits prescribed in Existing Documentation (p. 8), forces the engineer to become acquainted with the bridge to a greater depth than a traditional load rating would require. This familiarity helps the analyst to identify critical members, design instrumentation plans, and implement a load test safely and effectively.

The FEM can be used to investigate and understand the influence of compounding factors like unintentional bearing stiffness, participation of the parapets or barriers, and other load-bearing mechanisms as described previously. The model can also be used for a staged analysis. For example, in a composite structure, the construction sequence can be modeled to find the effect of these different stages and the change from noncomposite to composite behavior on the deflections (*75*).

Finally, the FEM can be used to develop predictions of responses, ensuring that the sensors selected are adequate; the locations for installation are likely to carry high levels of response; and that the expected loading is adequate to overcome transient components (like frozen bearings) which cannot be included in a load rating.

Nondestructive Evaluation

To determine the material properties, where applicable, nondestructive tests are recommended prior to executing a load test. The results of these nondestructive tests can be used to improve the analytical models that are used for the initial load rating of the bridge as discussed in Analytical Model Development (page 9) and improve the preparations of the load test. For the phase of the analysis of the results, verified material properties will eliminate one of the sources of uncertainty in the analytical model.

For concrete bridges without plans, nondestructive techniques can be used (*20*) to estimate the reinforcement layout. For steel bridges, nondestructive techniques can be used to estimate the residual stresses in the sections. Current techniques for estimating residual stresses include ultrasound (*76*) [with promising results in laser ultrasonic measurements (*77*)] and magnetic Barkhausen noise (*78, 79*).

TYPES OF LOAD TESTS

Diagnostic Load Tests

The majority of load tests carried out in practice are diagnostic load tests. These tests are typically carried out with controlled and known loads. Diagnostic load tests (*39, 80–83*) can be used on newly opened bridges to verify the behavior of the structure to adjust predictions of an analytical model and can also be used on older bridges. Several countries, such as Italy (*3*), Switzerland (*84*), and France (*85*) require a diagnostic load test upon opening of a bridge. This information is useful, as it can be referred to later on, when a load test is carried out on the existing structure. The effect of material deterioration on the distribution of live load force

effects can then be analyzed based on the reduction in stiffness between the newly opened bridge and the bridge after decades of service life.

In a diagnostic load test, the load effects (i.e., strain–stress, rotation, crack widths, or deflections) are measured in bridge members in response to applied loads. The measured load effects can be interpreted to determine the member forces and moments. With all measurements zeroed before the beginning of the load test, the distribution of the live load effects is measured directly.

The measured load effects, or derived member forces and moments, can be compared with the values as calculated based on an analytical model (such as a FEM). The difference between the measured and calculated values is used to update the load rating of the tested structure or member. The measured responses should agree with the load effects determined in the preliminary calculations, or a rational explanation for the differences needs to be provided. If significant differences between measured and simulated responses are identified, a more thorough investigation may be required to resolve the differences and further analysis should not be undertaken until the differences can be resolved or fully explained.

The following sources of uncertainty in the rating and analytical assessment of the structure or tested member can be better assessed through a diagnostic load test:

- Influences on capacity (present condition and as-built condition)
  - Material properties,
  - Effectiveness of repairs, and
  - Deterioration and damage.
- Structural uncertainties
  - Load distribution,
  - Dynamic load allowance,
  - Boundary conditions,
  - Composite action, and
  - Barrier contribution.

The influences on capacity, such as the effect of material degradation and deterioration can only be quantified in a smear manner through a load test (e.g., by measuring the deflections and thus estimating the effect on the global stiffness). To identify the nature and source of material degradation and deterioration, other techniques [such as visual inspections, nondestructive evaluation (NDE), or material testing–sampling] are required. Load tests cannot provide information on these effects on the ultimate load capacity.

Nonstructural members can enhance the behavior and stiffness of a member at service load levels but may cease to contribute at higher load levels and towards the ultimate capacity. The applied load should be sufficiently high to properly model the behavior of the bridge at the rating load level. In the final analysis, the contribution of mechanisms (*18*) that may not be reliable at the load levels representative of the ultimate limit state, cannot be accounted for. These contributions should be subtracted from the final total capacity. Examples include unintended composite action or unintended support fixity.

Parameter-Specific Tests

Parameter-specific load testing refers to collecting sensor measurements from a structure with the intent of determining the contribution of a specific bridge element to the behavior of the

structure (Table 2-1). The end goal may not be to conduct a bridge load rating, but rather to simply provide insight into the performance of a specific element or component as well as its impact to the behavior of the structural system. It is not possible to describe all of the different scenarios that might fall into this category, instead we have provided the following list of example tests.

Proof Load Tests

Proof load tests (*42*, *81*, *86*, *87*) are typically carried out on bridges in service. In a proof load test, a target load is applied to a bridge, and observations are made to determine if the bridge carries these loads without damage. Since large loads are applied, the loads should be applied in increments and according to a loading protocol determined prior to the test, and the bridge should be closely monitored during the experiment to observe warnings of possible distress or nonlinear behavior. Careful preparation and experienced personnel are required to analyze the response of the bridge and make decisions about the safety of continued loading on the structure. Caution is required to avoid damage to the structure, or injury to personnel or the public.

For this reason, the bridge needs to be equipped with adequate sensors in suitable locations. The measurements have to be analyzed during the proof load test to verify that the stop criteria are not exceeded. In proof load tests, stop criteria are of the utmost importance because they indicate when certain thresholds for damage are about to be exceeded, thus resulting in an immediate ending of the proof load test. If the stop criteria are exceeded before reaching the required maximum load, the bridge will not be approved for the studied live load model, or particular live load configuration.

TABLE 2-1 Examples of Parameter-Specific Load Tests

Parameter	Instrumentation
Damaged structural element	Instrument-damaged element along with all elements connected to the damaged element. Load test will identify the change in load distribution surrounding the damaged element.
Retrofit or repair	Instrument the retrofitted or repaired element. Load test will determine the load carried by the retrofitted or repaired element, which can then be compared with the design.
Composite behavior of the deck-girder system	Instrument girder cross-section (near top flange, near bottom flange and intermediate height) to determine neutral axis location.
Forces into a connection detail	Instrument all elements that are attached to the connection detail. Elements should be instrumented in such a way to calculate axial or bending forces, depending on the project goals.
Movements of expansion bearing	Instrument girder ends at concerned expansion bearings for movements due to temperature or live load. Sensors should also be installed at structural sections where undesirable force effects are expected due to frozen expansion bearings. An alternative solution is to measure the movement of the bearing (and tilt of the substructure) to identify how this compares with free expansion of the bridge.
Performance of pin or hinge	Instrument-concerned pins or hinges for movements due to temperature or live load as well as attached structural members for undesirable force effects due to a partially or fully frozen condition.

The result of a proof load test is a better understanding of the behavior of the bridge, which can be used as input for a probabilistic analysis (*88–92*). The change in the probability density function (PDF) of the capacity side of the equation, R_d, is then as given in Figure 2-1.

In practice, a maximum load is determined prior to the proof load test that is necessary to approve the capacity of the bridge for a certain live load model or a particular test load. During the proof load test, the net capacity to carry live load is measured.

Proof load testing is currently used in the assessment of existing bridges in the Netherlands (*93*), Germany (*16*), and the United States (*94–96*).

Dynamic Load Allowance Estimation

Dynamic load allowance, or the impact factor, applied in load rating the structure can be conservative from most structures and is typically more influenced by roughness of the approach or expansion joint, which induces vehicle dynamic that results in an impact on the structure. The dynamic load allowance is applied as a 33% increase to the static live load effects of the design vehicle applied to the structure which is a considerable load factor against the capacity of the structure; therefore, conducting a load test for the purpose of identifying the true impact to the structure can be beneficial.

Conducting load tests to identify the dynamic load allowance that may be used in place of the code-based value in load rating should be considered carefully. While span length can contribute to the dynamics of the structure, some of the more difficult load parameters to accurately apply to a structure—such as vehicle dynamics (speed, weight, and suspension characteristics), roadway roughness, expansion joints, support conditions, and influence of secondary elements—are a few items to consider (*97*). Typical load tests conducted under normal traffic conditions may not be produce the dynamic response that should be considered in load rating. Controlled load tests designed to simulate the various conditions that may produce a reasonable estimate of dynamic load allowance is the best approach. It is the responsibility of the engineer to develop the load testing procedures so that a reliable dynamic load allowance can be measured and used in place of the code-specified value.

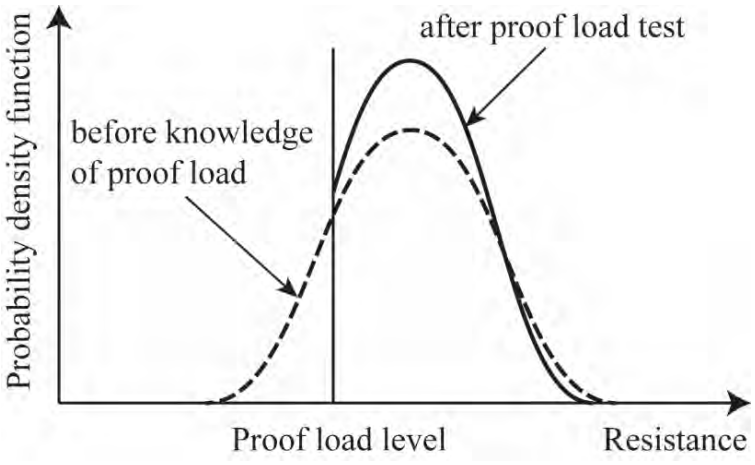

FIGURE 2-1 Truncation of PDF of resistance after proof load test, based on Nowak and Tharmabala (*90*).

Vibrational Methods

Even though most live loads applied on bridges are dynamic, static or pseudo-static analysis is generally used in bridge analysis for vehicular loads (i.e., inertial loads are ignored). Diagnostic and proof load tests considered in this document implicitly assume that load is applied in such a way that inertial loads can be neglected. This assumption is not true when the structure is subjected to excitations such as earthquakes, blasts, waves, etc. In such cases, the natural frequencies of structures play an important role in the way a bridge behaves under the dynamic loads. These effects should be considered, using structural dynamics, in the design of tests. Testing involves finding and analyzing dynamic characteristics of structures such as modal frequencies, mode shapes, damping ratios, and time histories. Often, this is referred to as Modal Analysis. Such analyses generally require a detailed FE type of model using system identification and model updating approaches.

Dynamic load testing for purposes of load rating does exist; however, it is still primarily a focus of academic research (*98–103*). Practicing engineers do not widely utilize dynamic testing for the following reasons:

> There are additional complexities when attempting to use dynamic data for FE model refinement—mainly having to adjust both stiffness and mass (inertial) matrices. When model refinement is done with diagnostic load test data, the primary focus is to adjust the stiffness parameters (element properties, element connectivity, and boundary conditions) such that the measured and simulated responses match. These parameters are typically well known from the design plans or can be simulated by simple assumptions. For example, to model the effect of a guardrail, a transformed stiffness element can easily be added to the model without having to match the exact configuration of that guardrail. Trying to accurately model both the mass values and mass distribution of a system can significantly increase the complexity of a model because simple assumptions cannot typically be made. Examples include determining the amount of water in a utility pipe at the time of testing, or accurately measuring the cross-slope variation of the wearing surface at the time of testing. However, dynamic testing also gives insight into the mass and mass distribution on a structure that live-load testing does not.
>
> In addition to the complexities of modeling for dynamic testing, the sensitivity of the overall system to change as well as the interpretation/usability of the results add to the challenges of dynamic load testing. Previous researchers have concluded that due to the inherently redundant design of civil structures and ability for redistribution of load, there would need to be significant “damage” to a structure in order for it to be detected through dynamic measurements (*104*). The identification and localization of problems is very difficult to do with any global method, whether static or dynamic.
>
> As is the case with all types of testing, environmental effects must be considered. Changes in temperature or humidity, or a combination of temperature and water presence, may affect dynamic test output (*105*, *106*). These environmental changes must be considered when test results are compared over long time windows, such as hours, days, or months.
>
> Dynamic characteristics (mode shapes, natural frequencies, and damping ratios) are more difficult for the practicing engineer to interpret because they are typically accustomed to dealing with static/design type characteristics such as bending moment, axial force, stress, etc. This difficulty with the use and interpretation of

results not being tied to what is typically considered in design makes the use of dynamic testing only reserved when complex analysis is required, or when vibration is of particular concern for the structure.

This document is focused on providing guidance for the use of load testing for existing structures. Therefore, a detailed treatment of dynamic testing is not provided here. The benefits of dynamic testing are considerable, and dynamic testing is appropriate for many applications. Some of these include field verification of dynamic properties in conjunction with a detailed analytical model; the determination of maximum vibration responses; and the determination of damping ratios for structures with very low damping. As familiarity with dynamic testing grows, practical applications and use may also increase.

LOAD TEST CONSIDERATIONS

When to Consider a Load Test Type

Diagnostic load testing can be used to update the rating of a given bridge based on the difference between the analytical and measured structural response. The differences between the field measurements and the structural–analytical model can be analyzed and attributed to different sources (*18*) including measurement and modeling errors. Each of these sources can be separated so that contributions that do not play a role at the ultimate limit state (i.e., unintended composite action in steel girder bridges with a concrete deck where the composite action stops to function at high loads) can be omitted from the analysis.

Proof load tests require higher load levels and as a goal have to directly demonstrate that a given bridge can carry the required load. Proof load testing is recommended when there are large uncertainties about the structure, and engineers have reason to believe that significant reserve capacity is available, but it cannot be quantified exclusively via analytical approaches. These uncertainties can be caused by a lack of structural plans, and no possibilities to develop plans, or by material damage, when there are uncertainties about the effect of the material degradation on the structural capacity of the considered bridge. Typical cases of proof load testing for bridges with material damage include testing of concrete bridges with corrosion-induced damage, or damage caused by alkali–silica reaction.

When Not to Consider a Load Test

Load testing of bridges is not recommended when the developed FEM results in sufficient rating. Other situations in which load testing is not recommended is when the safety cannot be guaranteed during the load test; for example, when there is a risk of a brittle failure during a proof load test.

STRUCTURAL CONSIDERATIONS

As discussed in Analytical Model Development (p. 9), the analytical model is a critical component to ensure test safety. Depending on the purpose of the load test, a hand calculation can be sufficient, or a full FEM can be necessary. The analytical model provides an external

check of the reasonableness of measured responses. Without a model, the engineer is left with only heuristics, or simplified calculations to guide the test effort. When a rigorous preparation is required, the combination of all three is preferred.

For proof load testing, high loads are generally applied on the bridge. The analytical model should be analyzed using the expected load levels and positions using, at minimum, the expected assumptions for varying parameters like boundary condition stiffness, concrete modulus, and composite action. Responses that can be directly compared to the field instrumentation should be produced. For complex structures, or situations where there is a real, heuristic-driven concern over safety, these parameters may be varied for a more robust sensitivity study. In this case, the response predictions are a range, as opposed to a single value. It should be noted that models are by no means guaranteed to be correct or superior to engineering judgement or heuristics. They should be combined and considered together.

BENEFIT–COST ANALYSIS OF USING LOAD TESTING

In order to estimate the cost of using load testing, it is important to evaluate the full life-cycle cost of the structure. Ideally, decisions with regard to when to carry out maintenance activities and when to load test are determined by minimizing the total life-cycle cost, while keeping the structural safety at a desired level (*107*). The expected total economic cost of a bridge structure can be determined as (*108*):

$$C_{ET} = C_T + C_{PM} + C_{INS} + C_{REP} + C_F \tag{2.4}$$

with

C_T = the initial cost;
C_{PM} = the expected cost of routine maintenance;
C_{INS} = the expected cost of inspections;
C_{REP} = the expected cost of repair; and
C_F = the expected failure cost.

An analysis of this optimization problem using an event tree related to the possible decisions showed that nonuniform time intervals are more economic and require fewer lifetime inspections and repairs than uniform time interval inspections (*108*). The way performance is expressed is typically determined based on strength and serviceability considerations. However, research on optimizing performance for durability is also under development (*109*).

When making choices with respect to structural health monitoring (SHM), the effect of costs can be considered as outlined in Frangopol and Kim (*9*):

$$C^*_{ET} = C^*_T + C^*_{PM} + C^*_{INS} + C^*_{REP} + C^*_F + C_{MON} \tag{2.5}$$

The superscript * denotes the cost updated with the information from the SHM system. The cost of the monitoring (C_{MON}) needs to be factored in as well. This factor consists of the cost of design and installation of the SHM system, the operation cost, the management cost, and the maintenance cost. From these considerations, it can be determined if a monitoring system is cost-

effective (*110*) or not. The expected deterioration plays an important role in the cost analysis of proposed solutions (*111*).

These principles can be applied to making the choice of load testing a structure. The difference is that for load testing, the cost consists of the cost of preparation, execution, and analysis of the load test. To maximize the benefit of using load testing, an optimum load testing procedure should be determined together with the optimum time during the life cycle of the bridge, and an optimum use of the data obtained from the load test. Cost-effective load testing should be based on analysis of the expected structural deterioration, and the associated expected damage detection delay (*110, 111*).

More transportation authorities are moving towards expressing the cost as a combination of the economic cost, the environmental cost, and the social cost (*112–114*). At this moment, no consensus has yet been achieved on how to quantify the environmental and social cost, and which aspects should be considered. Guidelines on how to assess the influence on climate change and use of resources are considered in the sustainability index for bridges (*115, 116*). The carbon footprint of different construction schemes or repair or rehabilitation measures can be assessed through the carbon calculator for construction activities (*117*). The social cost comprises a large number of aspects such as visual impact, driver delays, job opportunities, and more (*118*). The driver delay cost is simpler to estimate, whereas other social factors need further study to quantify. Social costs depend on the location of the bridge and should be studied on a case-per-case basis. However, preliminary studies (*118*) have shown that indirect social costs caused by driver delays can be about nine times higher than the direct economic cost in the construction phase of a bridge in a densely populated area. The challenge for bridge owners and designers lies in combining methodologies from different disciplines and weighing their importance before opting for a certain repair or replacement scheme. At all times, two counteracting effects need to be taken into account: the life-cycle cost should be minimized, while the performance of the bridge should never go below certain limits. Trade-off solutions are required to balance cost and performance.

Additionally, the cost analysis is moving from being decisions related, to a single-structural element or single structure, to the analysis of the entire road network (*119*). Some of the concepts that are applied to a single bridge structure can be extended to the entire network. However, in a transportation network it is important to acknowledge the interdependencies among the components. It was shown in (*119*) that a bridge maintenance schedule that yields the optimal network performance is not the same as the sum of the optimal schedules of the individual bridges. For an analysis at the network level, computational issues regarding the uncertainties involved or regarding numerical optimization can be a challenge and are a topic of current and future research. In the future, it is expected that decisions on when to load test, and which structure(s) to load test, will be made by analyzing the full sustainability cost and performance of the entire bridge network.

CHAPTER 3

General Load Test Preparation

SREENIVAS ALAMPALLI
New York State Department of Transportation

JESSE GRIMSON
BDI Bridge Diagnostics, Inc.

MARVIN HALLING
Utah State University

DAVID KOSNIK
CTL Group

EVA O. L. LANTSOGHT
Universidad San Francisco de Quito and Delft University of Technology

Y. EDWARD ZHOU
AECOM

INTRODUCTION

After an inspection and preliminary calculations, as described in Chapter 2, a program for load testing can be developed. This load test program should state the test objectives and identify the data and information required to meet those objectives. Once that required data is identified, the locations for measurements, and specific sensing technologies are selected, and data acquisition, aggregation, and analysis methods determined. When making these choices, one should pay particular attention to what analyses or observations ought to be made in real time during the test, and what analyses should be conducted post-test. These topics are discussed in this chapter.

TEST OBJECTIVES

The first step in the design of a load test is identification of test objectives (i.e., the specific questions to be answered by the test data). For example, an engineer might conduct a diagnostic load test to quantify lateral load distribution and stiffness or specify a proof load test to approve a bridge for a certain live load. Correspondence between specific load test goals and test types was discussed in Chapter 2.

The test objectives dictate the necessary field measurements. Some common bridge load test objectives include

- Quantification of in-service structural response to live load in a bridge with special structural features, such as high skew, curvature, unusual barriers or curbs, special diaphragms or braces, excessive fill above deck, or embedded box culverts
- Validation of various types of analytical models and development of a field-verified model
- Calculation of key parameters for load rating—for example, refining live load distribution factors (LLDFs) in multi-girder structures, or identifying unintended deck-girder composite action (such as may be found in bridges without shear connectors in original construction)
- In-situ measurement of local stresses (i.e., for fatigue calculations), particularly for features that are difficult to represent accurately by analytical methods such as distortion-induced stresses in unsupported web-gap areas, welded cover plate ends, or connection stresses in rocker linkages of suspension bridges
- Characterization of effects of in-service deterioration such as frozen rocker bearings or pinned connections, or member section losses due to steel corrosion or concrete spall.

PLANNING AND PREPARATION OF LOAD TESTS

General

Detailed planning is key to a successful load test. Once the test objectives are determined, the required measurement types and locations, as well as appropriate sensors, sampling rates, and post-processing schemes to obtain the desired measurements must be identified. A representative analytical model can be used for this purpose. Site-specific limitations, or difficulties with access to specific components of the structure, might make desired sensor positions impractical in some situations. These limitations warrant careful consideration during the planning phase. The load test plan will also include consideration of personnel requirements and the development of a safety plan.

In addition to the instrumentation scheme, the load test plan should include provisions for interpretation of sensor measurements and stop criteria. Especially for proof load tests, the stop criteria will identify situations in which the test must be prematurely aborted. The specific stop criteria are determined by the anticipated failure mode or modes; these anticipated modes are given by calculations or models developed prior to the test. Detailed discussion of stop criteria is included in Chapter 5. Briefly, typical stop criteria are related to material cracking, member deflections, and nonlinear structural responses. The measurements from the load test itself are used as stop criteria. As such, responses at stop-critical locations should be monitored in real time throughout the test (in addition to recording data from all instruments for post-test analysis per the test objectives).

Site-Specific Limitations

Preparations for a load test should include a site inspection. Inspection results will help identify and assess possible limitations at the site, which may include

- Requirements to keep part of the bridge open to traffic during the test, particularly using lane(s) adjacent to the tested lane(s), which can affect the measurements;
- Limited and/or difficult access to certain bridge members to where it becomes difficult to instrument these members directly;
- Limited work space for instrument installation (i.e., due to low vertical clearances);
- Required accommodations for possible road, rail, or water traffic passing under the structure (e.g., to avoid fouling railroad tracks or obstructing navigable waters with load test equipment);
- Availability of test vehicles with desired axle loads or axle configuration;
- Availability of work zone traffic control–protection, as well as restrictions on times of day during which lanes may be closed for testing (i.e., to avoid rush hours);
- Weather or other environmental conditions such as river stage; and
- Lack of stable or suitable reference point for deflection measurements (e.g., a bridge over deep water).

These limitations should be identified prior to the load test and accounted for in the test plan, as they may affect the instrumentation plan, the application of test load and other parameters, and the introduction of site-specific safety concerns.

It is good practice to present a safety and risk analysis report to local authorities and bridge owners–managers prior to the load test. This report should identify site-specific hazards, as well as possible problems arising from the load test itself. It should also document how, and to what practical extent, these hazards may be mitigated.

Instrumentation Plan

An instrumentation plan includes a sensor layout (type and position of all sensors), a data collection plan (data logger type, sampling rates, test controls, and data transmission means), and mounting and wiring details. Prior to developing the instrumentation plan, measurement parameters need to be determined. The following parameters are typically measured in bridge load testing:

- Strain in specific direction(s) at identified locations of interest (e.g., longitudinal strain on the bottom flange of a steel beam at the mid-span),
- Displacement or rotation in specific direction(s) of a member relative to a reference point at identified locations of interest (i.e., vertical deflection of a concrete girder at the mid-span relative to the ground and longitudinal and rotational displacements of a steel beam end relative to the abutment at an expansion bearing),
- Opening and closing of existing cracks,
- Surface temperature of steel or concrete members at various locations of interest, and
- Temperature of the ambient air and humidity.

Descriptions of some appropriate sensors to measure these quantities can be found in the literature (*120*), and should be revised in the light of ongoing technological advancements. Test preparation should include estimation of the location and magnitudes of the responses to be measured based on the available analytical model. These estimated magnitudes—along with test duration, site conditions, and structural material properties—inform selection of individual sensors (i.e., required measurement range, accuracy, and response type). All selected sensors should be suitable for field

testing (i.e., ruggedized against environmental conditions encountered in the field). Particular attention is required for sensor selection on concrete structures, as the time-dependent behavior of the material (creep effects) can result in larger structural responses. As it is common to lose some instrumentation during testing, or have sensors with an inaccurate reading, it is recommended to build in some amount of redundancy in the instrumentation plan.

Understanding how measured parameters are correlated to structural components and specific loading is very important. For example, even though deflections are specified in many specifications as a serviceability limit indicator and used extensively as a good indicator of the global behavior of the bridge system in the past, it is very hard to measure deflections using traditional gages. Correlation of deflection readings to the structure also requires knowing the specific loading on the structure, span length, and material properties, and investigation of such issues as neutral axis location and end fixity are not feasible with deflection measurement. Strain is dimensionless and stress is load per unit area. Thus, strain and stress values are less dependent on properties such as length and cross sectional. Deflection, on the other hand, depends greatly upon cross section area and length. Thus, it is not generally recommended to depend solely on deflection measurements during a load test used for load rating. Similarly, if a girder is only subjected to axial force, one strain gage may be enough to obtain the strain value. But, if both axial and bending strains are prevalent, it requires at least two strain gages positioned at appropriate location of the instrumented section to obtain a good picture of the total strain and to separate axial and bending strain components.

Data Acquisition and Visualization Requirements

The data acquisition (DAQ) equipment employed for a load test must have a sampling rate sufficient to capture the desired response to the test load. Depending on the particular load application, data acquisition speed may be considered as quasi-static, or dynamic. The DAQ, or connected analysis and visualization tools, must provide real-time output of measurements in engineering units for the test engineer to evaluate throughout the course of the test. Spatial plots are helpful to interpret the data. Examples include plots of deflected shapes, strain variations throughout a cross-section, or strain variation longitudinally within a girder. Such plots show erroneous data quite readily. These outputs are used both to evaluate the bridge response (and compare to stop criteria), as well as to provide verification of correct instrumentation operation (or to aid in troubleshooting of instrumentation before continuing the test).

As anticipated, structure responses and stop criteria depend upon position of the applied load(s) and responses must be analyzed jointly to interpret the test measurements. The test plan should include provisions for programming the test vehicle configuration for each test and the position of the test vehicle on the bridge throughout each test.

Prior to the load test, sensor calibration factors should be verified, and the correct calibration factors entered into the DAQ, or data visualization system, to provide real-time output in engineering units. Similarly, functionality of the sensors, DAQ, and data display systems should be checked prior to each load test.

Personnel Requirements

A qualified bridge engineer is responsible for the planning and execution of the load test. Experience in testing and instrumentation, field investigations, and knowledge of bridge structural behavior are required.

Adequate staff should be available to perform the load test to provide traffic control during the test and to assist in evaluating the results.

Local agencies or bridge owners may require specific personnel certifications, or training in site safety, first aid, or other aspects of industrial health and safety. It is prudent to review these local requirements prior to the load test and include required provisions in the test plan.

Loading Requirements

Once the objectives of the load test are identified, preliminary calculations are conducted to select test loads, to test vehicle configurations, and to estimate anticipated structural response. The structural response may be estimated from a variety of analytical models, depending on specific test objectives.

The following criteria may inform selection of test vehicle(s) for a load test, in terms of gross vehicle weight and axle configuration:

- Original design live load of the bridge,
- Rating vehicles required by applicable standards,
- Weights and axle configurations of heavy vehicles expected to use the bridge,
- Controlling failure mode of the bridge for each considered heavy vehicle configuration, and
- Availability and practicality (i.e., suppliers, loading method, weight limits, costs).

The configuration and number of test vehicles to be employed is determined by a preliminary structural analysis. The results of this analysis should include comparison of the load effects of the test vehicle with those of the design live load, rating vehicles, and heavy vehicles expected to use the bridge. Specifically, the purpose of this analysis is to ensure that the test vehicle(s) will represent the design and rating vehicles for the same controlling failure mode. The results of this analysis will also provide a quantitative indication of how the test load compares with the maximum live load for this bridge.

For diagnostic load testing, the test load should be sufficiently high to represent the heaviest service load for proper validation of structural behaviors that may vary at different loading levels, for example, unintended composite actions. Selection of test load levels for proof load testing is discussed in Chapter 5: Determination of Target Proof Load (p. 39).

Safety and Traffic Control

The load test plan must include provisions for the safety of the load test team and the traveling public, and for the protection of the bridge itself. The pre-test inspection report should include identification of general and site-specific safety hazards, as well as possible problems arising from the load test itself. In particular, consequences and corrective actions related to equipment installation/failures, structure access, adverse weather or site conditions, and other concerns should be identified. All personnel involved should be presented with a job safety analysis, job hazard analysis, or equivalent risk analysis report. All work should also be carried out according to governing safety guidelines for the jurisdiction or project site.

Maintenance of traffic (MOT) is typically the dominant safety concern and requires careful consideration to ensure a safe work zone for all aspects of the load test. While this

document is not intended to outline proper work site safety requirements—as each site or jurisdiction may have different requirements—it is recommended that prior to the load test the team consult with the owner of the bridge and identify the requirements for MOT. In the United States, the *Manual on Uniform Traffic Control Devices for Streets and Highways* (MUTCD) (*121*) defines standards used by road managers nationwide to install and maintain traffic control devices on all public streets, highways, bikeways, and private roads open to public travel. The MUTCD is published by the Federal Highway Administration (FHWA) under 23 Code of Federal Regulations, Part 655, Subpart F. State and local authorities may have more restrictive or specific guidelines or requirements for highway work zones.

It is the responsibility of the load testing team to outline roadway closures required to execute the load test clearly. The selected closure scheme should be designed to limit impact on the traveling public as much as possible. If short detours are available, full closures may have less impact than intermittent closures. The load test should also be conducted when traffic is minimal, such as at night. It should be kept in mind that closures may be required both on the structure to be tested, as well as on a roadway passing beneath the subject structure. For example, a roadway passing beneath a bridge to be tested may be obstructed by access equipment during installation or removal of load test instruments. The closure times should be defined so that the MOT can be designed to accommodate the entire load testing operation.

In addition, the load test team is responsible for addressing and mitigating risks to the traveling public that are specific to the load test; that is, risks that are not otherwise present on the subject bridge or roadway. In particular, a traffic control plan and a possible temporary detour of traffic must be coordinated with road authorities. Before the test, testing personnel should meet with personnel providing MOT to discuss the test plan as well as the traffic control plan to assure safety of test personnel as well as public, and also be in constant communication throughout the testing. Testing personnel should be flexible and be prepared to accommodate unexpected situations or traffic flows as they develop. Weather conditions can change suddenly; as such, a weather contingency plan should be included in the load test plan.

Environmental Effects

Environmental factors such as temperature, humidity, and wind can affect structural response and should be properly accounted for during the test preparation, during the testing, and also during the post-test analysis.

There are two main mechanisms by which temperature may affect the test include (1) unwanted responses of the sensor(s) or the instrumentation system due to temperature changes and (2) stresses or thermal deformations in the structure itself due to ambient temperature changes or temperature differentials or gradients. The influence of load effects induced into the structural members caused by changes in temperature should be evaluated. When evaluating test data, it is important to decouple thermal load effects from applied (i.e., test vehicle) load effects. In other words, temperature and applied load effects should not be simply summed. Temperature-driven effects on load test output can be minimized if the duration of the load test is short and the temperature is steady.

Strategies to quantify effects of temperature on structural response include:

- Deployment of a reference, or “dummy” sensor, on a coupon or unstressed member made from the same material, and subject to the same temperature changes, as a loaded member

of interest. The response of the dummy sensor is purely thermally driven and may be subtracted from the total response of the loaded member to obtain the purely load-driven component of response.

- Measurements under “no load” cases where the test load is removed completely over a period of time during which the ambient temperature varies. Analyzing the results of “no load” cases will provide a baseline for the response of the instrumentation system to the ambient environment including temperature. Such baseline can be used to make adjustments to the sensor responses during load test if deemed necessary.

Strategies for reducing the effect of temperature on the instruments themselves include:

- Selection of sensors, or sensor configurations, with inherently small temperature sensitivity such as resistive strain gages with built-in temperature compensation
- Applying instrument temperature corrections as provided by the manufacturer.

The effects of humidity changes, especially condensation, may also be significant for certain sensing elements. Particular care should be taken on bridges over bodies of water, where humidity is locally higher, and condensation may form on bridge elements at certain times of day.

STRUCTURE TYPE CONSIDERATIONS

Additional considerations are required for particular structure types or failure modes. Some examples of typical structure type- or material-specific considerations are presented in this section.

Steel Bridges

For steel bridges, strain measurements can fulfill a variety of test goals. For example, measured in-service strains can be compared to theoretically predicted strains to verify design assumptions and/or verify performance of the bridge over time; strain profiles over girder depth can indicate whether composite action occurs between the girder and deck. For fracture- and fatigue-critical members, the test preparations should address structural safety and performance thresholds during the test.

Concrete Bridges

Load tests of RC structures warrant special consideration to avoid shear failure, punching, or other brittle failure modes. In particular, loads during proof load tests of RC bridges should be selected and applied in such a manner as to preclude such failures.

The geometry of RC slab bridges precludes strain measurements over the depth of the cross section; thus, analysis must be based on strains on the bottom face of the slab and deflection profiles. For girder bridges, on the other hand, strain measurements over the depth of the girders is possible, and a strain profile can be developed to check if the cross section behaves as uncracked or cracked.

Measuring strains in RC bridges requires relatively large gage lengths. When using very small gage lengths, the heterogeneous nature of concrete results in strain variations. When using

small gage lengths, the effect of local cracking can result in strain variations. The gage length should be large enough to capture cracking effects in a smeared way.

For prestressed concrete (PS/C) bridges strain measurements can fulfill a variety of test goals, similar to applications to steel bridges. For example, strains can be measured over the depth of the girders (in the same way as for steel girders) to evaluate composite action between the girder and deck. During proof load tests, the load configuration should be set up so that the girder is the main loaded element; punching of the wheel prints through the deck or other brittle failure modes should be prevented. This issue should be addressed during the preparation stage.

Stone, Masonry, and Unreinforced Concrete Arch Bridges

Stone and masonry arch bridges are complex structures which display a three-dimensional load-bearing behavior as a result of the interaction between the arch barrel and the spandrel walls (*15*). To study the behavior of masonry arches, proof load tests can be used (*28*). For historical masonry arch bridges, an extensive program of nondestructive tests can be used during the inspection stage prior to the load test. These nondestructive tests can be used to verify key input parameters required for the numerical analysis that is developed to prepare the load test. Special attention should be paid to the presence of internal voids, flaws, layering condition, and the mapping of nonhomogeneity, moisture content, etc. (*28*). Measuring the strains due to temperature variations and comparing these strains to the analytically predicted strains of a fully restrained model of the bridge can be used to quantify the lateral stiffness of the foundation (i.e., the ability to confine the arch).

For historical unreinforced concrete arch bridges (*122*) load tests are suitable to determine the stiffness of the structure in the presence of large cracks and material degradation. The collaboration of the arch, spandrel walls, fill layers, substructure and additional elements such as curbs and barriers can be evaluated with a load test.

For stone arches, similar recommendations as for masonry arches can be formulated (*15*). The FEM that is used to prepare and analyze the load test needs to be a 3D model using solid elements. In this FEM, it is recommended to assign a tensile strength to the masonry–mortar continuum. A value of 2% to 5% of the compressive strength has been shown to be a good, conservative estimate (*15*).

A combination of diagnostic load testing and proof load testing is recommended, so that the change in behavior from low to higher load levels can be observed. Special attention needs to be paid in the analysis of the FEM and test results with regard to the interface between the arch barrel and the spandrel wall. Deterioration of this interface significantly changes the load-bearing behavior of the stone arch bridge. Similarly, for open spandrel arch bridges, the construction sequence should be correctly modeled in the analytical model. If this sequence is not properly modeled, a disparity between the load test results and expected structural responses from the analytical model will result.

Timber Bridges

Timber bridges can be evaluated in terms of overall performance as well as static and dynamic load distribution characteristics through load testing (*123*). To determine the state of a timber bridge prior to a load test, a condition assessment is necessary. This assessment can combine visual inspections, photographic and video documentation, and moisture content measurements

(*123*) to determine the extent of wood deterioration. Diagnostic load testing of timber bridges can be used to determine the distribution of loads (*123*), or to evaluate the performance of rehabilitation measures (*124*). During the test, timber strains and deck deflections can be measured (*125*).

Long-Span and Signature Bridges

For long-span and other signature bridges, members can be evaluated with the general recommendations from this document, but additional steps need to be taken to load test for the behavior of the full structure. Therefore, long-span bridges as a whole are outside the scope of this document; however, some components of a long-span bridge may be considered such as the floor system where live load is reasonably easy to apply and measure directly. Typically, each long-span bridge will need a detailed preparation and the particular behavior of the bridge will drive the required choices for the load test.

CHAPTER 4

Diagnostic Load Tests

SREENIVAS ALAMPALLI
New York State Department of Transportation

JESSE GRIMSON
BDI Bridge Diagnostics, Inc.

MARVIN HALLING
Utah State University,

DAVID KOSNIK
CTL Group

EVA O. L. LANTSOGHT
Universidad San Francisco de Quito and Delft University of Technology

Y. EDWARD ZHOU
Delft University of Technology

INTRODUCTION

The goal of a diagnostic load test is to measure actual responses of the structure (e.g., strain, deflections, rotation, and accelerations) against known loads so that realistic analytical models can be established to determine the effects of various loads. Diagnostic load tests are often intended to reduce the uncertainties associated with actual as-built conditions that cannot be modeled easily using theoretical or analytical models such as material properties, boundary conditions, transverse distribution, secondary nonstructural elements, effectiveness of repair and strengthening measures, and stiffness reduction due to material deterioration. Diagnostic load tests involve relatively low load levels, usually at or around the service load level, and can be executed in a relatively short amount of time.

Preparation for diagnostic load tests in general was described in Chapters 2 and 3. Briefly, preparations include pre-test inspection and document review. In addition, if the results of the load test will be used to update the bridge load ratings, the bridge should be rated analytically according to the applicable/prevailing standards [such as the AASHTO MBE (*57*) or owner–state-specific procedures].

The recommendations in this chapter relate to specifics of diagnostic load testing. The test results are then used to compare with analytical predictions, develop field-verified analytical models, remove unreliable mechanisms that should not be considered during load rating, and ultimately calculate refined load ratings to reflect the actual performance of the bridge. Ultimately, the diagnostic testing approach involves load testing for the purpose of developing a more realistic structural or analytical model than the design model (i.e., to reflect as-built or in-service

conditions), which is then used for refined structural evaluation including load rating. The updated load rating can then be interpreted by the bridge owner to select the appropriate level for posting, if required, or issuing permits for overloads.

Figure 4-1 shows a flowchart of the steps and considerations during the preparation, execution, and analysis stages of a diagnostic load test.

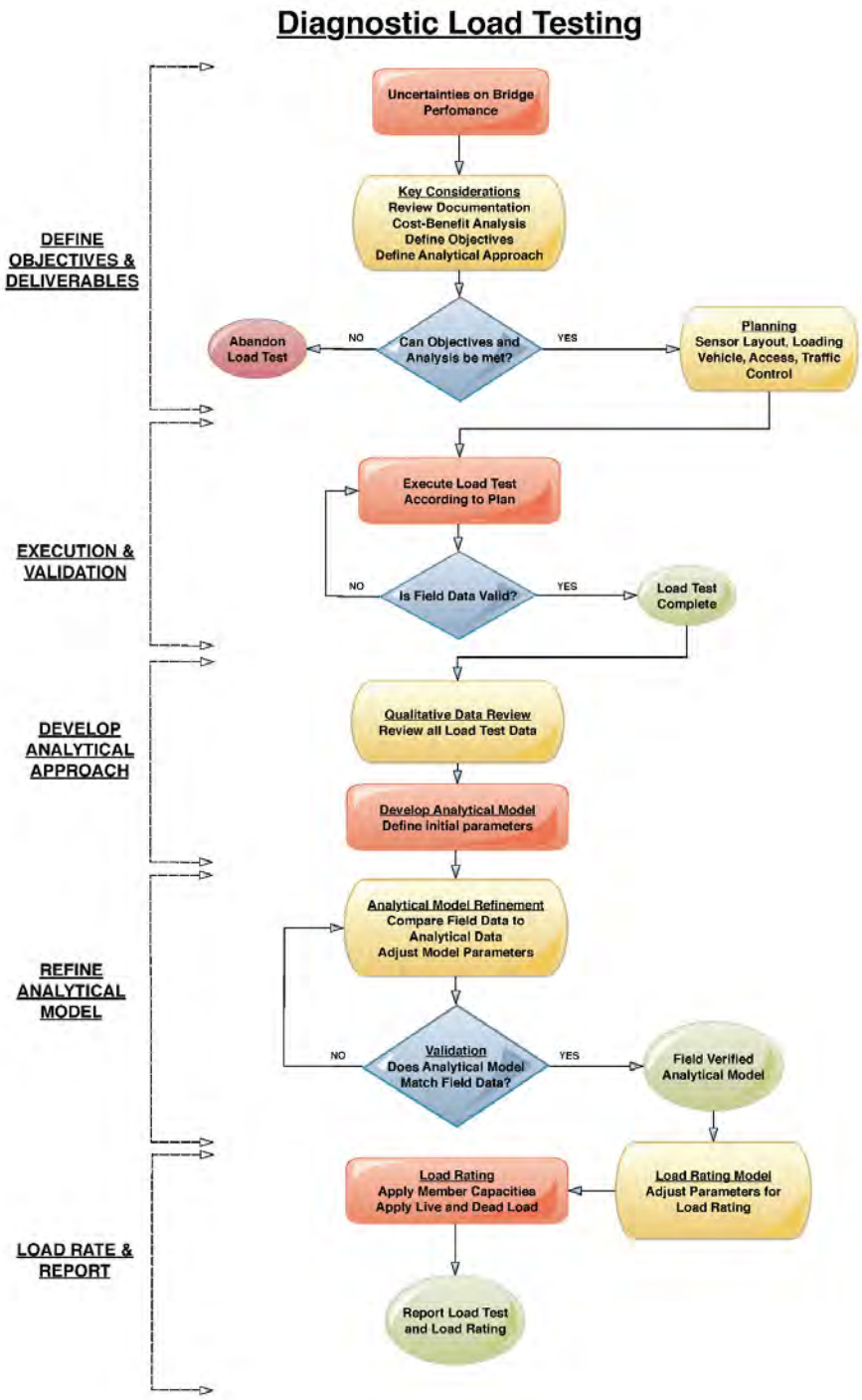

FIGURE 4-1 Diagnostic load testing flow chart.

KEY CONSIDERATIONS

Prior to the execution of a diagnostic load test, as with any load test, the specific objectives of the test must be clearly described and understood by all stakeholders. Typical reasons for performing a diagnostic load test include

- Field verification of design assumptions,
- Distribution of live load effects,
- Measurement of stress response in certain members,
- Determining actual performance of bridge appurtenances that affect structural boundary conditions (i.e., expansion joints or pinned connections),
- Measuring the maximum unexpected stresses in members connected to a “frozen” pin or other malfunctioning appurtenance, and
- Development of load ratings for particular vehicle configurations.

Several of these typical load test objectives relate to reserve strength of the bridge. For instance, the additional capacity provided by non-structural members (i.e., sidewalks, barriers, and parapets) that are not included in design can add significant load carrying capacity. In these cases, one should have an idea of the source of the reserve strength before the testing is initiated—the diagnostic load test is to verify and quantify these sources of reserve strength.

Some additional key considerations, beyond the preceding and the general preparations discussed in Chapters 2 and 3 include

- Specific objectives of, or reasons for, performing the load test (i.e., load ratings for particular vehicles, stress responses in certain members, actual performance of expansion bearings or pins, the maximum unexpected stresses in connected members, and verification of design assumptions);
- Physical measurements needed to accomplish the objectives (i.e., maximum strains or deflections in specific members due to certain loads);
- Critical members and load carrying capacities of the structure based on a review of available information and field observations;
- Instrumentation plan to acquire the needed physical measurements, including sensor types and locations, sampling rates, etc.;
- Magnitude and configuration of test load and method of application (i.e., number of test vehicles, vehicle weights, test runs, vehicle combinations, arrangements, and speeds);
- Overall scale and detail levels of analytical model for comparisons with field test measurements; and
- Cost–benefit analysis of the load test itself (see Benefit–Cost Analysis of Using Load Testing, p. 15).

EXECUTION OF DIAGNOSTIC LOAD TESTS

General

As diagnostic load tests are carried out at load levels that are a fraction of the full factored live load, these tests can be executed in a short amount of time (typically 1 day) and most activities can be carried out on a subset of the traffic lanes of a bridge while the remaining lanes remain open to traffic. Full closures are only required during the data collection phase, which can typically be completed 5 to 15 min per load path. With busy roadways, traffic can be cleared between load paths.

When access to the underside of the bridge is necessary, partial closures of the roadway under the bridge may be required. Scaffolding or manlifts may be required for the activities under the bridge. For bridges over water, specialized access equipment is necessary.

Specialized field measurement equipment may be helpful to reduce setup time in the field as well as to prevent disruption of the measurement due to the vagaries of field work. In other words, some structural instruments that are familiar and trustworthy in a laboratory environment may be impractical for field use due to factors such as exposure to weather or other harsh environmental conditions, time and access requirements for sensor wiring and configuration, or other considerations. Some examples of the specialization of equipment could be

- A user interface that does not require programming in the field can be practical;
- Sensor wiring can be simplified or eliminated using pre-assembled wiring harnesses or wireless sensors; or
- Easy-to-install sensors employing transducer electronic data sheets, or another self-identification mechanism, can further speed installation and reduce probability of mistakes (*55*).

Monitoring Bridge Behavior

It is prudent to monitor the measured bridge behavior in real time during any type of load test. The test engineer should follow instrument outputs (e.g., strain and displacement) as well as the predicted versus actual load-displacement diagrams for critical locations throughout the test. Graphical displays, particularly with allowable limits superimposed on the sensor data plots, make this easier. However, special provisions for alternative real-time displays may be necessary for very dense instrumentation schemes.

Environmental Effects During Diagnostic Load Tests

As discussed in Environmental Effects (Chapter 3, p. 23), effects of the environmental factors, such as temperature and humidity, on sensor performance should be established prior to any load test. Basic information on temperature and humidity effects should be available in the sensor manufacturer's data sheets. If this effect is large, experimental results should be adjusted for this difference as well.

Typically, diagnostic load tests use a slowly moving test vehicle to cross the bridge traveling less than 5 mph (8 km/h), resulting in a very short loading cycle. Accordingly, the ambient temperature–humidity may be reasonably assumed to be constant during the test, and the corresponding effects on the sensors neglected. However, complex load tests may take

sufficiently longer to complete due to temperature and other environmental factors that may change significantly during the course of the test. This effect is particularly pronounced in situations where some or all of the sensors are exposed to direct sunlight. In these cases, substantial differences in sun exposure, and thus sensor temperature, may be induced by changes in cloud cover, wind, or the diurnal movement of the sun. Field protection of the sensor or testing at night is recommended to reduce such differential heating where possible. Alternatively, it may be helpful to deploy temperature sensors near such affected sensors to at least provide a basis for applying thermal correction factors.

The environmental effects are not only limited to the effects caused by changes in temperature and humidity over the course of the test. For example, the stiffening of asphalt overlays and foundation-soil system under low temperatures can greatly influence the overall behavior of the bridge. Data obtained under low-temperature conditions should not be used directly to generate load ratings, as these mechanisms are not present when the temperature rises.

On-Site Data Validation

As mentioned in Monitoring Bridge Behavior (Chapter 4, p. 29), the prudent test engineer will monitor the graphical output of the measurements during any load test. In addition to addressing structural response and safety questions, such real-time monitoring is useful as a means of on-site data validation, as certain types of sensor malfunctions may be clearly indicated by measured responses that diverge from expected structural behavior in particular ways.

The graphical outputs required during the test are typically to view the sensor responses in their engineering units in real-time. For moving test vehicles, response histories as a function of the load position allow for the most straightforward interpretation in the field. It is important to make sure that an unexpected measurements are not caused by sensor malfunctioning, but indeed a valid observation can be made with a few on-site checks.

In general, bridge load tests are expected to result in structural responses that are reproducible, linear, and symmetric. In other words, similar responses should be obtained from repeated tests using the same testing vehicle on the same load path (though, as mentioned in Environmental Effects During Diagnostic Load Tests (Chapter 4, p. 29), small effects of changes in temperature and humidity may appear). The principle of linearity indicates a linear relationship between load and response. In other words, if through a second passing the load testing vehicle is twice as heavy, the response should be twice as large. Finally, when bridge geometry is symmetrical about midspan or some other reference point, the load response is expected to be symmetrical as well.

Divergence from the patterns of reproducibility, linearity, or symmetry indicates either an unexpected structural response or a sensor or instrumentation malfunction. In practice, sensor malfunctions and installation mistakes are probably the most common source of such errors. Regardless, any such error should be taken seriously and evaluated on the basis of sound engineering judgement.

An experienced test engineer will typically have a “feel” for some of the signal patterns associated with various common malfunctions or errors. Some typical problems with sensor output include

- A sudden shift in the measurements caused by an impact to the sensor and/or the wiring;

- A constant response value known as a “flat line” (i.e., if the sensor has reached the limitations of its measurement range);
- Displacement and strain readings in the opposite of the expected direction caused by reversed signal wires;
- A sudden offset or response that does not return to zero could indicate that the sensor has detached from the structure;
- A noisy signal (poor signal-to-noise ratio) due to missing or improperly configured amplifiers, crosstalk, or other electrical phenomena; and
- Drifting sensors due to grounding issues.

Occasionally, site-specific conditions may present additional challenges. For example, instrumentation on bridges near facilities with high levels of radio emissions (e.g., broadcast towers, highway maintenance depots, or police–fire stations) may experience higher-than-typical levels of electromagnetic interference on sensor inputs. This results in higher-than-expected noise on the output when the sensor or DAQ does not have the appropriate mitigation for electromagnetic interference or radio frequency interference. In many cases, such interference can be mitigated by hardware filters, or reduced in post-processing.

Nonlinear and Inelastic Response Validation

While the intent of typical diagnostic load tests is never to generate non-linear responses in the structure, it is very important to identify such conditions, should they occur during a test. Such behavior will likely affect subsequent analytical modeling requirements, or may be an indication of a problem within the structure itself. If the instrumentation system has been thoroughly validated on-site and is believed to be in proper working order, the test engineer must make an engineering decision whether to proceed when indications of nonlinear or inelastic response become apparent. It is good practice to calculate the expected responses prior to conducting the load test so that the test engineer can establish realistic thresholds for the on-site data validation process.

An inelastic response is typically identified through a measured response that does not return to the original state after the load is removed. This type of response may be the result of multiple reasons including permanent deformation (e.g., steel yielding) or may simply be the response of a change of state of the structure (e.g., locked bearing becoming free).

INTERPRETATION OF DIAGNOSTIC LOAD TEST RESULTS

Qualitative Review of Load Test Data

As discussed in On-Site Data Validation (p. 30), the initial review of load test data should be conducted in real time during the test to validate sensor performance and reveal unexpected structural behavior. This section describes data review, post-processing, analysis, and applications upon return from the field site.

Some post-processing is typically required following the load test. For example, strain measurements may require correction for the influence of temperature and humidity (Environmental Effects During Diagnostic Load Tests, p. 29), deflection measurements may

need to be corrected for the deflections measured at the supports, load position may need to be corrected for any offsets in starting position, and/or filters may need to be applied to reduce ambient noise. In some circumstances, smoothing of electrically noisy dynamic data may be helpful.

Following post-processing, the structure responses are plotted versus time or load position for the various loads and load paths. Some common plots include

- Response histories of all sensor outputs as a function of (*a*) time and (*b*) applied load. These plots provide a synoptic view of the bridge response and also serve as a backup to in-field identification of sensor functionality (On-Site Data Validation, p. 30);
- Applied loading schemes;
- Deflections in the longitudinal direction;
- Measured strains over the structural member's depth;
- Spatial distribution of strains with time or load;
- Response histories near supports to help identify restraint at the support condition; and
- Movements at the joints.

Development of Analytical Model

An analytical model, typically an FEM or a structural "stick" model, may be developed to simulate the diagnostic load test. All reasonable efforts should be made to ensure that the model is a faithful representation of the bridge structure, with particular care given to geometry, based on as-built plans and verified by field measurements. Maintaining the 3D geometry of the bridge while using 1D (beam) and 2D (shell) elements generally requires a number of offsets or link elements. These considerations are especially important to properly model composite action, cross-frames, and supports (which should be located at the base of the girder, not at the end of the corresponding element). Material properties are generally based on nominal values from the as-built plans. However, if deemed necessary, material samples can be collected from the bridge and test results are used. If a previous routine or in-depth bridge inspection indicates section loss of steel members due to corrosion, or other deterioration of primary load-carrying elements (e.g., broken strands in a PS/C girder), the model should reflect the reduced section geometries.

Other important considerations in development of analytical models include

- Use of proper element types and mesh sizes comparable to the sensors used in load test;
- Inclusion of secondary members such as barriers, sidewalks, diaphragms, etc. that provide additional stiffness and capacity not reflected in design calculations, and that might influence the response behavior of the bridge;
- Definition of support conditions at bridge bearings (i.e., points, lines, or patches, and with or without friction);
- Quantification of elastic modulus of RC (uncracked or cracked cross-section, long-term effects);
- Modeling of member intersections or connections (of partial member cross-section, steel to concrete without shear connectors, bolted connections consisting of angles, gusset plates, etc.); and

- Definition of geometric eccentricities at connections of different structural members.

Validation and Refinement of Analytical Models

After an analytical model is established, it should be used to predict sensor responses from the load test. The analytical load cases applied to the model should simulate the test loads in terms of the magnitude, arrangement, as well as lateral and longitudinal positions of loading forces such as the crossing of the testing vehicle of known axle weights and configuration. The model will only consider the truck live loads, as the measurements are zeroed at the beginning of the diagnostic load test, and thus only measure live load effects. The analytical output, such as strains, stresses, or deflections, should be at the same locations and orientations as where sensors were mounted on the bridge during the load test.

A recommended first step is to compare plots of the load test measurements and corresponding analytically determined responses for a blind comparison. This initial comparison serves to identify gross modeling errors and verify the correctness of the basic model (*55*). It is common that the first-round of analytical predictions do not agree with the field measurements in magnitudes to varying degrees. However, if the patterns of analytical responses—such as general shapes, locations of peaks, valleys, and zero points—differ significantly from field measurements, the computer model needs to be checked for correctness in geometry, structural continuity or discontinuity, support conditions, and load cases. The analytical model may need updating to reflect observations from the load test data. For example, if unintended composite actions between adjacent members (deck-girder, floor system-truss, etc.) is observed in the testing, the model should be adjusted to account for it. Similarly, if distribution factors in a multi-girder structure were noted to be very different than those used in the design, actual distribution factors should be applied to the structural, or analytical model. Uncertain model parameters should be the first parameters considered for model updating. Table 4-1 provides guidelines for a (non-exhaustive) list of parameters that can be adjusted to refine the analytical model for improved agreement with load test measurements.

The actual optimization of the FEM is an iterative process. The properties to be adjusted (Table 4-1) can be determined as variables, and a parameter set for which the best correlation between the model and the data obtained is sought, while bearing in mind that the final values should reasonable considering the realistic parameter properties. The two basic parts of this refinement process are the heuristic part and the automated error-minimization part.

A fully automated error minimization is not desirable, just as engineering judgement is always necessary when analyzing test data. However, methods exist to compare the errors achieved when selecting different values for a given parameter. A least-squares approach can be used to determine the parameter for which the lowest error is achieved. Crucial in this process is the selection of the correct parameters to be optimized. The engineer should also define reasonable limits to the parameters, so that realistic values can be achieved, and so that possible problems with the method of developing the field-verified FEM can be identified.

TABLE 4-1 Common Adjustment Parameters for Refining an Analytical Model

Adjustment Parameters	Refinement of Analytical Model for Improved Agreement with Load Test Results
Element type and mesh size	Strain or stress output, depending on the element type and mesh size at sensor locations, must be comparable to the gage length and orientation of strain sensors used in load test.
Secondary members	Secondary members—such as barriers, sidewalks, diaphragms—need to be properly included for their geometrical, material, and stiffness properties.
Bearing support conditions	Typical bridge bearings—of fixed or expansion—provide a rectangular patch support to the superstructure. Expansion bearings usually have frictional resistance. Use of idealized fixed or roller point or line supports in the analytical model may cause discrepancies with load test measurements due to simplifications.
Elastic modulus of concrete (e_c)	E_c is usually estimated from the specified concrete compressive strength (f_c') using an empirical formula. In reality, most concrete mixes are placed at a higher strength than design requirements, and concrete continues to gain strength over time. When modeling the sectional stiffness, both the effect of the concrete strength and the provided reinforcement are considered. If test data is available, using the actual material properties instead of nominal values will improve the fidelity of results from the model.
Link members for eccentricities	Use of line or planar elements in a FEM requires the use of link members to address the eccentricities between intersecting or connecting bridge members. Proper definitions of the stiffness properties of the link members are important to simulate the overall behavior of the structural system, including intended or unintended composite actions between adjacent members.
Member end connection stiffness	For steel members of I-shaped or other types that do not have a full moment connection at the end in the framing system, e.g., the commonly used partial web height double-angle bolted connection, the actual rotational stiffness of the connection falls between those of a fixed and a pinned connection. Depending on the type of elements used in the model, adjustments can be made to the rotational stiffness for better agreement with field measurements. For example, a rotational stiffness constant can be defined at the connection when beam members are used in the model.

The heuristic method requires experience and is based on the visual examination of the field measurements versus the analytical model output. Individual element parameters can be adjusted, and restraints at the supports can be identified and adjusted. As all the identifier parameters are adjusted through this iterative process, a field-verified model can be achieved.

After refinement and validation, the analytical model can be used to determine structural responses for other load cases or combinations for needs such as load rating analysis based on the field-verified model. The extrapolation should be done carefully using sound engineering judgement.

LOAD RATING CONSIDERATIONS

General

After the model refinement procedures, the resulting field-verified model can be used for load rating. When a simplified analytical model is used, the procedure to determine the experimental rating based on field measurements from (*18*) can be used. It is important to address questions about the applicability and extrapolation of the test results and the field-verified model to future ratings (*55*).

The different load rating methods are the allowable stress method, the load factor method, and the LRFR method. The load rating can be based on capacities at the inventory level and operating level as defined in the MBE (*57*). The inventory level corresponds to design levels of safety recommended by the AASHTO specifications. The operating level corresponds to the upper bound of allowable safety permitted by the MBE.

Any refined parameters that could change over time, or that may be unreliable with heavy loads or damage, should be assessed and adjusted as appropriate. For example, beneficial unintended composite action encountered under typical loads may be lost under heavy loads. Similarly, effects of future maintenance decisions must be taken into account. Bearing maintenance provides a useful example: frozen bearings can reduce the span moments, but the bearings can be repaired, so this reduction is not generally applicable for future load ratings.

If the refined FEM is the result of a diagnostic load test, then the model is most applicable to inventory rating values, because it is assumed that all measured and computed responses are within the linear-elastic range of the structure. It is important to keep in mind that load testing does not provide information about the ultimate strength of structural members. To evaluate this limit, collapse tests are necessary. However, it must be noted that load responses should never be permitted to reach the inelastic range, since this reduces the lifetime performance of the structure.

The equation for the LRFD rating factor, given in the Introduction of Chapter 2 (p. 6), describes the ratio of available capacity for live loads to live load demands, taking into account the dynamic load allowance. If the rating factor is larger than, or equal to 1, the bridge rates sufficient for the considered live load model. If the rating factor is smaller than one, and depending on the loads imposed on the bridge, the test engineer may recommend posting of the bridge (*74*). In light of the interplay between condition–maintenance and bridge capacity, it may be helpful to use the results of the model as a tool for directing bridge inspectors to areas of concern during inspections.

Live Load Effects

When diagnostic load testing is used for load rating, the results of the diagnostic load test are used to determine the effects of live loads (sectional shears and moments) in a way that corresponds to the actual behavior of the bridge. All types of rating loads (standard design, legal, and permit) can be rated with the field-verified model, using the load combinations and limit states required by the MBE (*57*). The field-verified model can be used to determine the induced forces and moments, and to evaluate how the bridge will respond when standard design loads, legal loads, and permit loads are applied to the structure, and thus to determine the load rating factors for each truck type, in the truck paths as determined by the MBE (*57*). The lateral truck positions must be defined to induce critical responses for all structural members under consideration. For completeness, multiple-lane loading scenarios should be included in the evaluation.

Capacity Calculations

The capacity of the structure is not changed or identified by a diagnostic load test. Capacity for the failure mode for which the load rating is done can be determined from the expressions available in the governing codes, such as the MBE (*57*), or can be based on refined models that

represent the structural behavior and possible sources for additional capacity that are typically not included in the simplified code equations. In order to carry out the capacity calculations, information about the geometry of the bridge and the material properties is necessary. If as-built plans are not available, nondestructive testing techniques can be used to estimate the geometry and material properties.

A variety of methods are available to determine geometry of bridges without as-built plans from field measurements. For example, geometric models for any bridge type can be obtained rapidly using laser scanners, lidar systems, or photogrammetric methods.

Material properties can also be determined with a number of nondestructive testing techniques. For concrete bridges, the concrete compressive strength (*126*), the position and sizes of the reinforcement bars (*127*), the amount of corrosion damage (*128*), and the extent of cracking (*21*) can be estimated with nondestructive testing techniques. A variety of devices to scan for reinforcement are available. In addition, if the owner agrees to allow minor damage to the structure, the concrete cover can be removed locally at a few positions to verify the results of the reinforcement scans. For steel bridges, nondestructive testing techniques can be used to estimate the presence of cracks in the steel, and to characterize the material based on particular properties such as hardness (*76–79*). For timber bridges, nondestructive testing techniques can be used to study the material properties, degradation, and moisture content (*123*). Similarly, for masonry bridges, a combination of nondestructive testing techniques with local sampling can be used to determine the material properties and ingress of moisture (*28*).

Besides nondestructive testing techniques, material samples can be taken from the structure, when permitted by the bridge owner, for testing in the laboratory. The results of these tests can be used to confirm the results from nondestructive tests.

Load Posting and Permit Loads

The engineers conducting the load test submit their recommendations for rating to the bridge owner. The final decisions to load-post the bridge, impose load restrictions, and issue permits are left to the bridge owner. This distinction is necessary because posting and permit procedures vary by jurisdiction.

REPORTING OF LOAD TEST AND LOAD RATING

The load test and rating report should contain all information pertinent to the load test and resulting rating. At a minimum, the following information should be included:

- With regard to the bridge
  - Name, location (e.g., milepost or feature crossed), and year of construction;
  - Representative photograph; and
  - Type of structure (e.g., slab, girder, truss) and material (e.g., RC, PS/C, steel).
- With regard to the preparations of the load test
  - Primary and secondary objectives of the load test;
  - Overview of the available information of the bridge such as original calculation reports, design or as-built plans, and material testing reports from the construction stage;
  - Recent inspection reports;

  - Current load rating;
  - Description of the analytical model used to prepare the test;
  - Description of loading trucks and load paths used for the test;
  - Instrumentation plan; and
  - Reference to the safety plan for a safe execution of the load test.
- With regard to the execution of the load test
  - Date and time of test;
  - Names and affiliations of persons conducting or observing the test;
  - Deviations from planned loading trucks or load paths, if any;
  - Observations during the load test;
  - Any unusual site conditions or discrepancies between as-built plans and actual site conditions; and
  - Pertinent environmental information such as temperatures, humidity, etc.
- With regard to the analysis of the load test:
  - Review of the measurements
    - Discussion on data quality,
    - Notable observed behavior (i.e., measured loading truck passings, strains as a function of time and load position), and
    - Any other conclusions based on the computations from measurements (i.e., maximum stresses, forces or moments, location of member neutral axis);
  - Comparison between analytical model results and field measurements; and
  - Description of development of field-verified model, including discussion of parameter refinement and final results.
- With regard to the final rating and advice
  - Discussion of which contributions to the difference between the original analytical model and field-verified model can be extrapolated to the ultimate limit state, and thus used for the final rating;
  - Adjustment of field-verified model for rating purposes, if necessary;
  - Rating assumptions: assumptions on rating procedure and factors, summary of member capacities used for rating, considered rating loads and configurations;
  - Resulting rating; and
  - Recommendations for maintenance based on the results, if any.

CHAPTER 5

Proof Load Tests

MARVIN HALLING
Utah State University

DAVID KOSNIK
CTL Group

EVA O. L. LANTSOGHT
Universidad San Francisco de Quito and Delft University of Technology

Y. EDWARD ZHOU
AECOM

INTRODUCTION

Two approaches exist internationally for proof load tests. The first approach, as outlined in the MBE (*57*), prescribes proof load tests as a method to demonstrate the ability of a bridge to carry its full dead load plus some "magnified" live load. This live load is represented by a rating vehicle in bridge load rating. The second approach, as used in European practice, is based on the use of high loads to create the same sectional force, or moment, as a load combination from the code to show that the structure can carry the loads as prescribed in the code. In that case, the live load model from the code (distributed lane loads and design truck and/or tandem) needs to be converted to an equivalent proof load truck or tandem.

Using high loads during proof load tests, however, involves certain safety risks, and can complicate test execution. In addition, such high loads introduce the risk of causing possible damage to, or even collapse of, the structure under test. These risks are quantified in Chapter 6.

As high loads are applied during proof load tests, an analysis of some efficient form should be performed during the preparation stage to correlate the test load with the critical force effect for the predicated governing failure mode. The extent of this analysis should depend on the goals of the load test, the expected behavior of the bridge, and the level of maximum proof load relative to service load. For example, a more thorough analysis may be required for a shear-critical concrete girder bridge than a flexure-critical RC slab bridge for assessing the maximum critical force due to test load with respect to estimated capacity.

A proof load test encompasses a multiple-step loading and unloading process in a progressively increasing manner towards a predetermined target proof load. Real-time measurements and on-site data reviews at each step are required to mitigate the risks inherent in proof load tests. During the proof load test, measurements such as strain, displacement, and rotation are evaluated and compared to predetermined thresholds, the so-called stop criteria. These thresholds indicate when the test load may be approaching or have exceeded the limit for linear elastic structural response. They may also indicate that a further load increase may result in irreversible damage to or any possible failure of the structure.

The MBE (*57*) describes target proof loads for bridges and formulates recommendations for execution of proof load tests. Other existing code provisions for proof load tests are found in codes for buildings, such as ACI 437.2M-13 (*59*) and the German guideline (*129*); these have limited application to bridges due to differences in support conditions and service loads (including quasi-static versus dynamic loads).

This chapter presents considerations for proof load tests, specifically, with regard to determination of the target proof load, test execution, and post-test analysis of experimental results. The steps of the process are outlined in Figure 5-1.

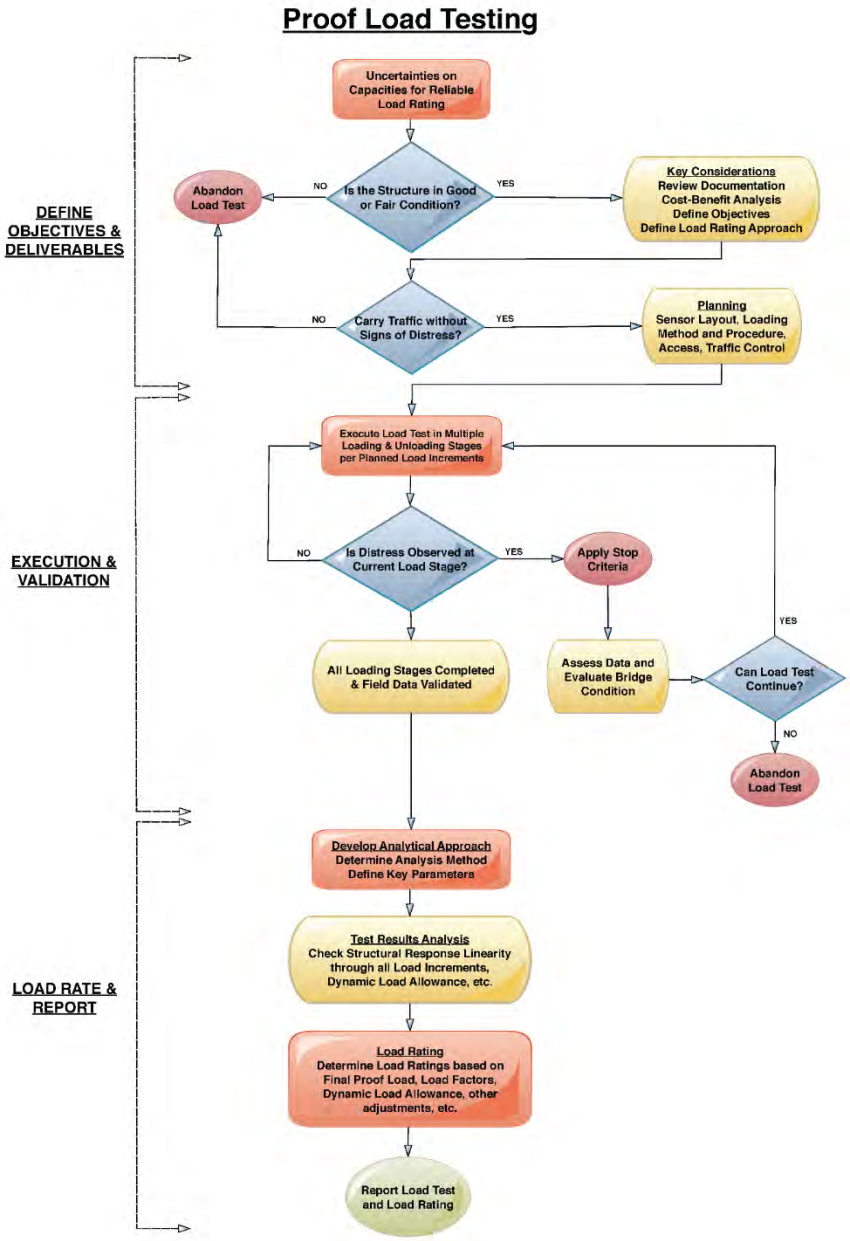

FIGURE 5-1 Proof load testing flow chart.

DETERMINATION OF TARGET PROOF LOAD

Method from the AASHTO *Manual for Bridge Evaluation*

The AASHTO MBE (*57*) prescribes that the "test loads must provide for both the rating vehicles, including the dynamic load allowance, and a load factor for the required margins of safety." The target live load factor, X_p, is the factor required to achieve a bridge load rating factor of at least 1.0 at the operating level. After the target adjusted live load factor X_{pA} is obtained, with adjustments for site conditions, the factor is multiplied by the rating load plus dynamic load allowance to get the target proof load. The MBE recommends a base value for X_p of 1.40; however, if the load rating is for a permit load, the permit load factors from Table 6A.4.5.4.2a-1 from the MBE should be used instead, which are generally less than 1.40 depending on the permit type.

According to the MBE, a lower-bound strength, R_n, based on the successful completion of a proof load test is:

$$R_n = X_{pA} L(1+IM) + D \tag{5.1}$$

with

L = live load effect,
D = dead load effect, and
IM = dynamic load allowance.

In comparison, the nominal strength R_n in bridge design is

$$R_n = \gamma_{LL} L(1+IM) + \gamma_D D \tag{5.2}$$

where γ_{LL} is the live load factor and γ_D is the dead load factor.

Equation 5.1 shows that the dead load in bridge load rating through proof load testing is deterministic without any load factor since the dead load does not change over the course of the test. The X_p factor, of a baseline value of 1.40, in Equation 5.1 as recommended by the MBE, reflects the live load factor for operating design load rating per the LRFR method, which has a reduced level of reliability compared with bridge design per LRFD or inventory design load rating per LRFR.

The adjustments to X_p are as given in Table 5-1, so that X_{pA} becomes

$$X_{pA} = X_p\left(1+\frac{\Sigma\%}{100}\right) \tag{5.3}$$

The value of $\Sigma\%$ is the sum of the adjustment percentages from Table 5-1 for the bridge under test. The target proof load L_T as a function of the load of the rating vehicle L_R is then

$$L_T = X_{pA} L_R (1+IM) \tag{5.4}$$

The background to this approach is given in the annex to the 1998 *Manual for Bridge Rating Through Load Testing* (MBRLT) (*58*). MBRLT employs a first-order reliability method based on normal distributions. The values assumed for the bias (mean to design value) and for the coefficient of variation are given in Table 5-2. The bias for the live load is based on weigh-in-motion measurements, and then extrapolated to 75 years to find the mean maximum load as 1.79 HS20 vehicles. The coefficient of variation on the live load is 18% when both the uncertainties on the heavy truck occurrences, and the uncertainties of the effect of these trucks on the members of the structure are considered, and 14% when only the uncertainties of the truck occurrences are considered. The target values of the reliability index β were defined as 3.5 for the inventory rating and design levels and 2.3 for the operating rating level, which reflects "past rating practices at the operating levels." The main uncertainties after a proof load test that need to be factored in are the magnitude of future live loads and possible future deterioration. The value of X_p was derived based on an example with an 18-m (60-ft) span with an equal dead load and live load effect, $D = L$, and was verified for a shorter span and longer span with $D/L = 3.0$.

Method Based on Equivalent Sectional Force or Moment

In European practice (61), a load is applied such that the resulting sectional force or moment is the same as the force or moment caused by the factored loads prescribed by the code. The general procedure is as follows:

- An analytical element model is developed as explained in Analytical Model Development (p. 9)
- The model is loaded with the following service loads: self-weight of the structure; superimposed dead load, and live loads (distributed lane load and design trucks/tandems in each lane) and
- Load factors are used to make the load combination.

TABLE 5-1 Adjustments to X_p [Table 8.8.3.3.1-1 from MBE (*57, 130*)]

Consideration	Adjustment
One-lane load controls	+15%
Nonredundant structure	+10%
Fracture-critical details present	+10%
Bridges in poor condition	+10%
In-depth inspection performed	-5%
Rateable, existing $RF \geq 1.0$	-5%
ADTT ≤ 1000	-10%
ADTT ≤ 100	-15%

ADTT = average daily truck traffic.

TABLE 5-2 Values for the Coefficient of Variation (COV) and Bias for Resistance and Load Effects as Used for the Derivation of the Target Proof Load Factor X_p

	COV (prior to test)	COV (after test)	BIAS
Resistance	10%	0%	1.12 1.0 distress in test
Dead load	10%	0%	1.0
Live load	18% truck + members 14% truck only	18% 14%	1.79 one lane 1.52 two lanes
Dynamic load allowance	80%	80%[a]	1.00

[a] Unless a moving load test is performed to investigate the dynamic load allowance.

- The critical position for the design trucks–tandems (i.e., the position that induces the largest sectional force or sectional moment) is determined for each span, based on the model output.
- The live loads are removed and replaced by the unfactored proof load wheel prints at the critical position. These wheel prints depend on the type of testing vehicle or loading setup to be used in the proof load test. For bridges with maximum three lanes, the wheel prints can be applied in a single lane.
- The target proof load is determined as the load on the proof load wheel prints required to induce the maximum sectional force or moment calculated previously.
- The load test is conducted in the field using a test setup corresponding to the target proof load.

For special cases, such as checking sectional shear in RC slab bridges via proof load test, the critical position can be known beforehand. Specifically, in this case, the critical position occurs when the face-to-face distance between the load and the support equals 2.5 d_l (*131*), with d_l the effective depth to the longitudinal reinforcement. For other cases and other members, the critical loading position must be determined with an analytical model.

Verification of Physical Capacities

It is recommended that key physical capacities of the structure (based on known or assumed material properties) be assessed through analytical means before the load test. These capacities serve as a check against possible failures of load carrying members, or possible collapse of the structure under the target proof load.

The calculated physical capacities provide an estimated level of the test load under which member or structural failure may occur. If the difference between the calculated capacity and the target test load is small, real-time measurements and data interpretations during the test must closely monitor the bridge response and condition change and have a detailed plan for stopping the test if determined necessary. Stop criteria, in terms of limit values of measured strains, displacements, or other physical parameters should be established before the start of proof load test.

For in-service bridges, an examination of the weights and types of vehicles that cross the bridge provides reference information on the actual loading condition experienced by the structure. Such information can also serve as a reality check to the calculated physical capacities.

Determination of Target Test Vehicle Weight Based on Target Proof Load

The target proof load L_T determined by Equation 5.4 is for the governing load effect in bridge load rating, e.g., maximum bending moment at mid-span, maximum shear force at a support, etc. Before the execution of a proof load test using test vehicles, the target test vehicle weight W_T corresponding to the target proof load L_T must be determined in order to accomplish the proof test goals.

If the test vehicle has identical axle configuration (spacing and weight distribution) as the rating vehicle, the target test vehicle weight W_T is simply

$$W_T = X_{pA}\, W_R\, (1 + IM)$$

where W_R is the gross weight of rating vehicle.

However, the test and rating vehicles being identically configured is usually not the case in reality; therefore, there is often a need to assess load ratings for multiple rating vehicles. As a result, it is necessary to determine a vehicle adjustment factor f_V for each rating vehicle to account for the axle configuration difference between the rating vehicle and the test vehicle. Thus, the target test vehicle weight should be determined as

$$W_T = X_{pA}\, f_V\, W_R\, (1 + IM)$$

A structural analysis using a line model is generally sufficient to determine an f_V for the test vehicle for equivalent governing live load effect L_R in load rating to each rating vehicle. f_V = 1.0 if the test vehicle is identical to the rating vehicle in axle configuration (spacing and weight distribution).

EXECUTION OF PROOF LOAD TEST

General

Execution of a proof load test involves applying the test load through a multiple-step loading and unloading process with increasing load levels before reaching the target proof load while structural responses are closely monitored through sensors.

Key considerations for executing proof load tests include the following:

- Method of applying test load (test vehicles or a fixed loading system with hydraulic jacks);
- Beginning level of test load based on actual traffic condition or analytical supports;
- Load increments for all loading steps before reaching the target proof load;
- Key response parameters of the governing failure mode(s) identified by analysis;
- Instrumentation plan (sensor layout, data collection, processing, or display methods);
- Measurements evaluation criteria for proceeding to the next loading level (zero-return of individual sensor responses, linearity of response-test load correlations, etc.); and
- Stop criteria for aborting the load test before reaching the target proof load.

For proof load tests on bridges, the application of the loading protocol with loading and unloading steps can be carried out by repeating truck positions, or by using a loading system with jacks. Among other reasons, multiple loading and unloading steps of increasing load levels are desirable as it allows the engineer to check the linearity of the structural response to increasing load. A larger response to the same load increase on subsequent applications indicates that nonlinear behavior is occurring in the structure, or that the applied sensors are not properly functioning. In either case, the test should be stopped to investigate the cause of the observations. Small fluctuations in the response as the result of the influence of temperature and humidity can take place during the test. Some engineering judgement is required to evaluate what constitutes a true nonlinear structural response versus response due to environmental changes.

Since proof load tests need to apply test loads higher than the service load, the loading protocol and the limiting values for the stop criteria have to be determined prior to the beginning of the load test and communicated with all parties involved. Safety considerations become important and sometimes govern the preparation and execution of the test (see Personnel Requirements, p. 21, and Safety and Traffic Control, p. 22). To evaluate the structural performance of the bridge during the load test and manage the associated risks, adequate measurements need to be provided that can be linked to the stop criteria for the type of test that is used. These measurements need to be continuously observed during the load test.

Load Application Methods

The system that is chosen to apply the load should be able to apply the proof load in a safe and controlled manner. If the loading protocol prescribes this, the load application method should be able to keep the load constant and apply the load in as-planned load increments. To check repeatability, the method of load application should be able to repeat the same load levels. The load application method should be able to apply the load to the wheel prints of the predetermined design truck or tandem. Given the large loads used for proof load tests, the load application method should also provide a means of safely aborting the test in the event of large deformations or exceedance of other stop criteria.

Some common proof loading systems include:

- Dead weights,
- Loading vehicles, and
- Hydraulic jacks in a loading frame.

Application of dead weights has several disadvantages. First, it cannot properly represent the concentrated wheel loads of the considered truck or tandem (either design truck or tandem, or rating vehicle). Moreover, when the structure starts to deflect, a gap between the dead weights and the structure can occur, causing some of the load to be redistributed to the support through arch action by the weights themselves. Finally, dead weights provide no method to quickly and safely abort the test in the event of large deformations—a major drawback from a safety perspective.

When loading vehicles are used for a proof load test, considerations must be given to

- Similarity of axle configurations between the loading vehicle and the rating vehicles;

- Physical capacity of the loading vehicle for being loaded to X_{pA} times the weight of the rating vehicle;
- Extra weight and a loader for loading and unloading the required number of vehicles to the target proof load;
- A loading–unloading site near the bridge so that test vehicles do not need to cross other bridges during the proof load test;
- Sufficient amount of scales for measuring the wheel weights of test vehicles and a flat area for obtaining accurate readings from the scales; and
- A travel route for transporting all the test vehicles, loader, and extra weight to the site without exceeding legal weight limits.

An army tank or similar heavy weight carried by a truck may provide an option (*132*) depending on the similarity of the axle configuration to the rating vehicles.

A third method for applying the load is using a loading frame with hydraulic jacks. This system, however, is time-consuming to build up. Another disadvantage is that, when the jacking system is supported by the bridge substructure, only the superstructure is loaded during the test since the forces will cancel out at the substructure. The overall bridge behavior, with both the superstructure and substructure loaded, will be unknown. Jacking has a considerable safety advantage, as the system can be operated in a displacement-controlled manner; thus, the applied load will be reduced when large deformations take place and a collapse will be avoided. When hydraulic jacks are equipped with load cells, the relation between applied load and structural responses can be visualized easily in real-time. Hydraulic jacks are commonly used in Europe, as a result of the geometry of the design tandem used in the Eurocode EN 1991-2:2003 (*133*). The European live load model was derived to result in equivalent sectional moments as those resulting from measured traffic, including safety factors. The design tandem is not a direct representation of a certain truck type.

Recommended Loading Protocol Using Test Vehicles

For multiple-lane bridges, including those carrying one lane in each direction, a minimum of two loading vehicles should be used.

The following loading protocol is recommended:

- Obtain two vehicles of the same axle configuration that is as close as possible to the rating vehicle of interest.
- Mark the bridge deck surface with lateral vehicle positions to properly check all load path components.
- Determine a realistic weight for the loading vehicle (W_{Real}) that the bridge experiences on a regular basis based on a traffic survey, legal weights, any postings, or site observations.
- Establish a maximum vehicle weight increment to be one third of the difference between the target proof load and the realistic load, or $\Delta W_{\max} = 0.33(W_T - W_{\text{Real}})$.
- Repeat the following steps at each increasing vehicle weight (W_{Real}, $W_{\text{Real}} + \Delta W$, $W_{\text{Real}} + 2\Delta W$, $L_{\text{Real}} + 3\Delta W$, etc.):
    1. Use one truck to cross the bridge at a crawl speed or position it at a stationary location at all pre-marked lateral positions.

2. Review sensor measurements and visually inspect the structure for any signs of distress.
3. Use two trucks side-by-side to cross the bridge at a crawl speed or position them at stationary locations at different combinations of lateral positions as allowed by deck geometry.
4. Review sensor measurements and visually inspect the structure for any signs of distress.

- If allowed by site condition and agreed by the vehicle owner and driver, repeat select single truck crossings by running the same truck at the speed limit, at the same lateral position, for assessing dynamic load allowance. This is usually practical and safe only at the lowest load level.

Loading Protocol Used With Hydraulic Jacks and Loading Frame

In Europe, it is common to use a hydraulic jacks and a loading frame to carry out proof load tests. This method is not commonly used in the United States, but has been included in this document for reference. An example of a loading protocol using hydraulic jacks and a loading frame during a proof load test is shown in Figure 5-2. This loading protocol, recommended for proof load tests on RC slab bridges (*134*), has the following characteristics:

- The loading speed is a constant value and should be between 3 kN/s (0.7 kip/s) and 10 kN/s (2.3 kip/s).
- Four load levels are used
  - A low level to check the functioning of all sensors,
  - A load level corresponding to the serviceability limit state (load factors = 1)
  - An intermediate load level, and

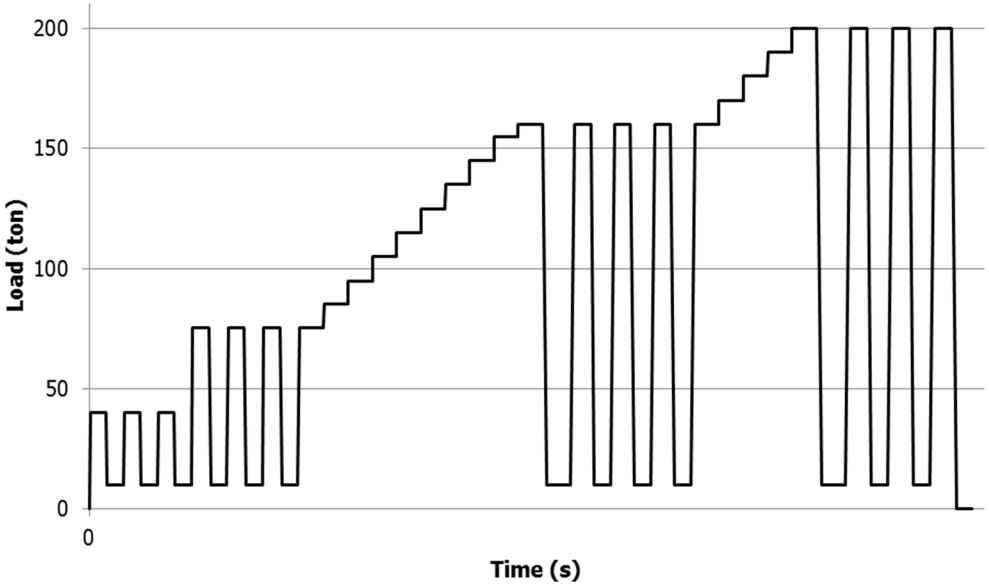

FIGURE 5-2 Example of a loading protocol (*131*).

  - The target proof load—a load level corresponding to 5% to 10% above the factored load combination for which the bridge needs to be evaluated to capture variability effects of the material.
- A baseline load level is used to make sure all measurements stay activated.
- Each load level is repeated three times, and each repetition is composed of 2 min at the maximum load and 2 min at the baseline load level.
- Each load level past the serviceability load level is approached incrementally and for each step, the load is increased and kept constant for three minutes—the time during which all measurements are analyzed, and the decision is made whether it is safe to add another small step.

Monitoring Bridge Behavior

According to the MBE (*57*), "the loads during a proof load test are applied in steps so that the response of the bridge under each load increment can be monitored for linear-elastic behavior and to limit distress due to cracking or other physical damage." If nonlinear behavior is observed, or if there are visible signs of distress such as buckle patterns appearing in compressive zones in steel or cracking in concrete, the test should be stopped. The MBE recommendations include monitoring of strain (stresses) in bridge components, relative or absolute displacement of bridge components, relative or absolute rotation of bridge components, and the dynamic characteristics of the bridge during the proof load test.

Some specific recommendations for monitoring bridge behavior during a proof load test are compiled in this section. Real-time monitoring of the following quantities at each load increment is recommended:

- The load-displacement diagram to identify if non-linear behavior is occurring,
- The strains in the members to verify if strain limits are exceeded,
- The width of existing cracks to see if cracks are activated in concrete bridges,
- All deformation output should be followed to see if the results are in line with the analytical predictions or if the predictions and measurements show significant changes, and
- The applied load on each wheel print should be measured separately when jacks are used, to verify if the load is distributed evenly across the wheel prints.

If nonlinear behavior is observed, the test should be paused for additional checks. In particular, the instrumentation engineer should check for any indications of sensor malfunction (see On-Site Data Validation, p. 30). In the absence of indications of sensor malfunction, nonlinear behavior (see Nonlinear and Inelastic Response Validation, p. 31) may be taken to indicate the onset of irreversible damage to the structure and may warrant immediate termination of the test.

During execution of the proof load test, the engineer analyzing the measurements must have direct contact (e.g., through walkie-talkie) with the load operator. The engineer analyzing the measurements will communicate to the load operator when the load can be increased, or when the load needs to be removed. These recommendations apply for load tests using a loading vehicle as well as tests employing a load frame with hydraulic jacks.

Determination of Stop Criteria

The MBE (*57*) and the MBRLT (*58*) require that a proof load test be terminated at the onset of non-linear behavior, or when damage occurs to the structure as described previously. Quantitative stop criteria based on measurements should be determined prior to the test. Since loading beyond such stop criteria may result in irreversible damage, it is important that the load test be terminated immediately upon reaching any one-stop criterion, even if the target proof load has not been achieved. In exceptional cases, and only with the consent of the bridge owner and an analysis of the possible risks involved, further loading can be permitted.

Prior to a proof load test, stop criteria should be defined depending on the bridge type and condition, based on the analytical model used for the test preparation, and by following engineering judgement. The stop criteria for the failure mode of flexure for RC buildings from the German guideline (*3*) are provided here as a reference:

- Limiting the sum of the concrete strain caused by the test load and the calculated strain caused by the permanent loads present at time of testing to 800 με
- Limiting the maximum concrete crack width to 0.5 mm (0.02 in.) for new cracks, and limiting the maximum increase in crack width to 0.3 mm (0.01 in.) for existing cracks and
- Limiting the residual crack width after a load cycle to 30% of the maximum crack width for a structure that was not cracked previously and to 20% of the maximum increase in crack width for a structure that was cracked previously.

An additional promising stop criterion—verified based on a number of bending and shear experiments on beams (*134*)—consists of imposing a limit to the allowable reduction of the stiffness defined as the slope on the load-deflection diagram measured by the sensor closest to the center of the load at its critical position for the considered failure mode. A recommended value is 25%. A qualitative evaluation also includes studying the deflection profiles at different load levels in the longitudinal and transverse direction to identify signs of redistribution and following the load-deflection diagram during the test for signs of nonlinearity. A more extensive proposal for stop criteria for flexure and shear can be found in (*135*). For shear-critical structures, stricter crack width limits may be necessary when aggregate interlock capacity is lost at small crack widths (*136*).

Crack widths smaller than 0.002 in. (0.05 mm) are negligible and should not be considered for determining the residual crack width. For a load test conducted to study sectional shear or another brittle failure mode, engineers with specialized training and experience should determine the stop criteria prior to the test and interpret the measurements during the test. The specialists should also apprise the bridge owner of the inherent risks of brittle failure before the test. Additional measurements, such as acoustic emission monitoring, may be useful to identify precursors to brittle failure modes in concrete structures.

For steel bridges, a stop criterion can be to limit the total steel strain (measured strain due to test load and calculated strain due to permanent loads) to 90% of the yield strain. For timber and arch bridges, the test engineer needs to determine suitable stop criteria prior to the load test.

Environmental Effects During Proof Load Tests

As discussed in Chapter 3 (Environmental Effects, p. 23) and Chapter 4 (Environmental Effects During Diagnostic Load Tests, p. 29), many sensing devices commonly used to monitor load test are subject to effects of ambient temperature and humidity changes. The effects of temperature on sensing elements should be established before the test (typically from the manufacturer's data sheet) and taken into account during data interpretation, if necessary. Since proof load tests use more extensive loading protocols than diagnostic load tests, the execution time tends to be larger than for a diagnostic load test. As such, a discussion of the environmental effects is necessary.

In many cases, a proof load test may be completed without substantial changes in environmental conditions before any significant changes in temperature. For example, temperature changes during a test conducted over the course of a few hours in the morning or at night when the bridge is not in full sunlight may be negligible. By contrast, a test in which different areas of the bridge are exposed to sunlight at different points during the test would likely require careful consideration of temperature effects.

When using a dummy sensor, as discussed in Chapter 3, and when using real-time data visualization, the compensation by the output of the dummy sensor can be preprogrammed in the data visualization system. The compensated structural response can then be used for an improved evaluation of the stop criteria.

On-Site Data Validation

To validate the measurements, it is recommended to use a loading protocol consisting of loading and unloading. In a first trial run of the loading vehicle, or in the first load step at a low load level when using hydraulic jacks, all measurements should be studied to verify the proper functioning of all sensors. Some basic checks include, but are not limited to comparison of sensor measurements with analytical predictions; zero return after unloading; etc. Data should be checked for linearity, reproducibility, and symmetry as discussed in Qualitative Review of Load Test Data (p. 31).

INTERPRETATION OF PROOF LOAD TEST RESULTS

General

When a bridge has passed a proof load test, structural calculations after the test are not strictly necessary if the test load well represents the expected service load. The proof load test itself served to directly demonstrate that a bridge can carry a given loading. However, post-test analysis of the acquired measurements is still recommended to provide better understanding of the structure's behavior and inform its future rating.

The analytical model initially used to prepare a proof load test can be developed into a field-verified model post-test based on the actual measurements obtained during the proof load test. The principles for updating the analytical model are similar to a diagnostic load test (see Validation and Refinement of Analytical Models, p. 32). The possible sources for differences (*18*) between the calculated and measured deformations and strains need to be identified (see Table 4-1), and the differences between the tested structure and the model should be minimized. The influence of mechanisms that are unreliable at the ultimate limit state should be removed from the field-verified

model before this model can be used for load rating purposes. Once the analytical model is updated, it can be used to rate the entire structure when only one span is proof load tested; or rate the bridge for other types of rating vehicles of different axle configurations from the loading vehicle. This field-verified analytical model can also be utilized for all future analyses of this bridge.

Load Rating After Proof Load Test

The rating factor for the test vehicle will be at least 1.0 at the operating level, after successful completion of a proof load test. The operating rating factor will be larger than 1.0 if the applied load was higher than the target proof load. As a goal, the method based on a target proof load from the MBE (*57*) is to apply a test load so that the operating rating factor is at least 1.0. After the proof load test, the operating rating factor RF_O for the test vehicle is determined as

$$RF_O = \frac{OP}{L_R\left(1+IM\right)} \tag{5.5}$$

with

$$OP = \frac{k_0 L_p}{X_{pA}} \tag{5.6}$$

with L_R the load of the rating vehicle, IM the dynamic load allowance, L_p the maximum proof load X_{pA}, according to Equation 5.3, and k_0 a factor which takes into account how the proof load test was terminated. The value of $k_0 = 1$ if the target load was reached and $k_0 = 0.88$ if signs of distress were observed prior to reaching the target proof load. The 12% reduction is consistent with observations that nominal material properties used in calculations are typically 12% below observed material properties from tests.

Bridge load ratings are for specific rating vehicles, but the test vehicle used in proof load testing is generally different from the rating vehicles in axle configuration (spacing and weight distribution). As discussed in Chapter 5, Determination of Target Test Vehicle Weight Based on Target Proof Load (p. 41), for determination of target test vehicle weight, a vehicle adjustment factor f_V can be established for the test vehicle for equivalent governing live load effect L_R to each rating vehicle. When load ratings for rating vehicles different from the test vehicle are desired, f_V can be used to derive such load ratings. It is important to understand that a rating factor of 1.0 at the operating level can be assured only for rating vehicles that have a live load effect L_R equal to or less than that of the successfully completed target proof load.

Another important consideration in assessing bridge load ratings from proof load testing is the value of dynamic load allowance IM to be used in Equation 5.5. Engineering judgements are required to properly account for field conditions, load test results from high-speed vehicle crossings in comparison with slow speed crossings, possible condition changes of bridge deck surface and joints in the future, etc.

Load Posting and Permit Loading

The engineers conducting the load test submit their recommendations for bridge load rating to the bridge owner. When a stop criterion is reached during a proof load test, this event indicates that the bridge does not fulfill the code requirements for carrying such load. As such, the engineers may determine the highest value of the load that can be safely carried by the bridge for the codes under consideration. The final decisions to load-post the bridge, impose load restrictions, and issue permits are left to the bridge owner. This distinction is necessary because posting and permit procedures vary by region, among other reasons.

REPORTING OF PROOF LOAD TEST AND RATING

Reporting of Observations

It is recommended to develop the following graphical output after the proof load test to be included in the report:

- Load-response (i.e., displacement or strain) time histories of the entire load testing process from all sensors as well as the load-response envelope diagrams; from these diagrams, it can be determined whether nonlinearity may have occurred, and if so, where, and what type(s) of nonlinearity may have occurred;
- Measured loading scheme of the total load and the wheel prints separately when using jacks, or of the vehicle when using a loading vehicle;
- Structural response profiles (i.e., deformation, strain, deflection) in the longitudinal and transverse direction; and
- Crack opening and closing as a function of time or applied load for concrete bridges.

When analyzing this graphical output, attention should be paid to the linear response of sensors under different loading cycles to the same load level. Effects of the time-dependent behavior of the materials can influence these responses to a certain amount. After unloading, the residual deformations can be analyzed with respect to the zero measurement at the start of the load test. These residual deformations, possibly caused by the time-dependent behavior of materials such as concrete and timber, should not be excessively large.

The analysis of the stop criteria from Chapter 5 (Determination of Stop Criteria, p. 46) should be added to show that the maximum load was achieved without exceedance of any of the stop criteria.

Proof Load Test Report

The proof load test and rating report should contain all information pertinent to the load test and resulting rating. At a minimum, the following information should be included:

- With regard to the bridge
  - Name, location (i.e., milepost or feature crossed), and year of construction;
  - Representative photographs; and

  - Type of structure (i.e., slab, girder, and truss) and material (i.e., RC, PS/C, and steel).
- With regard to the preparations of the proof load test
  - Overview of the available information of the bridge, such as original calculation reports, design or as-built plans, and material testing reports from the construction stage;
  - Recent inspection reports;
  - Current load ratings;
  - Justification for the need of a proof load test (i.e., sources of uncertainty);
  - Description of analytical model used to prepare for the test;
  - Determination of target proof load and critical loading positions;
  - Estimation of average capacity of critical members to identify if a proof load test can be carried out safely;
  - Stop criteria and their derivation;
  - Instrumentation plan; and
  - Reference to the safety plan for a safe execution of the load test.
- With regard to the execution of the proof load test
  - Date and time of test;
  - Names and affiliations of persons conducting or observing the test;
  - Measured loading protocol;
  - Observations during the load test;
  - Any unusual site conditions or discrepancies between as-built plans and actual site conditions; and
  - Pertinent environmental information such as temperatures, humidity, etc.
- With regard to the analysis of the proof load test
  - Review of the measurements:
    - Discussion on data quality,
    - Notable observed behavior (e.g., load-displacement diagram, deformation profiles in longitudinal and transverse direction, strains as a function of time and load position), and
    - Any other conclusions based on the computations from measurements (maximum stresses, forces or moments, location of member neutral axis, etc.);
  - Comparison of stop criteria to measured structural responses;
  - Comparison between analytical model results used for the preparation of the test or initial rating and field measurements; and
  - Development of field-verified model, if requested by the owner.
- With regard to recommendations for bridge load rating, weight posting, and maintenance
  - Comparison between total load applied and target proof load;
  - Rating assumptions: assumptions on rating procedure and factors, summary of member capacities used for rating, and considered rating loads and configurations;
  - Rating based on the proof load test result; and
  - Recommendations for maintenance based on the results, if any.

CHAPTER 6

Estimating the Reliability Index and Remaining Service Life

DAN M. FRANGOPOL
DAVID Y. YANG
Lehigh University, ATLSS Research Center

DAVID KOSNIK
CTL Group

EVA O. L. LANTSOGHT
Universidad San Francisco de Quito and Delft University of Technology

INTRODUCTION

Uncertainty in applied loads and various aspects of a structure's ability to resist those loads plays an important role in the study of bridge performance in general and load tests in particular. Therefore, probabilistic approaches based on reliability, statistics of extremes, availability, and damage detection delay should be used (*9*). In this chapter, a brief overview of the state of the art related to determining the probability of failure of a bridge structure (before, during, and after a load test), the remaining service life, and finding the system reliability is given. Possibilities for future inclusion of information from a load test are indicated where direct derivations are not available. These principles are also linked to optimal scheduling of maintenance, repair, rehabilitation, inspection, and load testing activities to minimize bridge life-cycle cost.

Over time, bridge performance can degrade as the result of structural aging, aggressive environmental stressors, and loading conditions under uncertainty. The main degradation mechanisms in concrete and steel bridges are corrosion and fatigue. The effect of deterioration is an increase in the probability of failure of the considered structural element or structure, and thus a reduction of the structural safety over time. This effect is discussed in this chapter and linked to the updated reliability index after a load test.

When probabilistic methods are used, the uncertainties on the knowledge with regard to the capacity, the reduction of the capacity over time, and the occurring loads have to be described. These uncertainties can be aleatoric (caused by the inherent randomness of a process) or epistemic (caused by imperfect knowledge). Load testing can reduce the epistemic uncertainties on the performance of a bridge and can contribute to a quantification of the uncertainties through probabilistic concepts and methods.

UPDATING THE RELIABILITY INDEX AFTER PROOF LOAD TEST

Uncertainties in structural behavior may be considered in terms of density distribution functions (also called PDFs) of the resistance R and the loading S. Recommended formulations for these PDFs for various resistance models, load types, and analyzed load effects are given in the Joint

Committee on Structural Safety (JCSS) Probabilistic Model Code (*137*). Once the PDFs of the resistance *R* and the loading *S* are defined, the limit state function can be described.

For most structures, the limit state function is $g = R - S$. Failure occurs when $g < 0$, and can be expressed as P_f, the probability of failure. The reliability index, β, which is the measure of structural safety used in most design codes, is determined as

$$\beta = \Phi^{-1}\left(1 - P_f\right) \tag{6.1}$$

where the function Φ^{-1} is the inverse normal distribution. For the case of incipient failure (i.e., $g = R - S = 0$), and when *R* and *S* are uncorrelated, the probability of failure P_f can be determined (*90*) based on the functions shown in Figure 6-1.

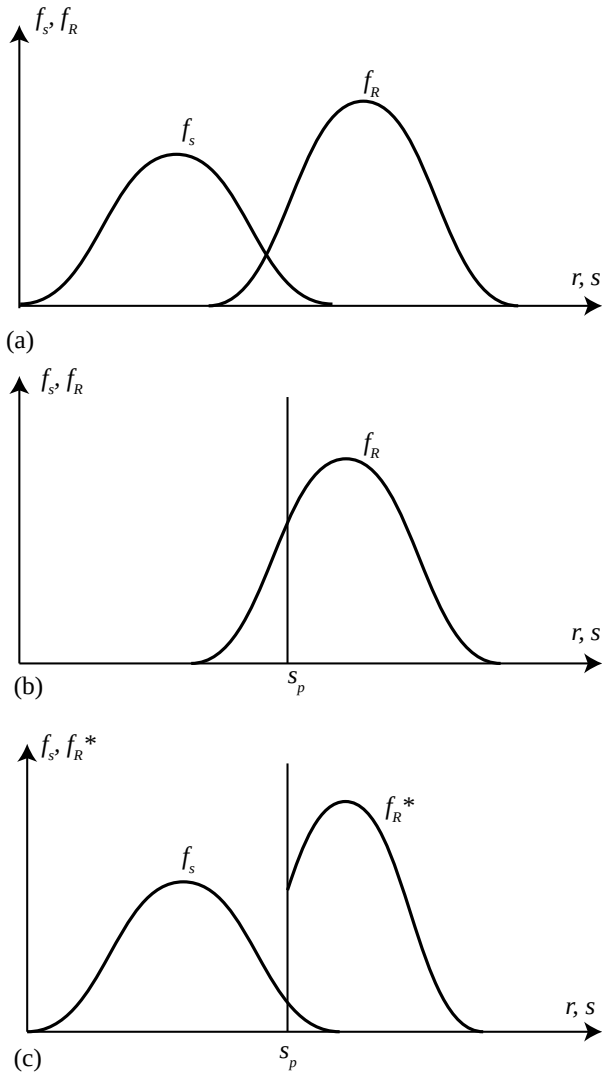

FIGURE 6-1 Determination of the probability of failure before, during, and after the proof load test (*90, 138*).

The probability of failure based on information available prior to a proof load test is given by the standard solution of the convolution integral (*138*):

$$P_{fb} = \int_{-\infty}^{+\infty} \left(1 - F_s\left(r\right)\right) f_R\left(r\right) dr \tag{6.2}$$

where $F_s(r)$ is the cumulative distribution function (CDF) of the loading S, and $f_R(r)$ is the PDF of the resistance R.

During a proof load test, the random variable of the loading is replaced by the deterministic value of the applied load in the test, s_p. As a result, the probability of failure during the test is described solely by the CDF of the resistance F_R,

$$P_{fd} = F_R\left(s_p\right) \tag{6.3}$$

rather than the convolution integral from Equation 6.2. If the bridge withstands the proof load without significant problems, the convolution integral from Equation 6.2 can be updated to reflect knowledge gained during the load test—specifically, that the resistance R is equal to or greater than the load effect caused by the applied load s_p. The updated convolution integral can be expressed as follows:

$$P_{fa} = \frac{1}{1 - F_R\left(s_p\right)} \int_{s_p}^{+\infty} \left(1 - F_s\left(r\right)\right) f_R\left(r\right) dr \tag{6.4}$$

When the load and resistance functions follow a normal distribution, the solution of the reliability index can be expressed more simply. The expression of the reliability index before the test, as a solution of the convolution integral from Equation 6.2, then becomes:

$$\beta_b = \frac{m_R - m_S}{\sqrt{\sigma_R^2 + \sigma_S^2}} \tag{6.5}$$

where m_R is the average resistance, m_s is the average loading effect, σ_R the standard deviation of the resistance, and σ_s the standard deviation of the loading effect.

During the proof load test, the applied load is the deterministic value s_p, so that the reliability index can be expressed as:

$$\beta_d = \frac{m_R - s_p}{\sigma_R} \tag{6.6}$$

A solution for the reliability index after the load test exists, and was derived (*138*) as:

$$\beta_a = -\Phi^{-1}\left(\frac{1}{1-\Phi\left(\frac{s_p - m_R}{\sigma_R}\right)} \times \int_{s_p}^{+\infty}\left(1-\Phi\left(\frac{r-m_s}{\sigma_s}\right)\right)\frac{1}{\sigma_R}\phi\left(\frac{r-m_R}{\sigma_R}\right)dr\right) \tag{6.7}$$

where ϕ is the PDF of the normal distribution and Φ the associated CDF.

The aforementioned procedure for updating reliability indices after load tests can also be used to evaluate the cost-effectiveness of proof load tests. Ideally, it is desired that the load level in a proof load test be as high as possible as long as the tested bridge does not show irreversible distress. As shown in Figures 6-1*b* and *c*, as the test load level increases, the failure probability in a load test increases accordingly while the updated failure probability after the test decreases (given no failure in the test). In other words, survival under a higher test load contains more valuable information but poses higher failure risk. The benefit and risk associated with a load test can be determined using the concept of value of information VoI (*139*) and the reliability updating procedure mentioned above. Specifically, the benefit of a test is represented by its VoI defined as follows:

$$VoI = C_F \cdot [\Phi(-\beta_b) - \Phi(-\beta_a)] \tag{6.8}$$

where C_F is the expected failure cost of the tested bridge. On the other hand, the total cost of a load test, considering the failure risk during the test, can be expressed as

$$C_{PLT} = C_{test} + C_F \cdot \Phi(-\beta_d) \tag{6.9}$$

where C_{PLT} and C_{test} are the total cost and test cost itself, respectively. Both VoI and C_{PLT} increase due to a higher test load level. Nevertheless, the ratio of VoI to C_{PLT} is the benefit-cost ratio of a certain load test procedure. This ratio can be maximized to determine the most cost-effective target proof load level. By the same token, the VoI and C_{PLT} can also be evaluated during a proof load test for its incremental loading steps so that more rational stop criteria can be selected. For real-time updating and VoI evaluation, an advanced decision-making model can be applied (*140*). The previous discussion can be extended to the life-cycle context of a bridge considering future live load magnitude and structural deterioration.

The PDFs of *R* and *S* before, during, and after load testing were shown in Figure 6-1. During the load test, the PDF of *S* is replaced by the deterministic value of the applied load, as illustrated in Figure 6-1*b*. After the load test, the PDF of *R* is updated; it is now known that the resistance is equal to or greater than the applied load s_p. Thus, the PDF of *R* – that is, f_R^* – may be updated, as was shown in Figure 6-1*c*.

The magnitude of the load before, during, and after the load test is shown in Figure 6-2*a*. This plot indicates that higher loads need to be used during the load test than the characteristic loads from the considered live load model. This plot also indicates that loads can increase over time. The effect on the reliability index is given in Figure 6-2*b* and *c*. If the target load is applied and the load test is successful, the outcome is a higher reliability index after the load test. If, however, the load test is not successful—that is, typically, the full target load could not be applied because nonlinearity in the structural responses was observed—then the outcome of the test may be a decreased reliability index. Note that, because of the high loads during the load test, the value

of the reliability index during the load test β_d is low. Finally, Figure 6-2*d* and 6-2*e* indicate the effect of decreasing resistance over time (i.e., due to time-dependent deterioration mechanisms such as corrosion) on the reliability index (*141*). Again, two different scenarios are presented. In Figure 6-2*d* the case of a successful load test is shown, which results in a higher reliability index β_a after the load test, whereas Figure 6-2*e* shows a lower reliability index β_a after the load test when the target load could not be reached.

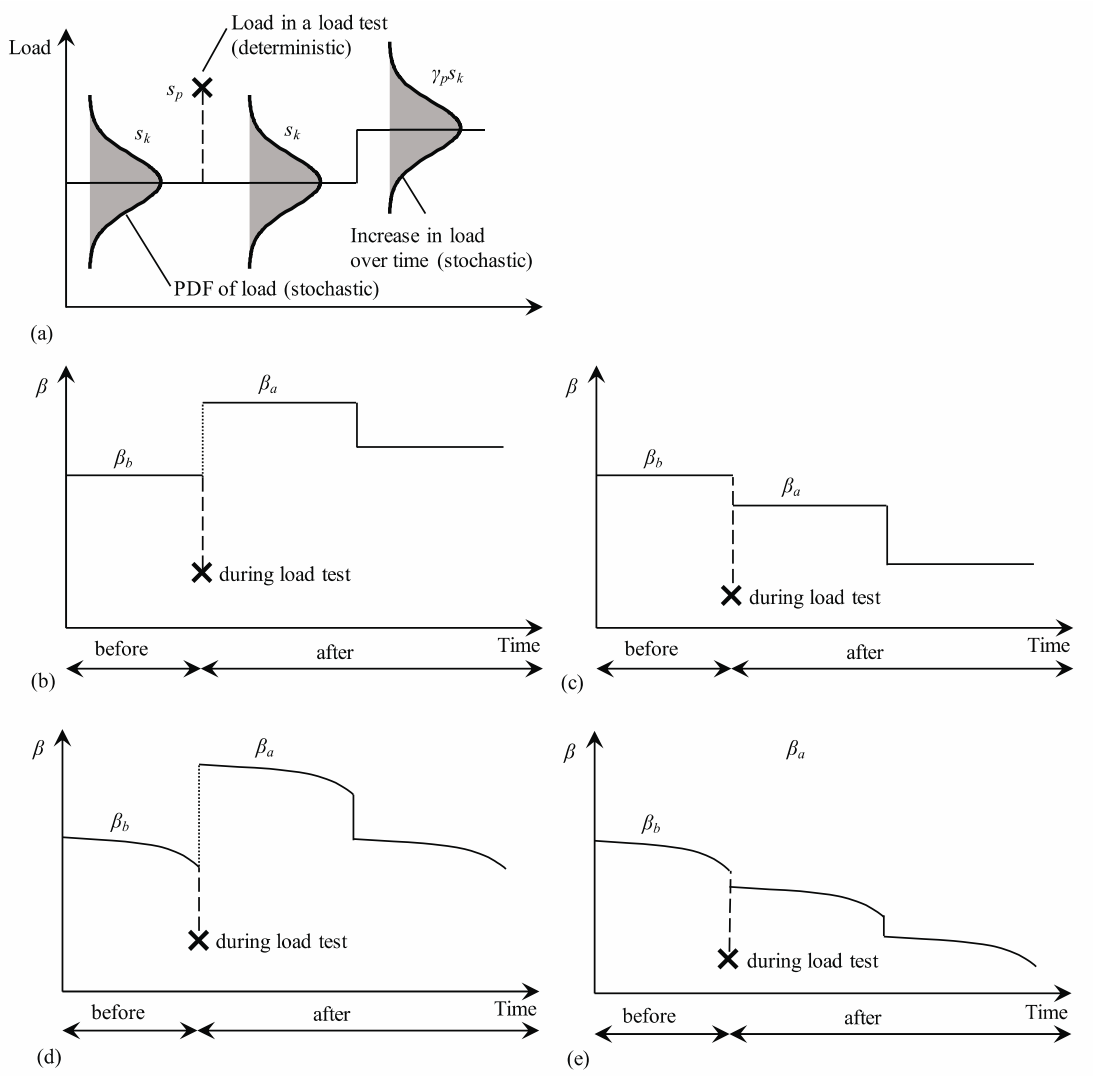

FIGURE 6-2 Change of reliability index before, during, and after load test (*138, 141*): (*a*) value of the load before, during, and after load test; (*b*) effect on reliability index for a load test in which the target load or higher was applied; (*c*) effect on reliability index for a load test in which nonlinear behavior occurred before applying the target load; (*d*) reliability index over time if deterioration is taken into account for the case in which the target load or higher was applied; and (*e*) reliability index over time if deterioration is taken into account for a load test in which nonlinear behavior occurred before applying the target load.

The time-dependent resistance function can be expressed by making the PDF and CDF of *R* a function of time. Additionally, the increase in loading over time can make the function of the loading *S* also time-dependent. The expression for the limit state function then becomes time-dependent (*141*):

$$g(t) = R(t) - \mathrm{S(t)} \tag{6.10}$$

Without intervention, $R(t)$ will decrease with time, due to time-dependent deterioration. $S(t)$ can increase over time to reflect increasing traffic loads. As a result, the probability of failure will increase over time, and the reliability index will decrease over time, as shown in Figure 6-2*c*.

Another approach (*142*) is to consider the reliability index as a function of time. The expression of the reliability index then takes the following form (141):

$$\beta(t) = \beta_0 \text{ for } 0 \le t \le t_{ini} \tag{6.11}$$

$$\beta(t) = \beta_0 - \alpha(t - t_{ini}) \text{ for } t_{ini} \le t \tag{6.12}$$

These equations take into account that, until a point in time denoted t_{ini}, the reliability index is constant—no increase in the loads takes place, and no degradation of the resistance takes place. After t_{ini}, the reliability index decreases. The expression is a function of α, the deterioration rate (1/year). An application can be found in the literature (*143*), where a combination of available maintenance data and reliability analyses was used to estimate the reduction of the reliability index over time. An additional challenge is that the available information of the condition of existing structures depends on the engineer performing the inspections, and thus shows large variability and poor reliability; however, this issue is beyond the scope of this document. Further discussion of the effect of degradation is given in Chapter 6 (Establishing Target Reliability Indices, p. 56).

ESTABLISHING TARGET RELIABILITY INDICES

The target reliability index for an existing structure upon assessment is lower than for a structure that needs to be designed (*144*). The target reliability index for assessment may be influenced by consequences of failure, reference period (time between assessments), remaining service life, relative cost of safety (upgrading) measures, importance of structure, and so on. Lower reliability indices result when the maintenance and repair costs are large, and the consequences of failure are minor. Stewart et al. (*144*) suggest a target reliability index for a 1-year reference period between 3.1 and 4.7. The target reliability index can be based on a code for existing structures, such as prescribed in the Netherlands by the Dutch Ministry of Infrastructure and the Environment for the Assessment of Bridges (RBK) (*145*), or based on the recommendations from Koteš and Vican (*146*), which should be combined with the Eurocodes for existing structures. For this case, a target reliability index was defined for bridges depending on the age of the bridge and the remaining lifetime of the bridges, not considering degradation mechanisms. The target reliability indices were found to be between 2.692 and 3.773. For rating at the operating level, a target reliability index of 2.3 was determined and for rating at the inventory

level a reliability index of 3.5 (*58*). The reliability index of 2.3 is below the lower bound of 2.5 for life safety (*147*).

Another possibility for carrying out a reliability analysis uses the results of a load test indirectly (*148*). In this approach, a diagnostic load test is used to develop a field-verified FEM. The combination of the field test and results from SHM can then be used to obtain a load rating and system reliability of the considered bridge over a long period of time. The reliability analysis is then executed based on the FEM.

DETERMINING THE REMAINING SERVICE LIFE

Determining the remaining service life of structures is related to the fact that structural deterioration increases the probability of failure over time, and thus decreases the reliability index over time, as was shown in Figure 6-2*d* and 6-2*e*. The design period and remaining service life of the structure can be estimated based on the associated reference period of the load factors for which the evaluation is carried out. When LRFR is used (*57*), three levels are considered. The design load rating level produces ratings at the inventory and operating rating level for the HL-93 live load. If the evaluation is carried out at the inventory load rating level, the associated reliability index is $\beta = 3.5$ with a reference period of 75 years. If the evaluation is carried out at the operating load rating level, the associated reliability index is $\beta = 2.5$ with a reference period of 75 years (*149*). If the evaluation is carried out at the legal load rating level, only a single safe load capacity is determined. The associated reliability index is $\beta_{minimum} = 2.5$ with a reference period of 2 to 5 years. For overload permits, the load factors are calibrated to a reliability index of $\beta = 2.5$ for routine or annual permits, and to $\beta = 3.5$ for special permits with a reference period of 2 to 5 years (*149*).

For concrete bridges, the main effect of service life reduction is corrosion of reinforcing steel. It has been found that under the same corrosion rate, the loss of reliability can be associated with flexural (*150*) and shear (*151*) failures as well as with the serviceability requirements (*152*). Spatial variation in the material properties of concrete and the ingress of corrosion-inducing chloride ions further complicate analysis. For example, chloride attack can be from three faces (bottom and both sides) when traffic spray is considered, or from only two sides (bottom and exposed face) when runoff is considered (*153*). Additionally, chloride attack can be uniform as a result of carbonation, or localized as a result of pitting corrosion (*154*). Variables such of these may be incorporated into models for the distribution of the failure modes, providing a probabilistic method to identify cost-effective repair approaches (*155*). To best estimate the capacity of the structure under corrosion attack, the use of nonlinear FEMs becomes necessary (*156*). A different approach would be to model the lifetime of concrete bridges as a random variable with a Weibull distribution. This distribution was fitted to complete lifetimes of demolished bridges and current ages of existing bridges (*157*).

For steel bridges, the main deterioration mechanism is fatigue and fracture, responsible for 80% to 90% of the premature removal of steel structures from service (*158*). Fatigue-prone details in existing bridges can reduce the estimated lifetime of the structure (*158*), which can be shorter than determined based on classically used models (*159*).

Inspection results can be used to update estimates of the remaining service life by improving the calibration of the probabilistic degradation model (*160*). Failure probability is then determined based on conditional probabilities (Bayesian analysis) (*159, 161*). The idea of

updating the effect of degradation after inspections can also be applied to load testing. The information from a load test can be used to update the estimate of the remaining service life. Inspiration can be taken from the practice of updating the estimated service life based on data from SHM (*162*). However, it must be noted that, because of the limited data available about the probabilistic effects on the performance indicators of interventions on the bridge structure, the incorporation of data from SHM is still a topic of research (*163*).

In European practice (*19*), the remaining service life after a proof load test is based on the load factors used to determine the target proof load. For example, according to NEN 8700:2011 (*164*), applied as well into the guidelines from RBK (*165*), load factors for assessment at different safety levels is described. When the load factors calibrated for a safety level with a reliability index $\beta = 3.3$ and a reference period of 30 years are used for determining the target proof load, then the conclusion from the proof load test is that the remaining service life is 30 years. This approach, however, does not account for time-dependent deterioration mechanisms, nor does it consider when the serviceability limits will be exceeded.

After a load test, the reliability-based analysis of the load test can be used to evaluate the safety of the bridge. With the information that a bridge has carried a certain load without any sign of distress, it can be concluded that the capacity of the bridge is equal to or larger than the applied load. This information is then used to update the PDF of the resistance R, and in turn the updated reliability index after the load test, β_a, can be calculated, as outlined in the previous sections. In order to follow this procedure, relatively high loads are necessary; thus, this procedure is typically conducted in concert with proof load tests.

A case study (*166*) showed that load rating is a reasonable approach to determining the strength and allowable load on a bridge. However, as load rating is a deterministic procedure (i.e., it is unable to account for both aleatoric or statistical, and epistemic or systematic uncertainties) intended for analysis of individual members, no information about the redundancy or robustness of a structure is provided, and correlation between failure modes is not considered. A system reliability analysis is required to account for these factors (*148*, *167–173*). This topic is discussed in Chapter 6: Linking Component Probability of Failure to System Probability of Failure (p. 58).

In a full analysis to determine the optimum times of carrying out a load test, a combination of the expected total life-cycle cost with the optimum times for all interventions (inspection, monitoring, load testing, maintenance, repair, etc.) must be developed. Integration of monitoring results into such a performance-based analysis is available (*174*), and can be taken as a starting point for the integration of load testing into a similar life-cycle cost analysis. This topic is further discussed in Chapter 6: Optimizing Life-Cycle Intervention Actions (p. 59).

LINKING COMPONENT PROBABILITY OF FAILURE TO SYSTEM PROBABILITY OF FAILURE

Updates to a reliability index following a load test are typically made on an individual component basis; for example, by comparing the sectional moment and the moment capacity of a given member. The next step is to determine the probability of failure at the system level (i.e., at the level of the entire bridge structure). Structural reliability theory offers a rational framework for quantification of system performance by including the uncertainties both in the resistance and the load effects and correlations (*107*). For an evaluation of the system, the failure domain under

specific loading conditions is considered. The bridge system can be modeled by considering the bridge system failure as series or parallel, or a series-parallel combination of bridge component limit states (*173*). The failure domain, *FD*, represents the violation of the system limit state, expressed in terms of component limit states:

$$FD \equiv \cup\left\{ g_k\left(X\right) < 0 \right\} \text{ for } k = 1:n \text{ for a series system} \tag{6.13}$$

$$FD \equiv \cap\left\{ g_k\left(X\right) < 0 \right\} \text{ for } k = 1:n \text{ for a parallel system} \tag{6.14}$$

$$FD \equiv \cup\cap\left\{ g_{k,j}\left(X\right) < 0 \right\} \text{ for } k = 1:n \text{ and } j = 1:c_m \text{ for a series-parallel system} \tag{6.15}$$

In Equation 6.15, c_m is the number of components in the *n*th cut set. Examples are available in which all bridge components (e.g., deck, girders, and piers) and all possible failure modes (e.g., flexure, shear, buckling, and fatigue) are considered (*141*). However, the extension of these approaches to include the results of load tests is still under development.

OPTIMIZING LIFE-CYCLE INTERVENTION ACTIONS

In the broader scope of bridge management, it is important to schedule intervention actions such as inspections, load tests, maintenance, and repairs in order to minimize life-cycle cost and maximize life-cycle performance (*141*).

As introduced in Chapter 2: Benefit–Cost Analysis of Using Load Testing (p. 15), the total life-cycle cost of a bridge includes the initial cost, the inspection, maintenance and repair costs, cost of load testing, salvage value (if recycle or reuse is considered), and the expected cost associated with structural failure (*108*). The last cost item, also known as life-cycle failure risk, should include both direct cost to bridge owners–managers and indirect cost incurred to society (*175*). The direct cost is induced by activities associated with system failure such as dismantling, cleaning, and rebuilding (*176*). The indirect cost is attributed to the extra travel time and extra travel distance of traffic users due to bridge failure as well as potential losses to business due to reduced accessibility. It should be noted that assessment of indirect cost may require analyses at a regional, road-network level (*177*) and may also contain considerable uncertainties.

Life-cycle performance of a bridge can be quantified by reliability-based indicators such as time–variant reliability index, redundancy and robustness, cumulative–annual failure risk, expected service life under reliability–risk thresholds, and lifetime resilience among others (*178–181*). The life-cycle performance can be described by a function of time in service obtained based on various deterioration models (*182*). Due to the aleatoric and epistemic uncertainties involved in the life-cycle analysis (*183*), failure probability and the associated reliability index may also be a random variable instead of a deterministic value (*142*).

The ideal times and types for inspection–SHM, maintenance, load tests, and repair can be determined by carrying out single- or multi-objective optimization (*163, 184*). Usually, different objectives of intervention planning may compete with one another (i.e., minimization of maintenance cost and maximization of reliability). Therefore, Pareto dominance can be employed to obtain a set of optimal compromises between two or more conflicting objectives

(*185*). This set of solutions, usually referred to as a Pareto front, can provide useful information to bridge owners/managers.

In the context of load tests, it is necessary to devise optimal load testing plans (e.g., time, type, and proof–diagnostic loads) so that (*a*) the total life-cycle cost can be minimized and (*b*) the life-cycle performance (e.g., expected service life) can be maximized. For this purpose, existing methods for inspection–SHM planning as mentioned above can be extended to account for load tests. Similar to inspection, load tests can provide updated information regarding structural capacities, either positive (stiffer reaction of the structure, better load redistribution, or other findings such that the load rating increases), or negative (the load rating decreases). Unlike inspection–SHM in which structural capacities are not affected by these actions, a load test might exert detrimental impact upon structural capacities (i.e., when nonlinear response is present during the test). Therefore, a combination of all these scenarios (*186*) needs to be studied using pre-posterior analysis (*187*). It must be noted that the final results (the optimal load test plans) depends strongly on the quality of the input data for the probabilistic analysis.

CHAPTER 7

Illustrative Examples

SREENIVAS ALAMPALLI
New York State Department of Transportation

JESSE GRIMSON
BDI Bridge Diagnostics, Inc.

DAVID KOSNIK
CTL Group

EVA O.L. LANTSOGHT
Universidad San Francisco de Quito and Delft University of Technology

Y. EDWARD ZHOU
AECOM

EXAMPLE OF A DIAGNOSTIC LOAD TEST

This case study presents a typical diagnostic load test on a rural one-lane structure. The structure, shown in Figure 7-1, is located in Yavapai County, Arizona, and was tested in February 2012. A previous load rating calculation had indicated that the bridge's load rating was below acceptable limits. A diagnostic load test was conducted to provide in-situ performance information to corroborate, or refine the previous calculations.

FIGURE 7-1 Diagnostic load test on rural one-lane concrete slab bridge.

The bridge is a four-span, cast-in-place RC slab structure with a slab thickness of 19 in. (483 mm). The overall width was approximately 16.17 ft (4.93 m) while the roadway width measured 14 ft (4.27 m). The bridge length is approximately 114 ft (34.7 m) overall. Relevant geometric details were verified during the field visit.

As the primary focus of the diagnostic load test was to determine the load rating for the superstructure, the instrumentation plans focused on superstructure load distribution. The structure was instrumented with 36 reusable surface-mount strain transducers, six cantilevered displacement sensors (Figure 7-2), and six surface-mounted rotation sensors (Figure 7-3). Only minor surface preparation was required to temporarily attach all sensors using a quick setting cyanoacrylate adhesive (Loctite 410 + Loctite 7452). Plan and section views of the instrumentation scheme are shown in Figure 7-4 and Figure 7-5, respectively. All instrumentation was removed after the load testing operations were completed.

Once the instrumentation was installed, a series of diagnostic load tests were completed with the truck traveling across the structure at crawl speed (3 to 5 mph/5 to 8 km/h). During testing, data was recorded on all channels at a sample rate of 40 Hz as the test vehicle (3-axle dump truck) crossed the structure in the westbound direction along three different lateral positions, referred to as Paths Y1, Y2, and Y3 (Figure 7-6). The truck's longitudinal position was also recorded with the sensor data so that the sensor data could then be viewed as both a function of time and vehicle position.

Information specific to the load tests can be found in Table 7-1. The test vehicle's gross weight, axle weights, and wheel rollout distance (required for tracking its position along the structure) are provided in Table 7-2. A vehicle "footprint" is also shown in Figure 7-7. The vehicle weights were obtained from certified scales at a local gravel pit, and all vehicle dimensions were measured in the field at the time of testing.

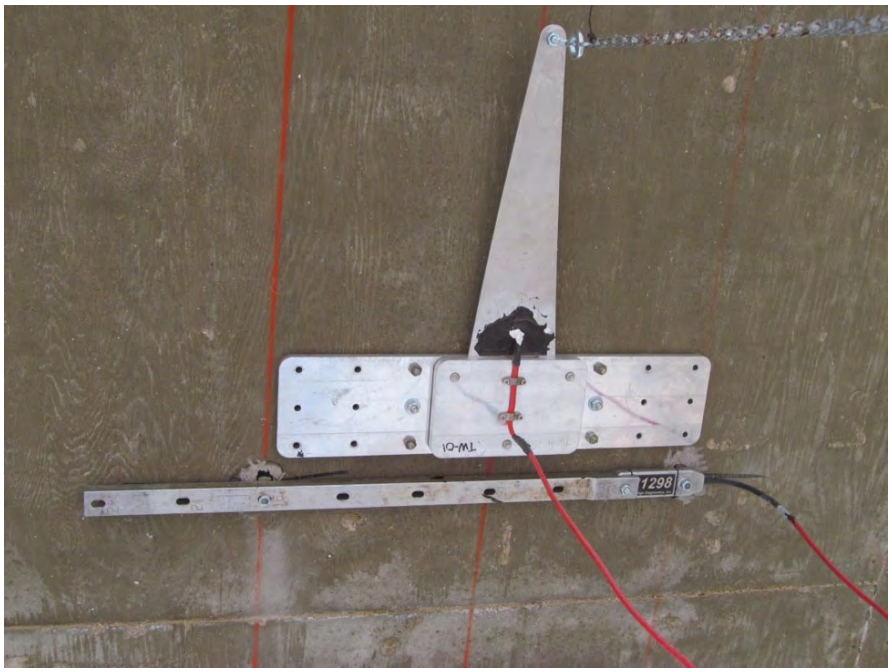

FIGURE 7-2 Surface-mounted strain transducer and cantilever displacement sensor.

FIGURE 7-3 Surface-mounted strain transducer and surface mount tiltmeter.

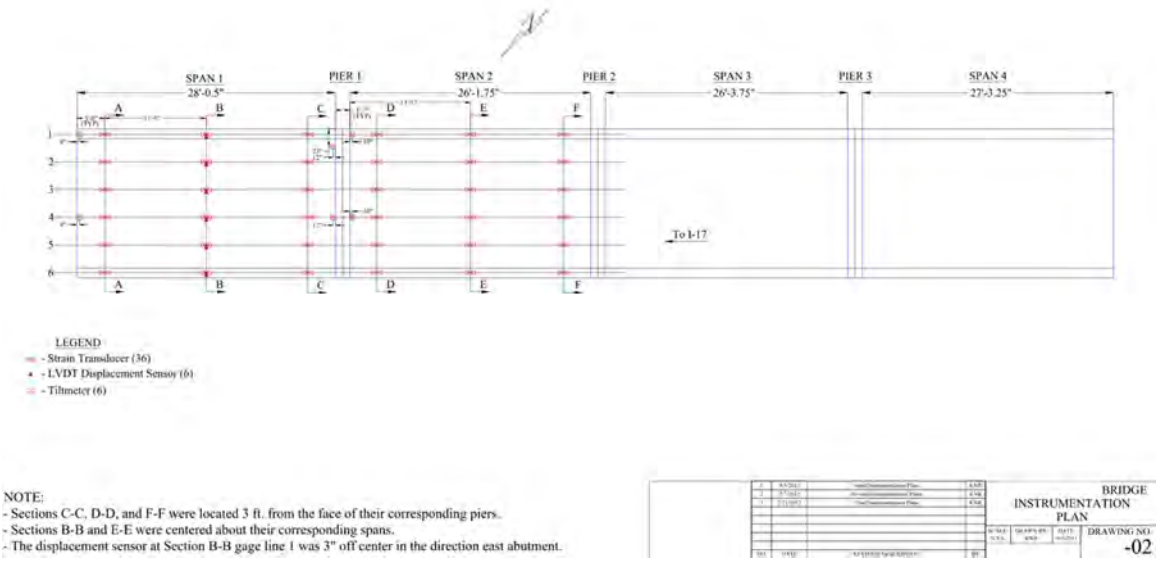

FIGURE 7-4 Instrumentation plan view.

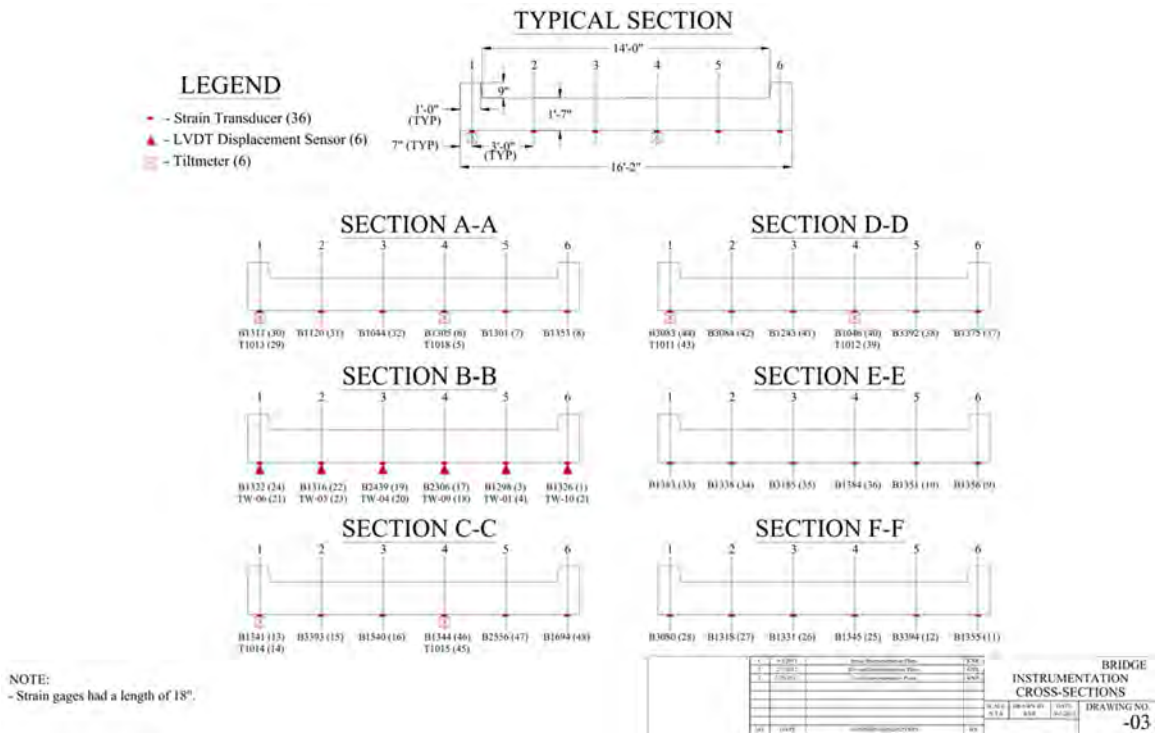

FIGURE 7-5 Instrumentation cross-section view.

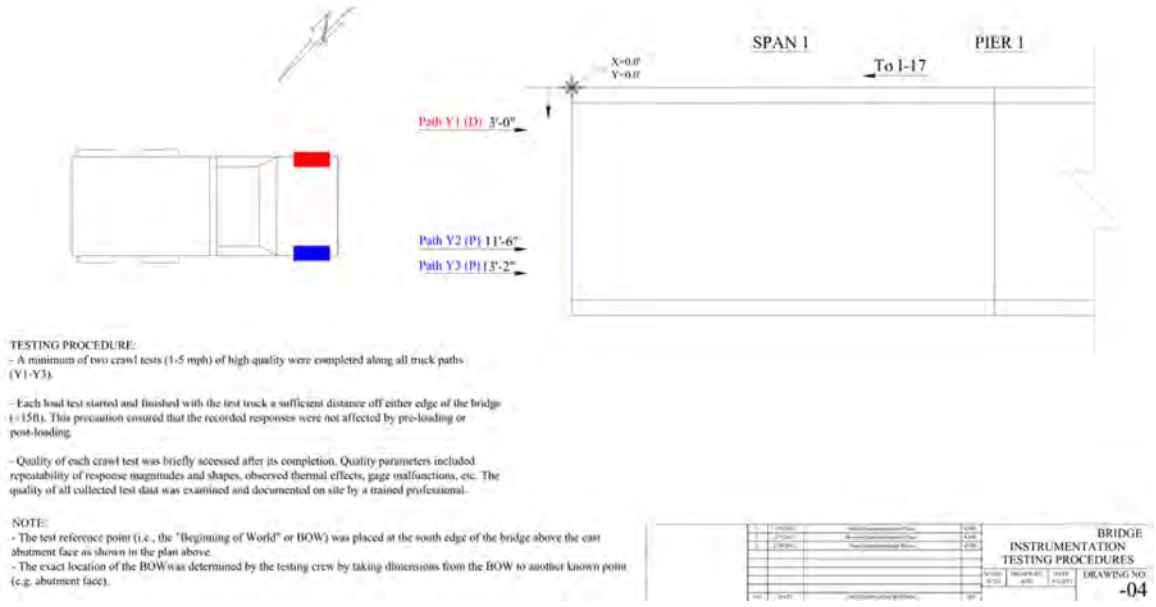

FIGURE 7-6 Load testing paths

TABLE 7-1 Load Testing Information

Item	Description
Testing date	February 15, 2012
Structure type	RC slab bridge
Total number of spans	4
Span lengths	Span 1: 28 ft, 1 in. (8.56 m) (clear span) 29 ft, 7 in. (9.02 m) (effective span used for rating) Span 2: 26 ft, 2 in. (7.98 m) (clear span) 27 ft, 9 in. (8.46 m) (effective span used for rating) Span 3: 26 ft, 4 in. (7.82 m) (clear span) 27 ft, 11 in. (8.51 m) (effective span used for rating) Span 4: 27 ft, 3 in. (8.31 m) (clear span) 28 ft, 10 in. (8.79 m) (effective span used for rating)
Skew	NA
Structure/roadway widths	Structure: 16 ft, 2 in. (4.93 m)/Roadway: 14 ft, 0 in. (4.27 m)
Wearing surface	NA
Other structure info	NA
Spans tested	2
Test reference location (BOW) ($X = 0$, $Y = 0$)	Southeast corner of the structure along the outside edge of the curb
Test vehicle direction	Westbound
Test beginning point	Front axle 15 ft (4.6 m) west of test reference location (BOW)
Number/type of sensors	• 36 strain transducers • 6 cantilevered displacement sensors • 6 tiltmeter rotation sensors
Sample rate	40 Hz
Number of test vehicles	1
Structure access type	Scaffolding/ladders
Total field testing time	1 day

NOTE: NA = not available.

TABLE 7-2 Test Vehicle Information

Vehicle Type	Tandem Rear Axle Dump Truck	
GVW	51,660 lbs (23,433 kg)	
Weight/width, axle 1: front	17,070 lbs (7,743 kg)	6 ft, 9 in. (2.06 m)
Weight/width, axle 3: rear tandem pair	34,590 lbs (15,690 kg)	7 ft, 2 in. (2.18 m)
Spacing: axle 1 – axle 2	15 ft, 2 in. (4.62 m)	
Spacing: axle 2 – axle 3	4 ft, 9 in. (1.45 m)	
Weights provided by	Yavapai County	
Wheel rollout distance	11 ft, 3.6 in. (3.44 m) per wheel revolution	

NOTE: GVW = gross vehicle weight.

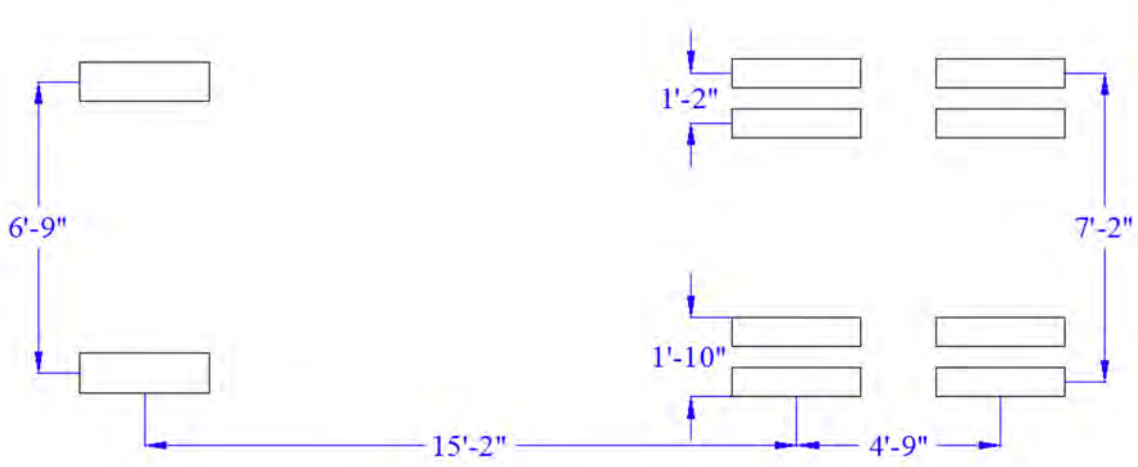

FIGURE 7-7 Load testing vehicle dimensions (conversion: 1 ft = 0.30 m, 1 in. = 25.4 mm).

After completing the field data collection phase of the project, the data is typically examined graphically to provide an initial qualitative assessment of the structure's live-load response. Some indicators of data quality include reproducibility between tests along identical truck paths, elastic behavior (i.e., sensor outputs returning to zero after truck crossing), and any unusually shaped responses that might indicate nonlinear behavior or possible gage malfunctions. This process can provide a significant amount of insight into how a structure responds to live load and is often extremely helpful in performing an efficient and accurate structural analysis. This is where it is important to know the vehicle position on the structure since viewing data as a function of position not only allows for a more meaningful graphical assessment but is also a key component in comparing analytical results to the load test results.

The following are typical items that should be reviewed to ensure all sensor data can be used in the analytical phase.

- **Reproducibility and Linearity of Responses.** The sensor responses from tests along identical paths should very reproducible as shown in Figure 7-8. Sensor responses should be linear with respect to magnitude and test vehicle position and sensor responses should return to essentially zero.
- **Thermal Drift.** Generally, temperature drift is not a concern for short duration load tests because the magnitude of the drift is very small compared to the live load responses. Depending on the type of sensor and duration of the load test, thermal drift may be present in the data and should be addressed by applying an appropriate filter (such as linear drift offset) to correct the data.
- **Lateral Load Distribution.** When evaluating a slab bridge for the purpose of developing a load rating, the bridge's ability to laterally distribute load is an essential characteristic to quantify. Lateral distribution is most easily observed by plotting the responses from an entire lateral cross-section, as done in Figure 7-9. Specifically, Figure 7-9 displays the midspan displacements from all three truck paths. The response values shown in this figure correspond to the longitudinal load positions producing the maximum midspan responses for each truck path. From this figure, it can be observed that the structure exhibited a reasonable level of lateral load distribution across its cross section.

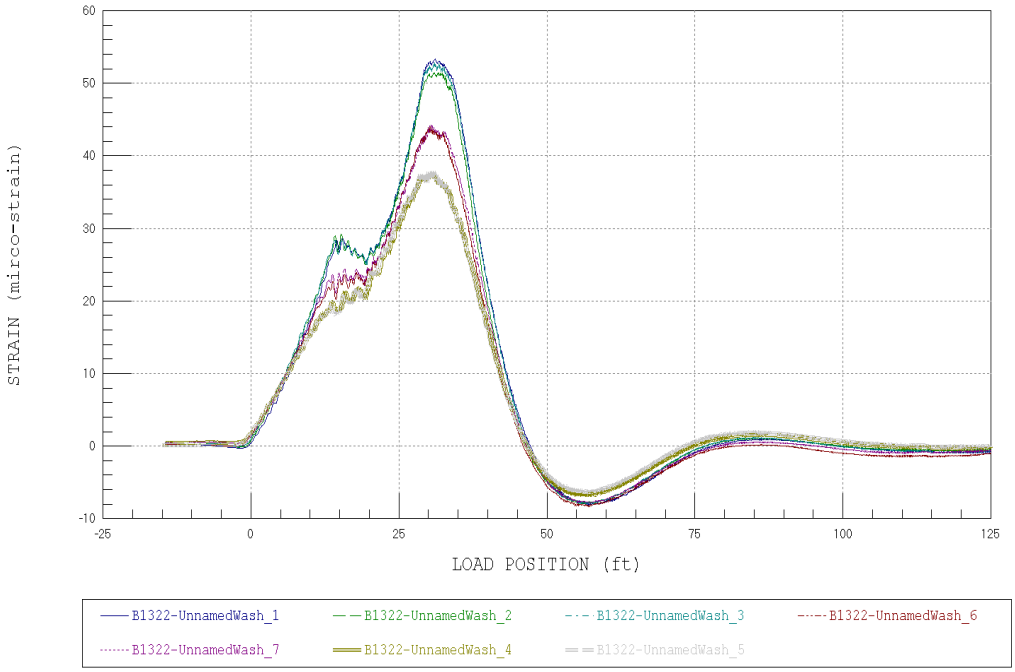

FIGURE 7-8 Example of reproducibility and linearity of strain gage response for three lateral paths.

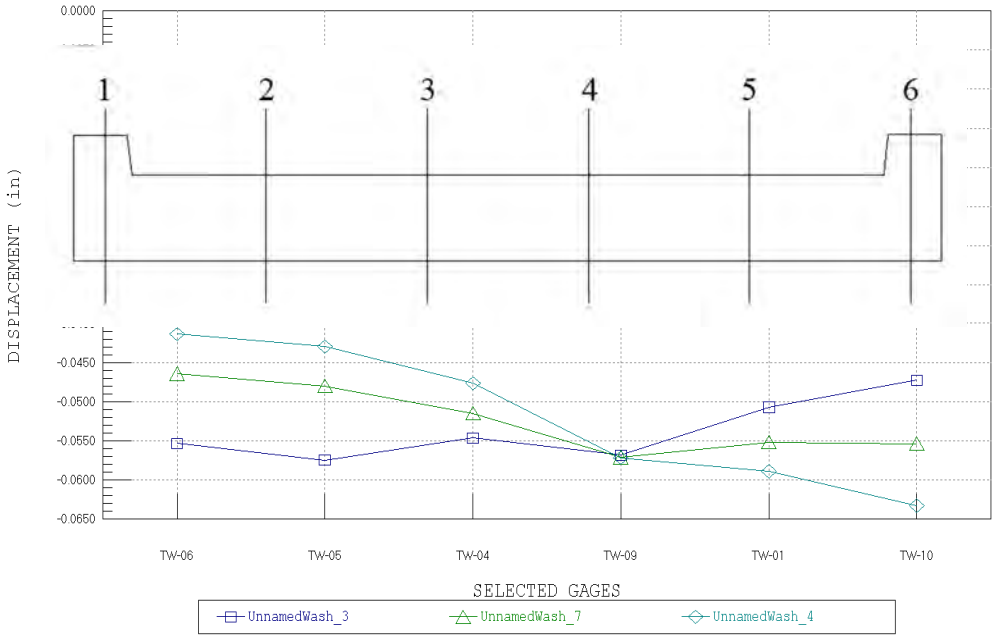

FIGURE 7-9 Lateral load distribution of observed deflection.

After completing this assessment, one data set for each path is selected as the data set that will be used to graphically and analytically compare to a FE analysis of the structure. The key objectives of refining a finite-element bridge model are to accurately simulate the behaviors recorded during load testing, and in turn utilize this model to accurately predict the structure's response under standard design loads or site-specific rating loads.

The 2D FEM geometry was developed based on as-built plans for the structure as well as field verified measurements. Initial model parameters were included based on material properties and section geometry while parameters like end restraint were initially estimated based on the results of the preliminary data assessment. Once the initial model was created, the load test procedures were reproduced within the model. This was done by moving a 2D footprint of the test truck across the model in consecutive load cases that simulated the designated truck paths used in the field (Figure 7-10). The analytical responses of this simulation were then compared to the field responses to validate the model's basic structure and to identify any gross modeling deficiencies.

The model was then refined by adjusting parameters within the model until an acceptable match between the measured and analytical responses was achieved. Specifically, refining consisted of iterative process of optimizing material properties and boundary conditions until they were effectively quantified. In the case of this structure, the majority of the refining effort was spent modeling the slab's effective stiffness in both positive and negative moment regions and the effects of the support conditions at the abutment and the piers. Since this was a continuous structure, faithful reproductions of flexural continuity over the piers was particularly important.

Following the FEM refining process, the final model produced a 0.986 correlation with the measured responses, which can be considered an excellent match for an RC slab structure. The parameters and model accuracy values used in the initial and final bridge models are provided in Table 7-3 and Table 7-4.

A general observation was that the areas of greatest moment (midspan and immediately adjacent to the piers) had greater crack density and therefore lower effective stiffness than the intermediate regions of the structure. This result can be considered typical of RC slabs.

The final FEM was found to closely match the member displacements and tilts, as shown in the comparison plots provided in Figure 7-11 through Figure 7-15. Note that in these comparison plots the measured responses are represented as solid lines while the FEM results are represented as discrete markers.

Upon successfully refining the FEM, load rating was performed on all appropriate bridge elements in accordance with the AASHTO LFR guidelines. Structural responses were obtained from a slightly modified version of the final refined FEM, and member capacities

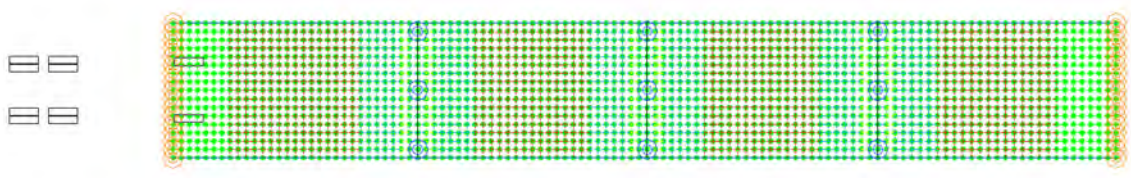

FIGURE 7-10 FEM of superstructure with imposed truck load.

TABLE 7-3 FEM Statistics

Analysis type	Linear-elastic FE–stiffness method
Model geometry	2D composed of shell elements, frame elements, and springs
Nodal locations	Nodes placed at the ends of all frame elements Nodes placed at all four corners of each shell element Nodes placed at all spring locations
Model components	Shell elements representing the slab elements Frame elements representing the curb Springs representing the end-restraint at the abutment walls
Live load	2D footprint of test truck consisting of 10 vertical point loads; truck paths simulated by series of load cases with truck footprint moving at 2.0 ft (0.61 m) increments along a straight path
Dead load	Self-weight of structure
Total number of response comparisons	36 strain gage locations x 204 load positions = 7,344 strain comparisons 6 displacement gage locations x 204 load positions = 1,224 displacement comparisons 6 rotation gage locations x 204 load positions = 1,224 rotation comparisons
Model statistics	1,955 Nodes 2,149 Elements 8 Cross-section–material types 204 Load cases 48 Gage locations
Adjustable parameters	Friction-based rotational resistance: bottom of the slab at piers (F_x) Slab stiffness: midspan slab (E) Slab stiffness: slab near abutments (E) Slab stiffness: slab near piers (E) Slab stiffness: slab adjacent to piers (E)

TABLE 7-4 Initial Versus Final FEM Results

Modeling Parameter: Slab Stiffness	Initial Model Value	Final Model Value
Slab at midspan, E	3,200 ksi (22.06 GPa)	2,600 ksi (17.93 GPa)
Slab near abutments, E	3,200 ksi (22.06 GPa)	3,300 ksi (22.75 GPa)
Slab near piers, E	3,200 ksi (22.06 GPa)	3,300 ksi (22.75 GPa)
Slab directly adjacent to piers, E	3,200 ksi (22.06 GPa)	2,150 ksi (14.82 GPa)
Translational spring resistance at piers, F_x	0	400 kip/in (70.1 kN/mm)
Model Correlation	**Initial Model Value**	**Final Model Value**
Correlation Coefficient	0.9782	0.9856

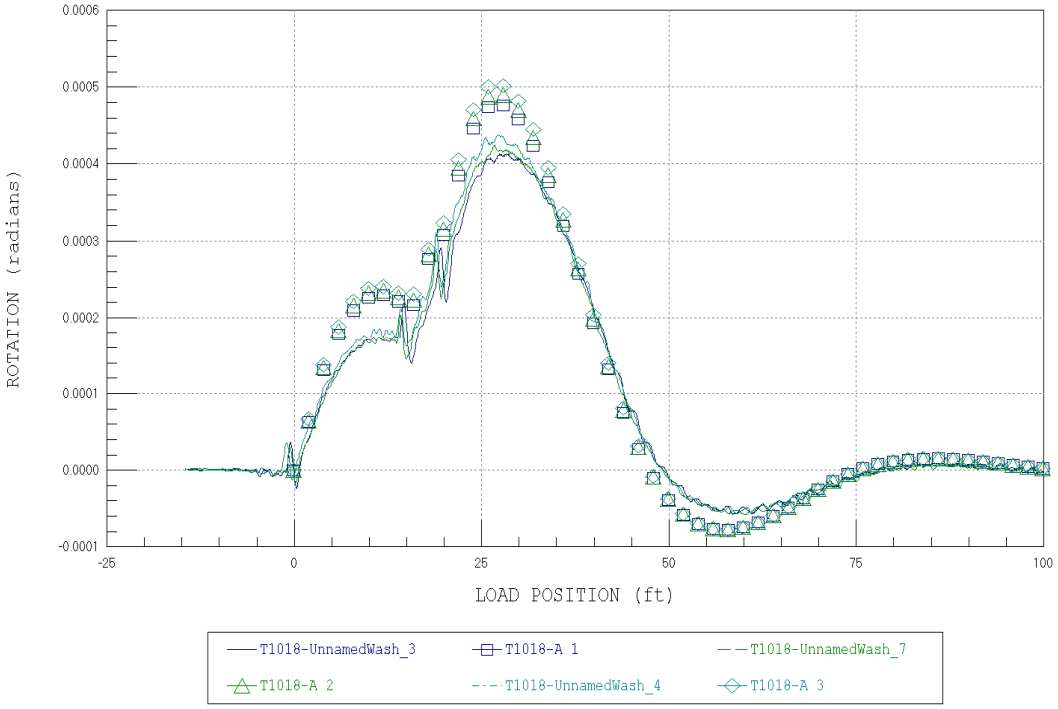

FIGURE 7-11 Comparison of FE rotation versus measured rotation along Section A-A.

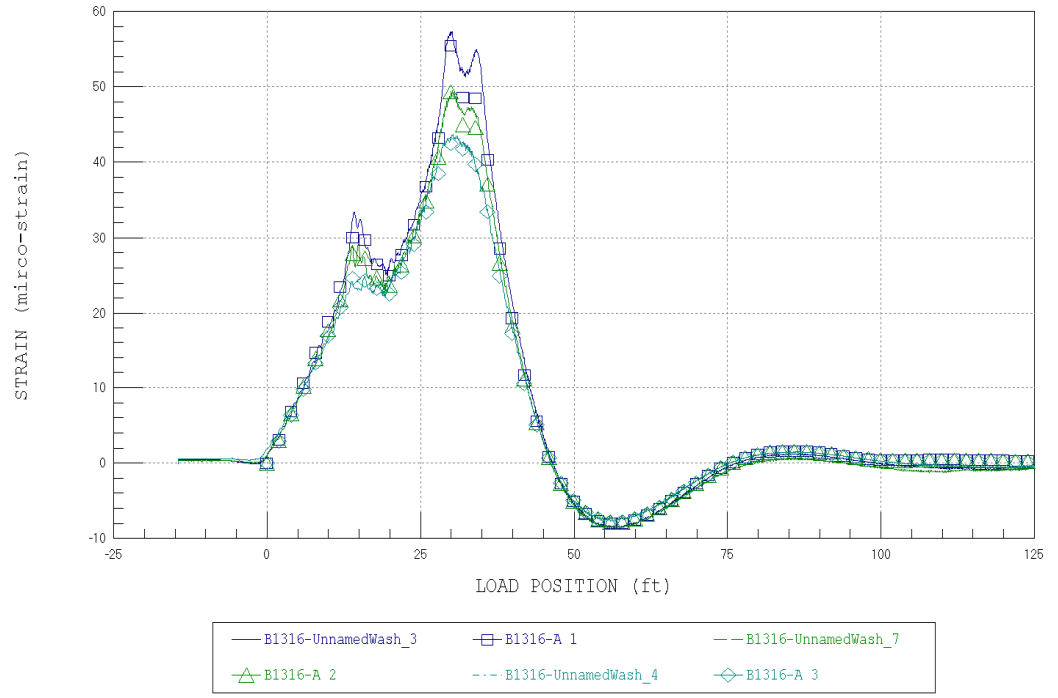

FIGURE 7-12 Comparison of FE strain versus measured strain along Section B-B.

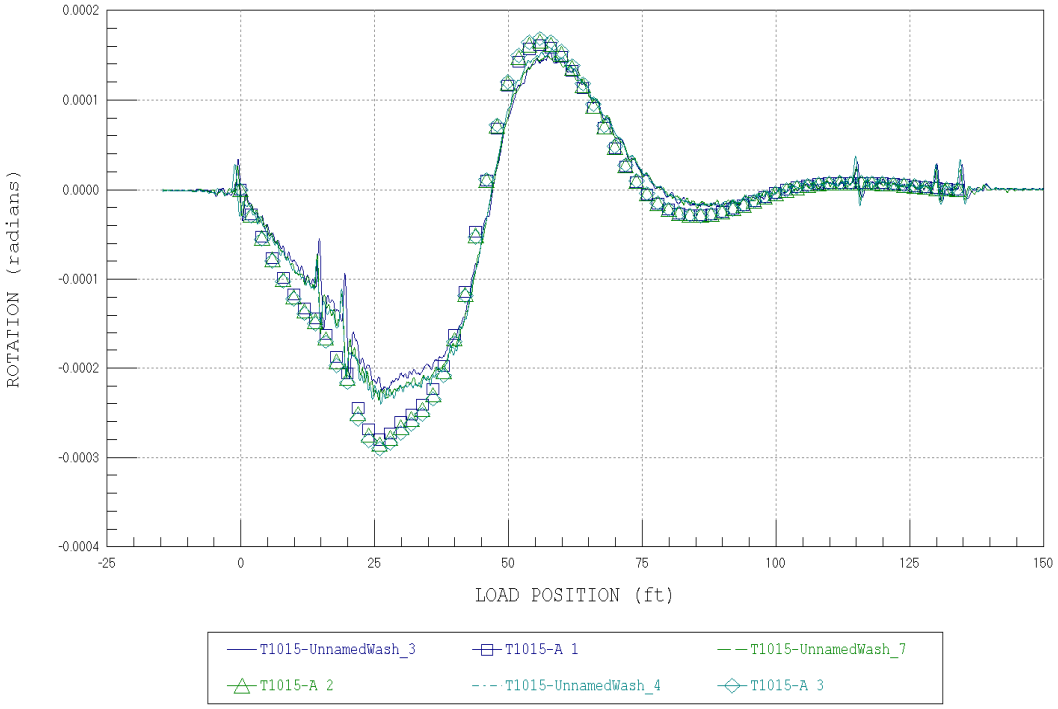

FIGURE 7-13 Comparison of FE rotation versus measured rotation along Section C-C.

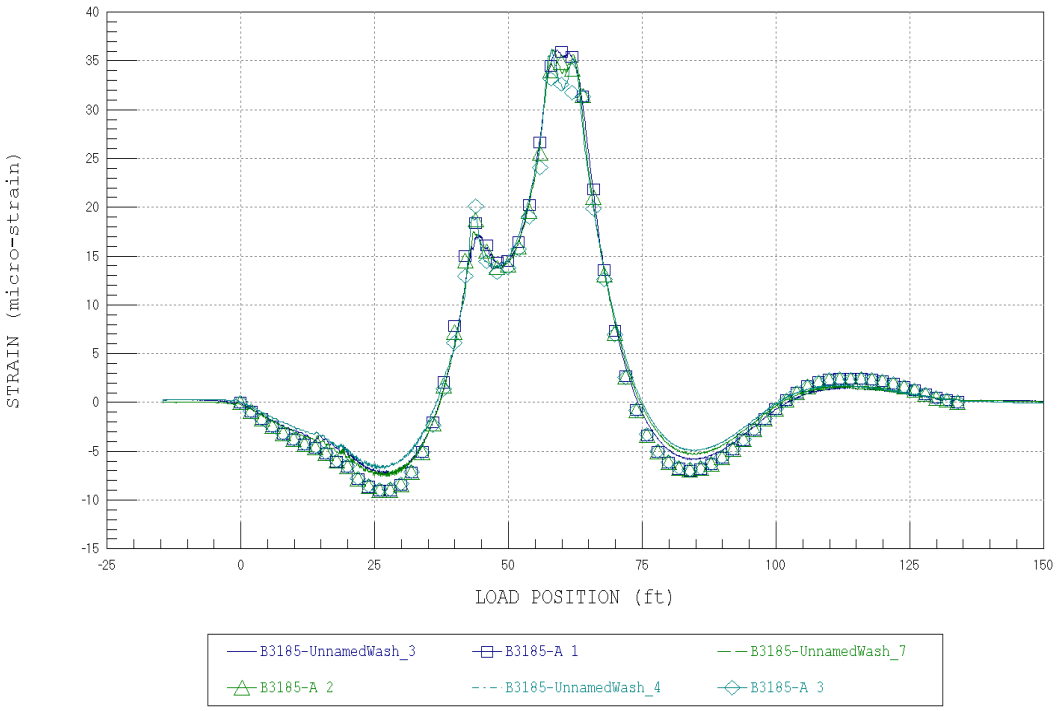

FIGURE 7-14 Comparison of FE strain versus measured strain along Section E-E.

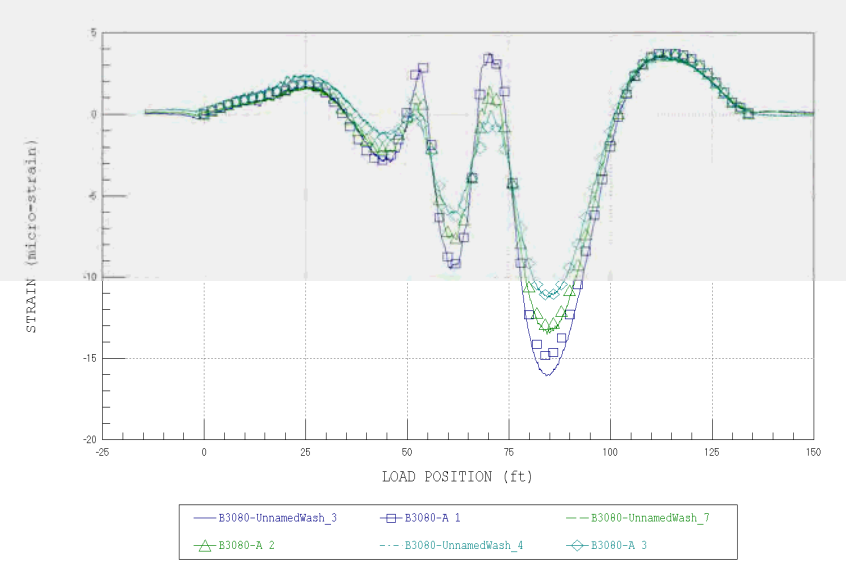

FIGURE 7-15 Comparison of FE strain versus measured strain along Section F-F.

member capacities were determined from the on-site bridge investigation and subsequent material testing. The rating methods used in this approach closely match typical rating procedures, with the exception that a field-verified FEM analysis was used rather than a typical AASHTO slab–strip analysis. This section briefly discusses the methods and findings of the load rating procedures.

Once the analytical model was refined to produce an acceptable match to the measured responses, some model parameters were adjusted to ensure the reliability of all optimized model parameters. This adjustment involved the identification of any refined parameters that could change over time or could become unreliable under heavy loads.

In the analysis of this bridge, the refined parameter that was determined to be unreliable was the moment–restraint provided by the piers.

- The piers' moment–restraint was reduced by 50% to ensure the responses would remain somewhat conservative over time.
- The slab's stiffness over the piers was adjusted to more accurately represent the expected behavior at the slab's ultimate strength state. At ultimate state it was assumed that the slab directly over the piers was fully cracked; therefore, the slab stiffness in these regions was reduced by the ratio between the gross and cracked section moment of inertia.
- The slab's stiffness adjacent to the piers was reduced by half to account for the additional cracking in these regions.
- The curb stiffness was conservatively reduced to zero for the dead load computations.

Member capacities were calculated based on the structural investigation of the superstructure and AASHTO specifications. A concrete compressive strength of 2.5 ksi (17.2 MPa) and a steel reinforcement yield strength of 33 ksi (227.5 MPa) were utilized based on the structure's age. During the existing NDE investigation, both the bottom and top reinforcing steel were found to be comprised of #8 bars (25 mm) spaced at 6 in. (150 mm) with the bottom reinforcement having 1.5-in. (38-mm) clear cover and the top reinforcement having 4.5-in. (114-mm) clear cover. A summary of the

calculated slab moment capacities and important member properties has been provided in Table 7-5. Note that the structure was only rated for flexure as per AASHTO guidelines.

Load ratings were performed on the field-verified FEM according to the AASHTO MBE (2003 revisions) (see Table 7-6 and Table 7-7 for applied rating factors). Given the 14-ft (4.27-m) wide roadway, only a one-lane loaded condition was considered for the rating. Figure 7-16 shows the load configurations for the standard load rating vehicles. All structural dead loads were automatically applied by the modeling program's self-weight function.

TABLE 7-5 Slab Moment Capacities (ΦMn, k-ft/ft)
(conversion: 1 in.^{2}/ft = 2,117 mm^2/m, 1 kip-ft/ft = 4.45 kNm/m)

Member–Limiting Capacity	Area of Steel (in.^{2}/ft)	Height (in.)	Distance from Steel Centroid to Compression Face (in.)	Design Moment Capacity (kip-ft/ft)
Slab–positive flexure	1.57	19.0	17	62.14
Slab–negative flexure	1.57	19.0	14	50.48

TABLE 7-6 Applied LRF Load Factors

Factor Type	Description	Factor Value
AASHTO Load Factors	Dead load—structural	1.3
	Live load—inventory	2.17
	Live load—operating	1.3
	Dynamic load allowance	30%
AASHTO Strength Reduction Factor	Flexure (moment) in RC sections	0.90

TABLE 7-7 Applied LRF Load Factors (conversion: 1 kip-ft/ft = 4.45 kNm/m)

Truck	Limiting Capacity	Dead Load[a] Moment (kip·ft/ft)	Live Load Moment[a] (kip·ft/ft)	Critical Inventory Rating Factor	Critical Operating Rating Factor
HS-20	Positive flexure	20.14	12.28	1.04	1.73
	Negative flexure	19.52	8.77	1.01	1.69
Type 3	Positive flexure	20.22	9.64	1.32	2.20
	Negative flexure	19.52	6.60	1.35	2.25
Type 3-3	Positive flexure	20.14	7.38	1.73	2.88
	Negative flexure	19.52	6.20	1.43	2.39
Type 3S2	Positive flexure	20.22	9.27	1.37	2.29
	Negative flexure	19.52	7.31	1.22	2.03

[a] Both the live load and dead load responses are unfactored responses.

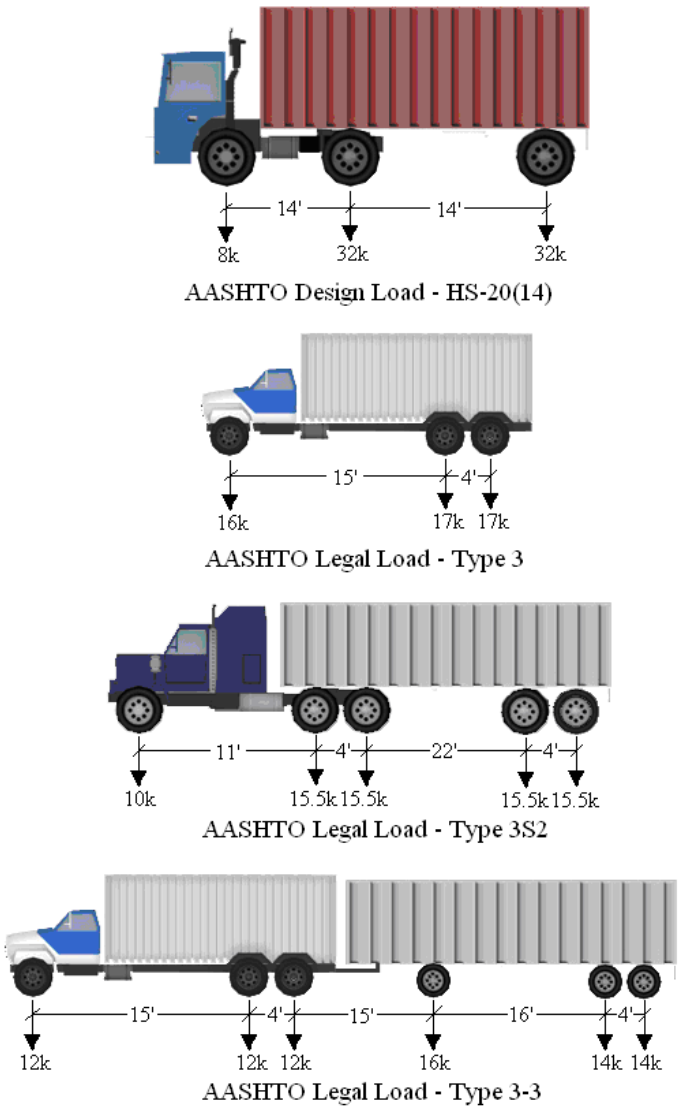

FIGURE 7-16 AASHTO standard load rating vehicle configurations.

The following is a summary of the load rating factors for the four AASHTO rating vehicles. As shown, the bridge met both inventory and operating rating criteria ($RF > 1.0$) for all standard design and posting loads, as shown in Table 7-7. The critical rating factor for all vehicles was controlled by the negative flexural capacity of the slab over the first pier under a single-lane loaded condition. Overall, rating results indicated that all rated vehicles can safely cross the structure.

In general, the response data recorded during the load tests was found to be of good quality and indicated no major signs of distress. The test data exhibited response magnitudes and shapes typical of an RC slab structure.

A two-dimensional FEM of the structure was created using the collected structural information, and subsequently adjusted until an acceptable match between the measured and

analytical responses was achieved. An excellent correlation between the measured and computed response was obtained during the modeling process.

Load rating results were controlled by the ultimate negative flexural capacity of the slab over a pier with a single lane loaded condition. The bridge met rating criteria ($RF > 1.0$) for all AASHTO standard design and posting loads.

EXAMPLE OF A PROOF LOAD TEST: ASR-AFFECTED SHEAR-CRITICAL REINFORCED CONCRETE SLAB BRIDGE

One example of a proof load test from the Netherlands that was carried out for research purposes, is the proof load test on the Zijlweg viaduct (*188*), pictured in Figure 7-17. This load test was carried out in the summer of 2015 (*19*) by Delft University of Technology. The Zijlweg viaduct is a four-span RC slab bridge with a skew angle of 14.4° carrying a single traffic lane. The geometry is shown in Figure 7-18 and Figure 7-19. Material damage caused by alkali–silica reactivity (ASR) is present in the viaduct, which has resulted in considerable cracking. Figure 7-20 is a map of cracking as observed prior to the proof load test.

FIGURE 7-17 Photograph of the Zijlweg viaduct.

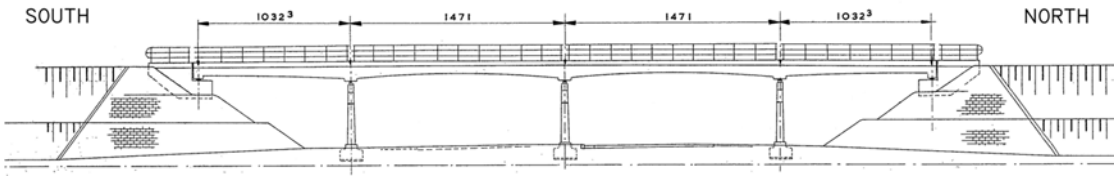

FIGURE 7-18 Elevation view of the Zijlweg viaduct, showing the four spans (units: m; conversion: 1 m = 3.3 ft).

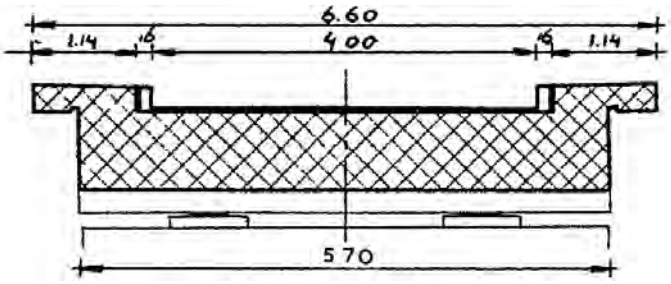

FIGURE 7-19 Sketch of viaduct cross section (units: m; conversion: 1 m = 3.3 ft).

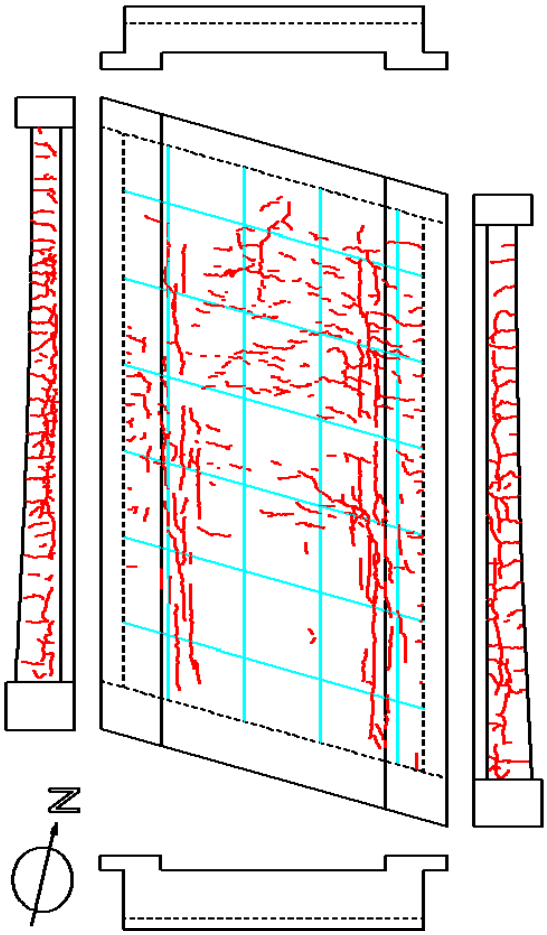

FIGURE 7-20 Map of cracking on bottom and side faces of Zijlweg viaduct.

Both shear and bending moment were studied, with their respective required loads and critical positions. Calculations at the design level of the RBK guidelines for the assessment of bridges (*165*) (load level with factors calibrated on a reliability index $\beta = 4.3$ for a reference period of 100 years) indicated that the viaduct did not have enough capacity in shear and bending moment. In particular, the shear rating was reduced due to the presence of ASR and its effect on tensile and shear strength of the concrete. Earlier research on the shear strength of ASR-affected structures (*189*) recommended a reduction corresponding to the measured tensile strength of the concrete. However, testing of ASR-affected beams, from an existing bridge, showed a maximum of 25% reduction (*190, 191*) in shear capacity as compared to Rafla's empirical shear formula (*192*), which was considered the capacity of an unaffected beam. Other experiments actually found an increase in the shear capacity (*193*) as measured on beams, with and without ASR damage, produced in the laboratory. Specifically, internal restraint against expansion of the gel induces a type of prestressing on the cross-section in the direction of the reinforcement, which sometimes can increase the shear capacity. From these observations, it is clear that estimation of ASR effects on structural capacity, and thus analytical evaluation of the Zijlweg viaduct would pose considerable challenges. Therefore, it was decided to subject the bridge to a proof load test.

Two positions were loaded in the northernmost span of the viaduct: one critical location for bending moment and the other for shear. Since the required proof loads exceeded that which could be obtained with a load test vehicle, a load spreader beam and counterweights were used, as shown in Figure 7-21. The weight is applied gradually to the bridge through a system of hydraulic jacks, where the jacks were positioned as to represent the four wheel prints described by the tandem from live load Model 1 from Eurocode NEN-EN 1991-2:2003 (*133*).

The worst-case position for bending moment was determined using a linear FE model of the bridge subjected to its self-weight, superimposed dead loads, and distributed and concentrated loads from live load Model 1 from NEN-EN 1991-2:2003 (*133*). The concentrated live loads were moved in the lane to find the most unfavorable position, and then the required proof load to create the same bending moment was calculated. The target proof load was found to be 1,257 kN (283 kip).

For shear, the critical position of the loading tandem was taken as a face-to-face distance of $2.5d_l$ (with d_l the effective depth to the longitudinal reinforcement) between the support and the first axle. The peak shear stress was distributed over $4d_l$ (*194*) to find the governing shear stress. The required load on the proof load tandem to have the same governing shear stress as caused by the live loads from the code was then determined. The target proof load was found to be 1,228 kN (276 kip).

The following structural responses were monitored during the load test: deflections of the slab; deflections at the crossbeams over the supports; crack widths; strains; rotations at the joint; and acoustic emission signals. An overview of the instrumentation [16 linear variable differential transformers (LVDTs) and 6 laser distance finders] is given in Table 7-8. Additionally, 15 acoustic emission sensors were applied. An overview drawing showing a schematic of the sensor plan is shown in Figure 7-22.

To apply the sensors in the field, more-detailed drawings, showing all relevant dimensions, were developed per structural response. An example with the details for the positions of the LVDTs that measure the slab deflections is given in Figure 7-23.

FIGURE 7-21 Load testing setup: steel spreader beam, counterweights, and hydraulic jacks.

TABLE 7-8 Sensor Summary (conversion: 1 m = 3.3 ft, 1 mm = 0.04 in.)

Name	Range (mm)	Application
LVDT1	10	Strain (1 m gauge length)
LVDT2	10	Strain (1 m gauge length)
LVDT3	10	Strain (1 m gauge length)
LVDT4	10	Reference for change in temperature
LVDT5	20	Deflection of the slab (on a longitudinal line)
LVDT6	20	Deflection of the slab (on a longitudinal line)
LVDT7	20	Deflection of the slab (on a longitudinal line)
LVDT8	20	Deflection of the slab (on a longitudinal line)
LVDT9	10	Displacement of the joint
LVDT10	10	Displacement of the joint
LVDT11	10	Displacement of the joint
LVDT12	10	Displacement of the joint
LVDT13	10	Deflection of the slab (on a longitudinal line)
LVDT14	10	Crack width
LVDT15	10	Crack width
LVDT16	10	Crack width
Laser1	100	Deflection of the slab (on a transverse line)
Laser2	20	Deflection of the slab (on a transverse line)
Laser3	20	Deformation of support (N)
Laser4	20	Deformation of support (N)
Laser5	100	Deformation of support (S)
Laser6	100	Deformation of support (S)

NOTE: The longitudinal or transverse line refers to the orientation of a line drawn on the bottom of the slab with respect to the position of the proof load tandem.

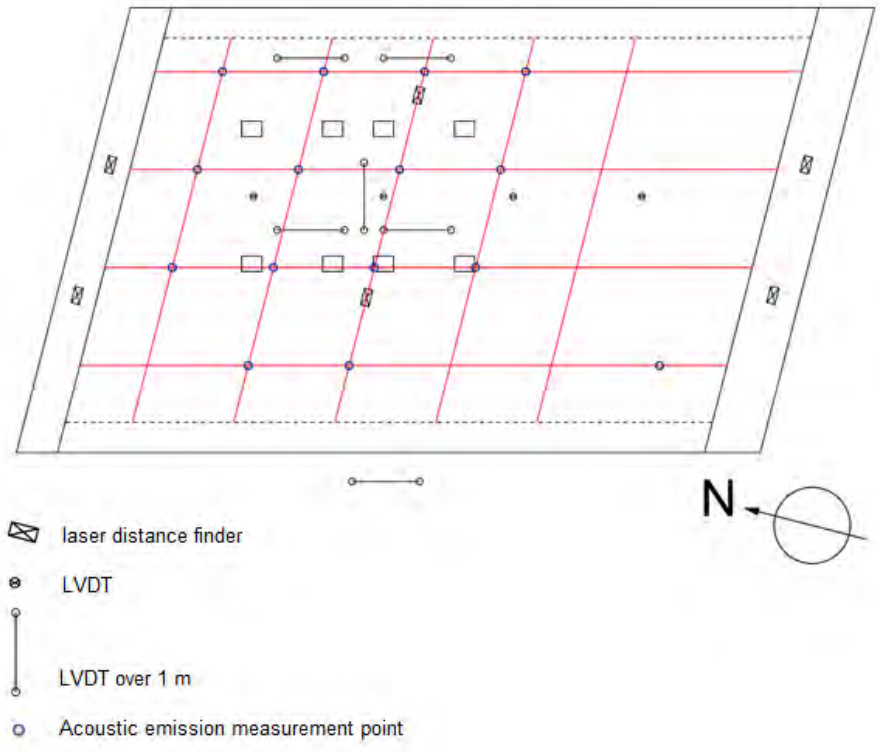

FIGURE 7-22 Instrumentation plan (conversion: 1 m = 3.3 ft).

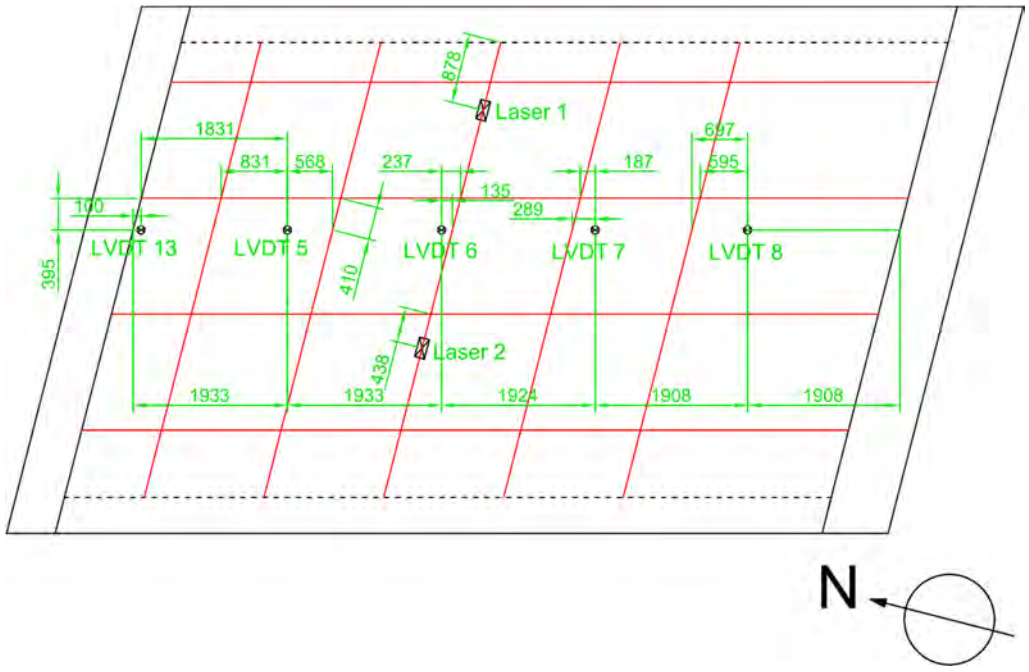

FIGURE 7-23 Locations of laser and LVDT deflection measurements (dimensions in mm; conversion: 1 mm = 0.04 in.).

As no particular stop criteria were defined prior to these proof load tests, specific working criteria were developed with guidance from existing standards and engineering judgement. For the bending moment test, the stop criteria from the German guidelines (*61*) were used as a reference. As no stop criteria for shear are available in current codes and guidelines, it was decided to heavily instrument the bridge and check the linearity, reproducibility, and symmetry of the responses after each load cycle. In addition, acoustic emission measurements were used to provide indications of cracking (*195*).

The loading protocol used during the proof load test for bending moment is shown in Figure 7-24. The total maximum load in the bending moment test was 1,368 kN (308 kip), which is equal to safety level RBK Design + 8.7%. The loading protocol used during the proof load test for shear is shown in Figure 7-25. The total maximum load in the shear test was 1,377 kN = 310 kip (i.e., safety level RBK Design + 12%). The total applied load is the sum of the load measured by the load cells and applied by the jacks and the load resulting from the weight of the jacks and steel plates used for the load application setup. During the proof load tests, no unexpected structural responses were observed, so the full target proof load could be applied. A deeper analysis of the measurements after the proof load test led to the same conclusion.

The RBK Design level has an associated reliability index of $\beta = 4.3$, for a reference period of 100 years. After the proof load test, it was thus concluded that the viaduct can carry the prescribed live loads safely and can remain open to all traffic (one lane), given that it is inspected frequently to assess the effect of ASR-related cracking on the durability of the bridge. This conclusion results from the current state of the art in Europe, which is based on determining the target proof load calculated using the equivalent sectional moment or force (depending on the considered failure mode). This practice is different from the North American practice of applying a magnification factor on a prescribed loading vehicle, because the European live load model uses a combination of concentrated and distributed live loads that does not

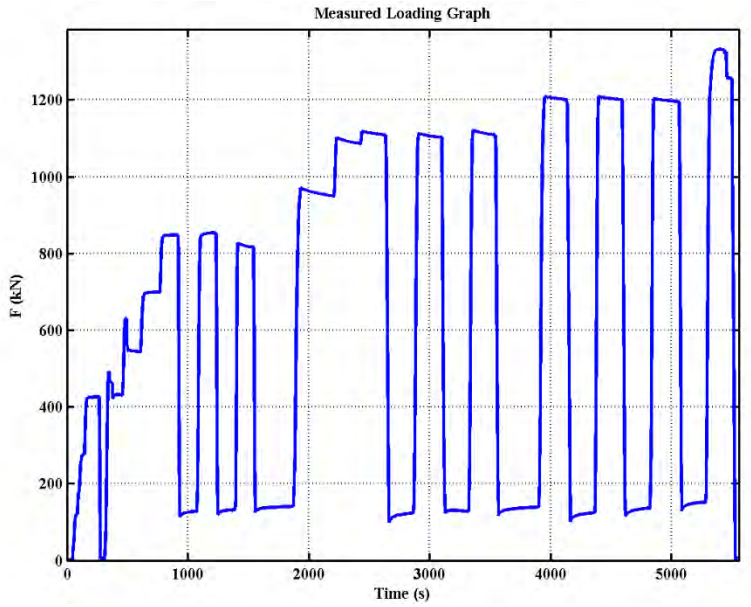

FIGURE 7-24 Measured loading procedure for bending moment proof load test (conversion: 1 kN = 0.225 kip).

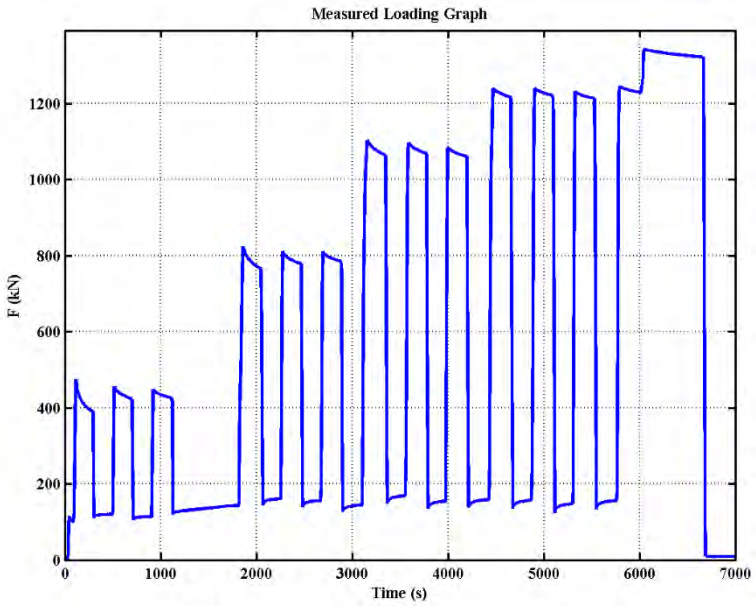

FIGURE 7-25 Measured loading procedure for shear proof load test (conversion: 1 kN = 0.225 kip).

directly represent a specific vehicle. Moreover, with this approach, it is assumed that using the load factors associated with a certain load level will result in the same reliability index when an equivalent target proof load is used. More research on the aspects concerning the uncertainties and aspects of structural reliability is necessary to determine the reliability index after a proof load test and thus to quantify the structural safety.

In the preceding case study, a load exceeding the highest load level was applied for research purposes. In practical load tests, however, applying such a high load is usually unnecessary.

SUMMARIZED CASE STUDIES

In this section, a number of shorter case studies are presented. These case studies show the application of load testing for specific purposes.

Load Test of a Bridge Retrofitted with a Fiber-Reinforced Polymer Bridge Deck: A Case Study Verification of Design Assumption and Evaluation of Long-Term Fatigue Performance

As noted in Chapter 1 (Objectives of Load Tests, p. 2), there are several reasons for diagnostic load testing of bridges. This case study describes one such diagnostic load test application that was used for (*a*) verification of design assumptions and (*b*) development of field-verified analytical models to gain knowledge on long-term fatigue performance of the bridge.

The New York State Department of Transportation (DOT) has been one of the pioneering states in using FRP materials in the 1990s when they were relatively new to the bridge infrastructure applications. Realizing that FRP materials are new to bridge industry and limited

performance data is available, periodic load testing was used to ensure adequate in-service performance of FRP materials and to gain more knowledge on their behavior and durability. This case study briefly describes one such application. More details on this case study can be found in Alampalli and Kunin (*31, 32*) and Chiewanichakorn, Aref, and Alampalli (*196*).

Structure

The bridge carries SR-367 in Chemung County over Bentley Creek (Figure 7-26 and Figure 7-27). The 42.7-m (140-ft) long and 7.3-m (24-ft) wide structure has the floor system comprising steel transverse floor beams at 4.27 m (14 ft) c/c spacing with longitudinal steel stringers. It was originally built as a single simple-span, steel truss bridge with a RC slab. In 1997, based on a capacity analysis, due to additional dead load from asphalt overlays and the deterioration of the steel trusses and floor system due to corrosion, it was rehabilitated by replacing the RC slab with an FRP deck to prolong the structure's service life as well as satisfying new load rating requirements.

The deck panels were designed to span between the floor beams. The steel stringers were left in place to provide bracing to the structure, although they no longer function in carrying live load. A total of six FRP panels were used to replace the roadway. More details of the structure can be found in (*31, 32*). The panels were connected to each other using epoxy and splice plates without any shear-key mechanism. The joints consist of a longitudinal joint that runs the entire length of the bridge and four transverse joints that each span one lane. Vertical surface joints between panel sections were glued together with epoxy. Top and bottom splice plates were bonded using an acrylic adhesive. A 10-mm (0.4-in.) thick epoxy thin polymer overlay was used as the wearing surface of both the deck and sidewalk. Most of the wearing surface was applied to the panels during fabrication. Portions of the wearing surface covering panel joints and bolt lines were applied on-site after the FRP surface was lightly sandblasted and cleaned.

(a) **(b)**

FIGURE 7-26 Elevation of (*a*) the bridge and (*b*) bridge with loaded trucks during the load tests.

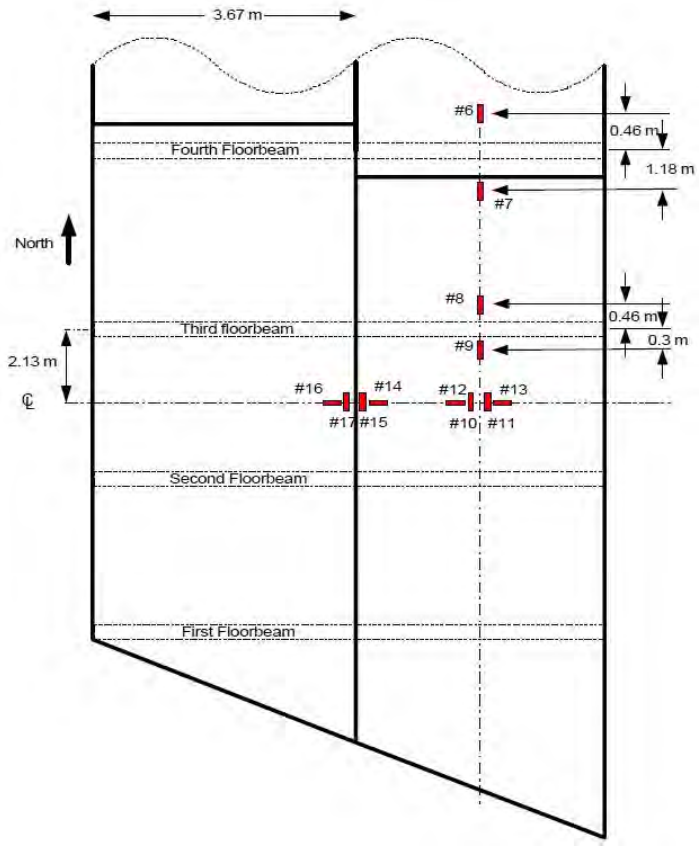

FIGURE 7-27 Strain gage configuration on top of the FRP deck (conversion: 1 m = 3.3 ft).

Test Objectives

Load testing objectives were

- Verify design assumption to ensure no composite action exists between the deck and the floor beams that attach the two together,
- Verify design assumption to ensure field joints are effectively transferring the loads between FRP panels,
- Verify the design load ratings of the deck, and
- Evaluate effects of the rehabilitation process on the remaining fatigue life of the structure.

Sensors and Instrumentation

Sensors and instrumentation were designed appropriately to suit the test objectives. Conventional, general purpose, uniaxial 350 ohms, self-temperature compensating, constantan foil strain gages were used to measure strains during the testing. The strain gages were bonded to steel and the FRP deck with adhesive and then waterproofed. A total of 18 strain gages were used: six placed on a steel floor beam to verify composite action and 12 placed on the FRP deck

to obtain the joint performance (Figure 7-27 and Figure 7-28). The data was collected using a computerized data acquisition system.

Testing and Analysis

Two fully loaded trucks of required configuration were used to load the bridge. Three separate load cases were utilized. Two New York State DOT dump trucks, each fully loaded resembling an M-18 (H-20) AASHTO live loading (*197*). The loads were positioned on the deck in such a way that the load testing objectives could be accomplished, and enough data could be collected for the development of the field-verified FEM that would be developed for further analysis. Truck configuration and weights used in the testing can be found in Alampalli and Kunin (*31*, *32*). Loaded trucks were also driven across the bridge at crawl speeds to create influence lines for the development of a detailed field-verified FEM.

Results

Strain Gages 0 through 5 that were mounted on a steel floor beam supporting the FRP deck were used to determine neutral axis of the deck–floor beam system. If there is no composite action between the floor beam and the deck, the neutral axis of the deck–floor beam system should coincide with the neutral axis of the floor beam. The results showed that the strains in bottom and top flanges are almost the same except for the sign (as expected) and represent a mirror image, with negligible strain at the center of the girder. The data indicates that the neutral axis of the girder is unchanged with the addition of the FRP deck and no composite action exists between the deck and the floor beams (Figure 7-29*a*). Redundant Gages 1, 2, and 4 also showed the same behavior.

To study the effectiveness of deck joints, strain gages were installed on both sides of the longitudinal joint and loaded trucks were positioned in both lanes of the structure one truck at a time (Figure 7-1). If the joint is transferring the loads effectively, strains recorded by the gages on either side of the longitudinal joints should be equal. The data showed that the joint is transferring approximately 65% to 70% of the load. The same trend was also observed using the data obtained from semi-static load testing (Figure 7-29*b*). These results indicated that the

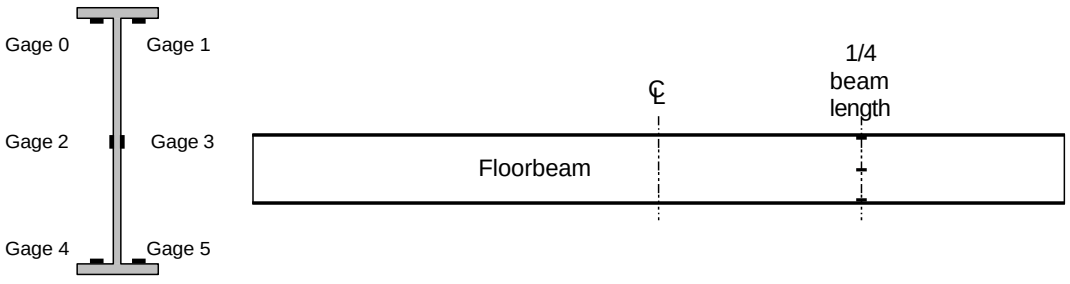

FIGURE 7-28 Strain gage configuration on the floor beam.

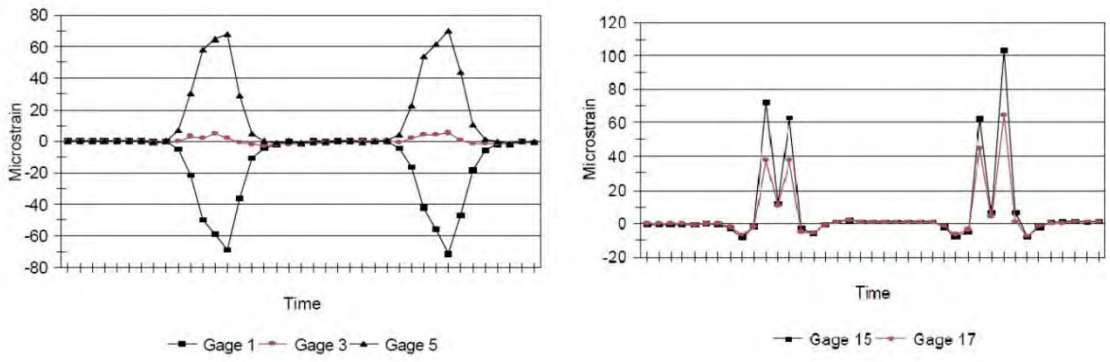

(a) **(b)**

FIGURE 7-29 Data from 5-km/h (3-mph) crawl test (*a*) showing no composite action between the deck and the floor beams and (*b*) effectiveness of field joints in the deck.

longitudinal joint is transmitting loads from one deck segment to the other, but the load is not completely carried across the joint. Since the deck joints were new at the time of the testing, it is recommended that testing be repeated after a few years to determine if in-service loads and environmental conditions have degraded the joint effectiveness.

The deck was designed for AASHTO MS-23 (HS-25) live load by the manufacturer. The ratings submitted to the department were based on a FEM developed using STAAD software. The reported governing operating and inventory load ratings of the deck under flexure were MS-300 (HS-330), and MS-226 (HS247). The strain data from the testing was used to verify these ratings in flexure. Note that access to deck panel webs was not available, thus shear stresses were not measured during the load testing. Load ratings for flexural stresses were calculated, assuming that the deck is simply supported on the floor beams. The operating and inventory load ratings based on flexure were calculated to be MS-292 (HS-318) and MS-219 (HS-239) respectively. These results agree closely with the ratings reported by the manufacturer.

If the intent of the test was solely to verify these design assumptions, it should be noted that no further analysis was required. A FEM of the entire bridge was developed, per the construction drawings, using a commercial FE modeling software and required analysis was performed using a general-purpose FE analysis package. This model with the FRP deck system was field-verified against load test results. Implicit dynamic time–history analyses were conducted with appropriate loading configuration for a moving design fatigue truck. Fatigue life of all truss members, floor-beams, and stringers were determined based on a fatigue resistance formula in the appropriate specifications used for bridge design (*196*). Based on the FE analyses, it was found that this bridge would expect to have 354 years, or presumably infinite fatigue life based on anticipated average daily truck traffic and new construction assumption. The results indicated that the fatigue life of the FRP deck system almost doubles when compared with the prerehabilitated RC deck system. Based on the estimated truck traffic that the bridge carries, stress ranges of the FRP deck system lie in an infinite fatigue life regime and thus, implies that fatigue failure of the trusses and floor system would not be expected during its service life. Fatigue life of critical members in one of the trusses of the FRP deck was found to be more than 1,000 years old.

Permit Load Verification Load Testing: Validating a Structure's Ability to Carry a Permit Load

The intent of this project was to evaluate the structure's ability to carry multiple super-heavy transports that were required to cross the structure. The initial study, which included a simplified FE analysis, resulted in acceptable LRFD load rating factors for all the super-heavy loads that were being applied to the structure. The favorable load ratings were a result of three primary factors: (*a*) the load was highly distributed due to the large footprint of the specialized transport; (*b*) the bridge was designed for custom vehicles which are significantly heavier than standard design vehicles; and (*c*) it was assumed that the bridge was in good condition. The last condition came into question as the PS/C bulb T-girders had significant cracks throughout the girders due to delayed ettringite formation (DEF). While the DEF cracks were a function of improper curing and not related to live-load effects, the New York State DOT was concerned that repeated heavy loads would negatively influence the cracks and the overall long-term performance of the bridge.

Due to the lack of reasonable alternative routes and the importance of the cargo, the department agreed that further investigation could be performed to determine if the bridge could serve as a viable route without experiencing any significant loss of serviceability. A series of load tests to examine how the DEF cracks and existing substructure cracks were influenced by heavy truck loads was selected for the investigation. In addition, load test data was used to generate field-verified load ratings for the heavy permit vehicles and thereby reduced any uncertainty in the current structural performance. Load tests were performed with a 156-kip (694 kN) single-wide transport. This truck was lighter than the permit loads but had a much smaller footprint. The goal was to apply a similar load to the bridge design load so as not to overload the bridge in any way but generate structural responses greater than typically experienced by the bridge. Results from the load test were favorable for allowing the permit vehicles to use the bridge.

Structural Testing Procedures

The bridge consists of 10 continuous spans, each composed of four PS/C girders and a RC deck. Span lengths range from 80 ft (24.6 m) to 115 ft (35 m) and are continuous for live load. There are also relatively large concrete parapets running along each side of the bridge deck that are continuous over the length of the bridge. The bridge crosses four lanes of a U.S. highway, several active railroad tracks, and a service road. Load tests were performed on Spans F and G as these spans exhibited relatively extensive DEF cracks in the girders and instrumentation could be performed with minimal impact on railway or roadway traffic below.

For the load test, the structure was instrumented with 56 reusable, surface-mounted, strain transducers, and six tiltmeter rotation sensors (Figure 7-30). Strain transducers were attached to each beam line at several cross sections to measure flexural bending and the rotation sensors were attached to the beams near the piers to provide a global measurement of continuity between spans.

Once the instrumentation was installed, a series of diagnostic load tests was completed with the test vehicle traveling at crawl speed of approximately 3 mph (5 km/h). During testing, data was recorded on all channels at sample rate of 50 samples per second as the test vehicle [156 kip trailer (694 kN), Figure 7-35] crossed the structure in the westbound direction along three different lateral positions, referred to as Paths Y1, Y2, and Y3. The vehicle's longitudinal

position was wirelessly tracked so that the response data could later be viewed as both a function of time and vehicle position. During the test procedures, traffic was periodically stopped so that the test vehicle was the only live load applied to the structure.

Information specific to the load tests can be found in Table 7-9. The test vehicle's gross weight, axle weights, and axle spacing are provided in Figure 7-35.

TABLE 7-9 Structure Description and Testing Information

Item	Description
Structure type	PS/C girders
Total number of spans	10
Span lengths	80 ft (24.6 m) to 115 ft (35 m)
Skew	13° 11 ft, 00 in.
Structure/roadway widths	Structure: 36 ft, 6 in. (11.13 m) / Roadway: 34 ft, 0 in. (10.36 m)
Wearing surface	Asphalt
Spans tested	F and G, both 102-ft (31-m) spans
Test reference location (BOW) (X = 0, Y = 0)	Centerline of Pier 7 and inside of east parapet
Test vehicle direction	Southbound all tests
Test beginning point	200 ft (61 m) north of BOW (centerline of Pier 7); start line skewed at same angle as piers
Number/type of sensors	56 strain transducers 6 tiltmeters
Sample rate	50 Hz
Number of test vehicles	1
Total field testing time	2 days (1 day instrumentation installation, 1 day for testing and demobilization)
Other test comments	Weather: sunny, ~75°F (24°C)

FIGURE 7-30 Surface-mounted strain transducers PS/C girders (typical).

FIGURE 7-31 Top and bottom strain transducers on parapet (typical).

FIGURE 7-32 Strain transducers mounted across girder DEF cracks to measure crack movement (typical).

FIGURE 7-33 Strain transducers mounted across pier cracks to measure crack movement (typical).

FIGURE 7-34 Tiltmeter installed near the pier wall (typical).

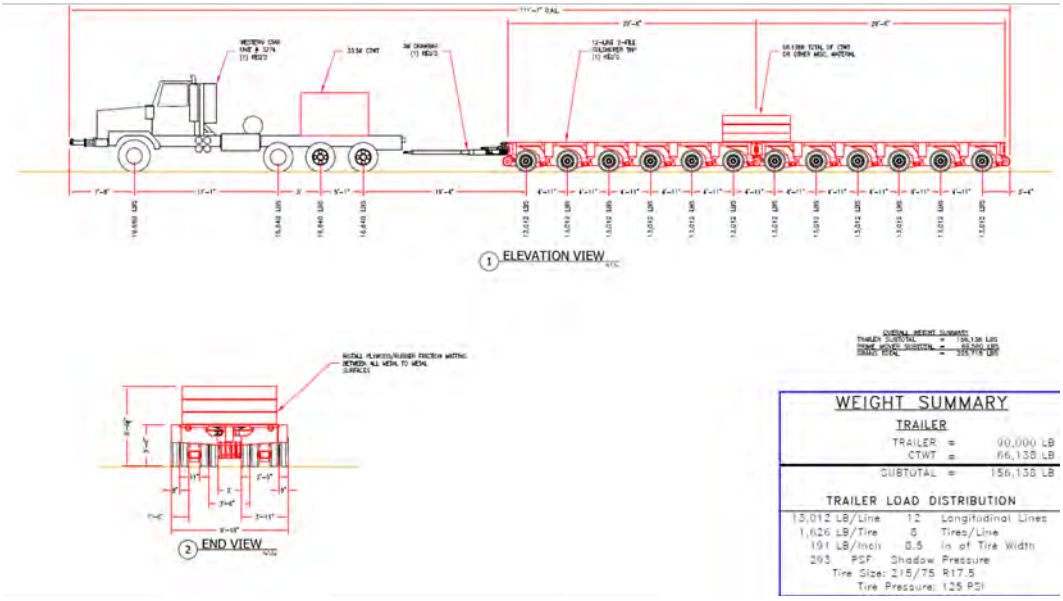

FIGURE 7-35 Test vehicle definition.

Preliminary Investigation of Test Results

All the field data was examined graphically to provide a qualitative assessment of the structure's live load response. Some indicators of data quality include reproducibility between tests along identical truck paths, elastic behavior (i.e., strains returning to zero after truck crossing), and any unusual-shaped responses that might indicate nonlinear behavior or possible gage malfunctions. This process generally provides insight as to how a structure responds to live load and is often extremely helpful in performing an efficient and accurate structural analysis.

- **Responses as a Function of Load Position.** Data recorded from the wireless truck position indicator was processed so that the corresponding strain and rotation measurements could be presented as a function of vehicle position. For the majority of data plots the graph's horizontal axis is the distance traveled relative to a reference point on the structure.
- **Reproducibility and Linearity of Responses.** The structural responses from identical tests were very reproducible. Figure 7-36 and Figure 7-37 contain multiple strain and rotation history plots for two repeated test runs. In most cases, it is difficult to identify that there are two plot lines for each sensor. In addition, all strains appeared to be linear with respect to magnitude and truck position, and all strains returned to the initial values. This result indicates the structure performed in a linear-elastic manner through all load cycles. All response histories had a similar degree of reproducibility and linearity, indicating that the data was of good quality.

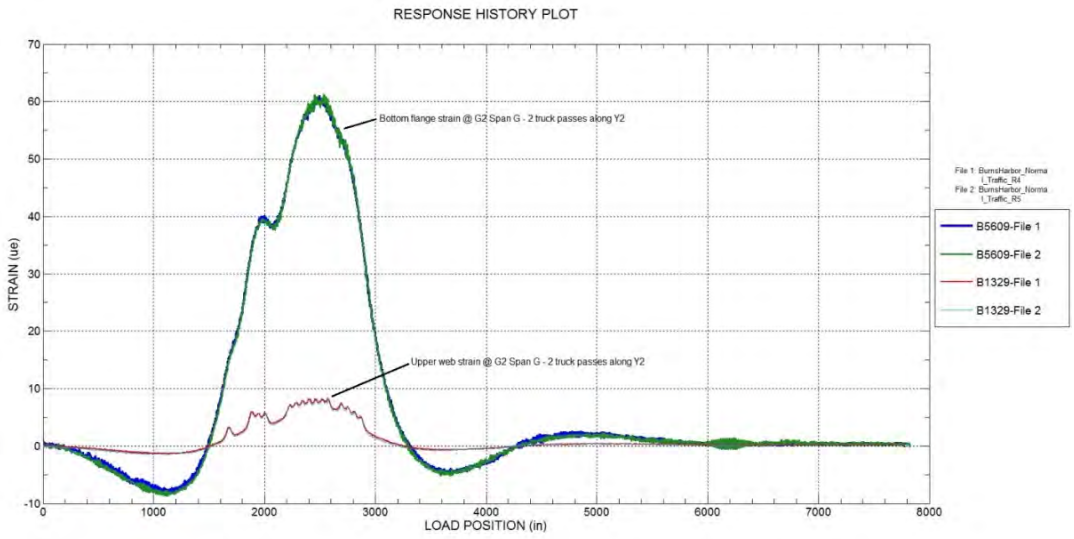

FIGURE 7-36 Example of strain response reproducibility.

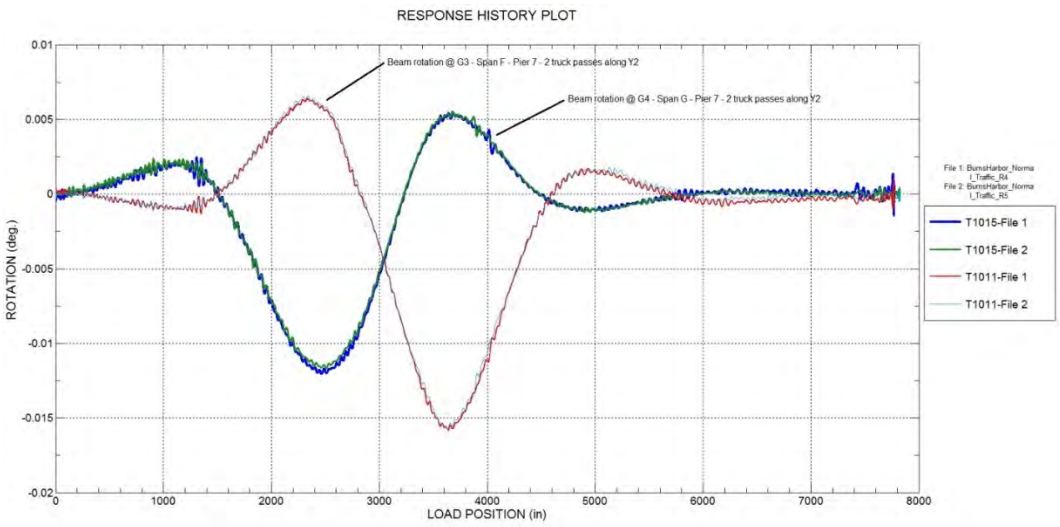

FIGURE 7-37 Reproducibility of beam-end rotation Span G, Pier 7.

- **Lateral Load Distribution.** When evaluating a response behavior to perform load rating, the bridge's ability to laterally distribute load is an essential characteristic to capture. Lateral load distribution can be observed by plotting responses from an entire bridge cross section, as done in Figure 7-38. Here midspan bottom flange strains are shown that correspond to the maximum midspan response from all three truck paths. While this plot illustrates lateral distribution as a function of relative girder response, the data cannot be used directly to compute lateral distribution factors. The effective stiffness and therefore the relationship between strain and load vary between interior and exterior girders. Furthermore, the load paths tend not to follow the geometric skew lines. The goal of the subsequent analysis will be to produce a model with identical lateral load transfer abilities.
- **Composite Behavior.** Having strain measurements at multiple locations on a girder cross-section allow for a graphical estimation of the neutral axis location. This process is simply based on similar triangles and the assumption that plane sections remain plane. Figure 7-39 shows the response histories from the upper-web strain gage and the bottom flange strain gages from Girder 3 at Span G. By examining the relative magnitude difference between the two responses it is apparent that the neutral axis of the interior girder at approximately the bottom of the top flange. The location of the measured neutral axis corresponds well with the theoretical neutral axis location.
- **Interaction of Parapet and Exterior Girder.** Neutral axis measurements generated for the exterior girder indicated the concrete parapets contributed to the exterior girder stiffness. In addition to the two strain gages located on the girder cross-section, two additional strain gages were installed; one at the bottom of the slab and the other near the top of the parapet. All four strain histories are plotted together in Figure 7-40. By examining the relative magnitudes and consistent behavior through the load cycle, it was apparent that a linear strain distribution existed, and that the neutral axis was significantly higher at the exterior girder than at the interior girder.

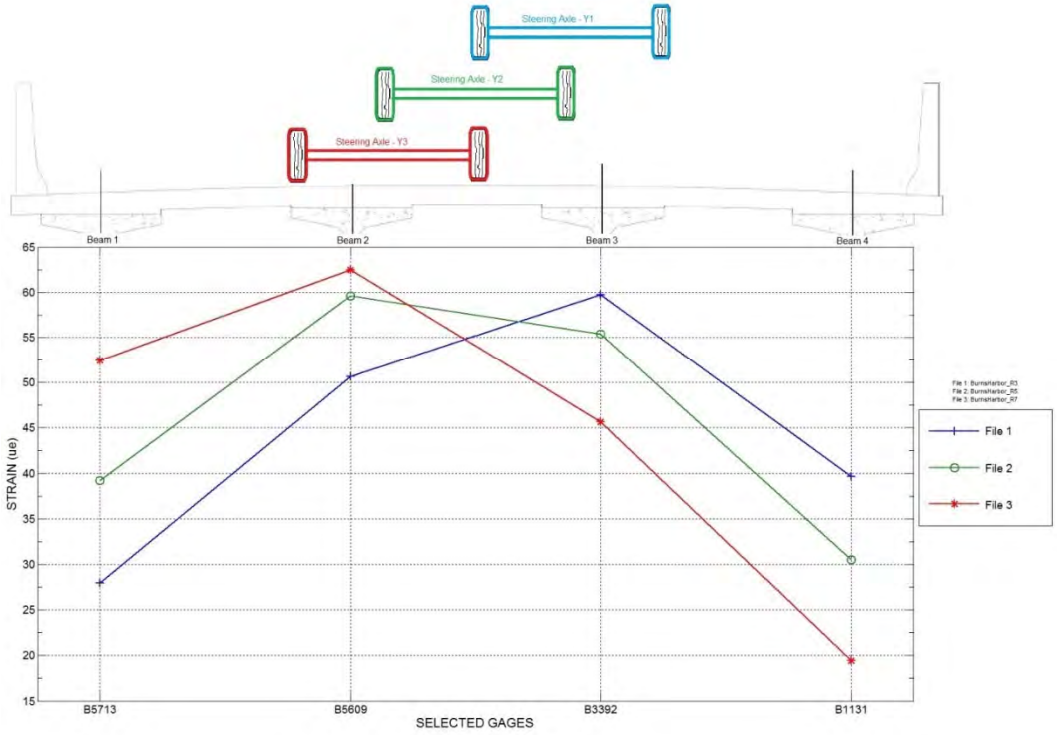

FIGURE 7-38 Lateral load distribution observed in midspan strain responses.

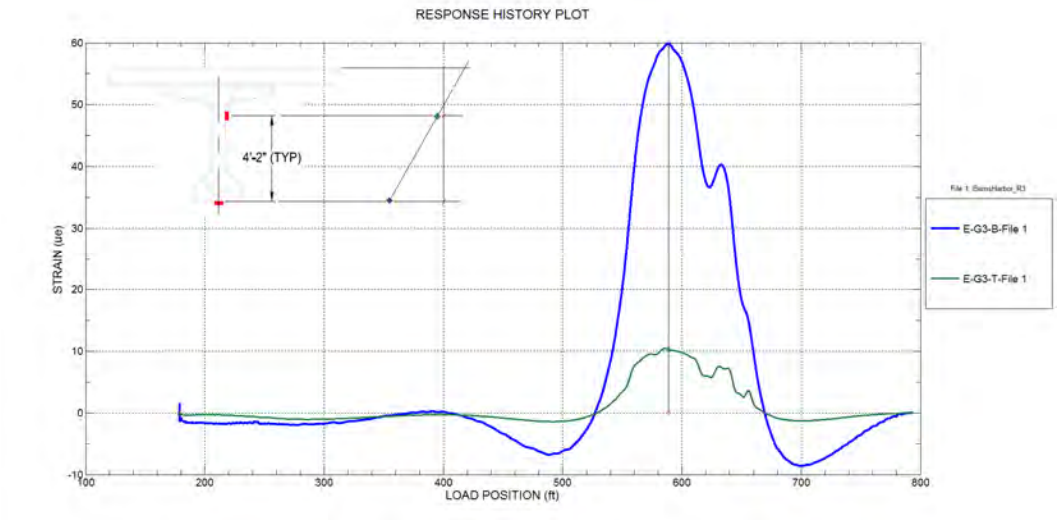

FIGURE 7-39 Neutral axis location of interior girder.

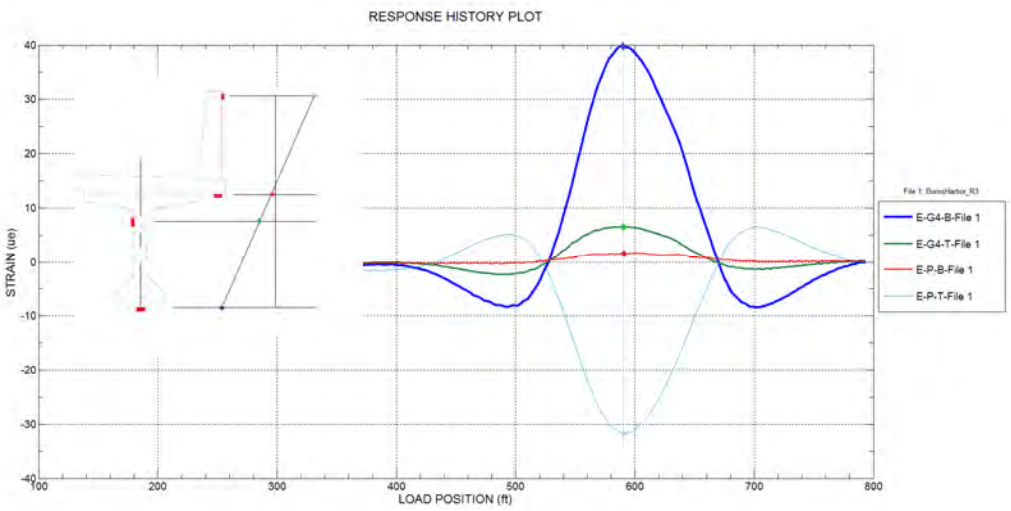

FIGURE 7-40 Neutral axis location of exterior girder.

- **DEF Girder Crack Movement.** Strain measurements were made across several girder crack locations. These cracks were all longitudinal and caused by curing issues. Load test measurements indicate that the cracks are not adversely influenced by live load. Strain transducers were oriented transversely to measure movement across the cracks. Strain measurements were converted to crack opening displacement by multiplying the strain measurement by the gage length (3 in. = 76 mm). The assumption is that all movement picked up by the strain transducer was caused by crack movement. Measurements of crack movement as a result of the test truck were very small; the maximum crack displacement was -5.5×10^{-5} in. (–1.4 μm). The direction of the crack movement was equally important as it was inversely related to the tension in the bottom flange; positive moment (tension in the bottom flange) resulted in a negative crack displacement indicating the cracks at midspan tended to close as the heavy load crossed. Figure 7-41 contains the midspan crack movement from Girder 3 at Span F for both the bottom and the side of the bottom flange. DEF crack movement was consistent for all four instrumented locations.
- **Crack Movement at Piers.** Crack movement was measured at four locations near the top of Piers 6 and 7. Strain gages were installed across the most visible cracks below the interior beam seats. As expected, these cracks opened as the test truck crossed the pier. Movement was small and elastic in that all measurements returned to the original positions after each truck crossing. Figure 7-42 shows the crack movement response from Pier 6 for all three truck crossings. The maximum measured crack movement was 0.00033 in. (0.0084 mm).

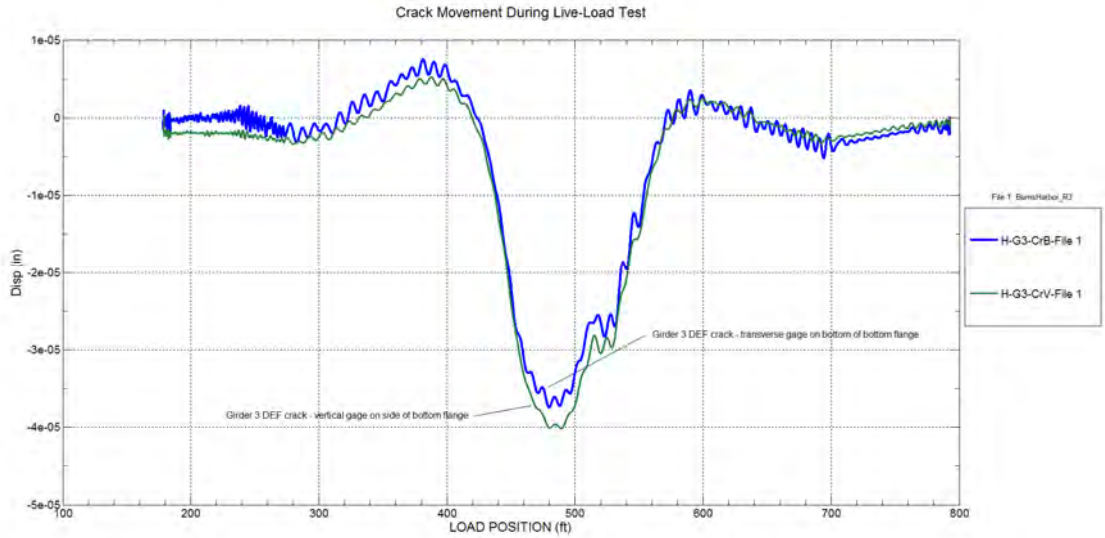

FIGURE 7-41 DEF crack movement on bottom flange of PS/C girders.

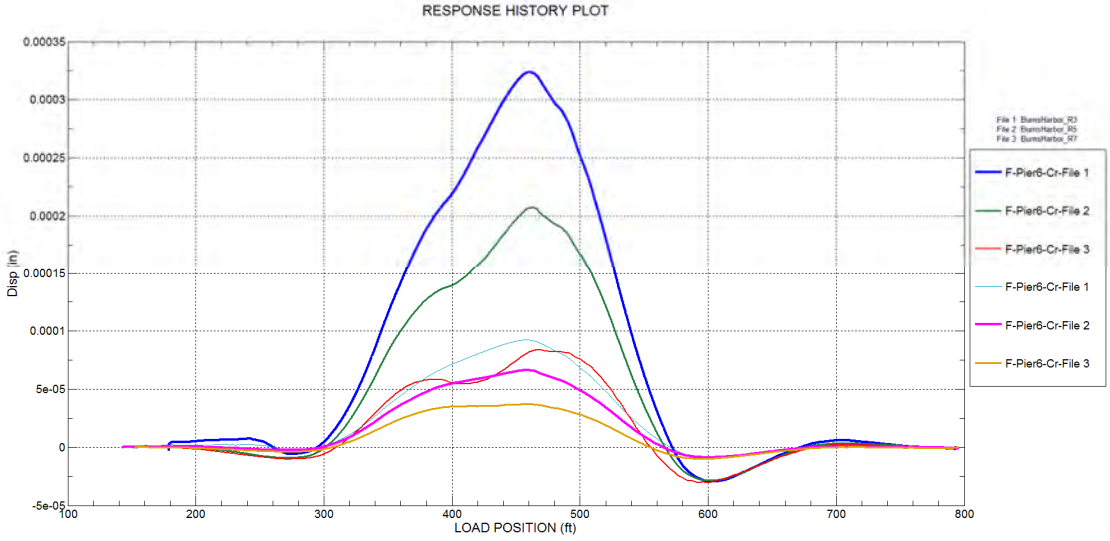

FIGURE 7-42 Pier 6 crack movement measured during all three truck paths.

Modeling, Analysis, and Data Correlation

This section briefly describes the methods and findings of the analysis procedures. A list of modeling and analysis parameters specific to this bridge is provided in Table 7-10.

First, geometric data collected in the field and insight gained from the qualitative data investigation were used to create an initial 2D FEM which is illustrated in Figure 7-43. Once the initial model was created, the load test procedures were reproduced using a structural analysis and data correlation software. This was done by moving a 2D footprint of the test truck across the model in consecutive load cases that simulated the designated truck path used in the field. The analytical responses of this simulation were then compared to the field responses to validate the model's basic structure and to identify any gross modeling deficiencies.

The model was then refined until an acceptable match between the measured and analytical responses was achieved. This refinement involved an iterative process of optimizing material properties, cross sectional properties or boundary conditions until they were realistically quantified. In the case of this structure, the majority of the refinement effort was spent modeling the interaction of the concrete parapet with the exterior girder, the correct deck and girder stiffness, and the continuity between spans. Two important structural conditions resulted from the model refinement. The first was the actual contribution of the parapets to the stiffness of the exterior girders and the lateral load distribution. The second item was the reduction in continuity between spans due to existing flexural cracks in the concrete deck immediately adjacent to the piers and cracks in the parapets over the piers.

TABLE 7-10 Analysis and Model Details

Analysis type	Linear elastic FE — stiffness method
Model geometry	2D composed of shell elements, frame elements, and springs
Nodal locations	Nodes placed at the ends of all frame elements Nodes placed at all four corners of each shell element
Model components	Shell elements representing the slab elements Frame elements representing the curb–parapet Springs representing the bearing seats at the piers
Live load	2-D footprint of pull truck and trailer consisting of 110 vertical point loads Truck paths simulated by series of load cases with truck footprint moving at 5-ft (1.5-m) increments along a straight path
Dead load	Self-weight of structure
Total number of response comparisons	15,984 response comparisons: • 42 strain gage locations x 333 load positions = 13,986 strain comparisons • 6 rotation gage locations x 333 load positions = 1,998 beam rotation comparisons
Model statistics	3,252 Nodes 4,859 Elements 20 Cross section–material types 333 Load cases (111 per truck path) 48 Sensor locations (crack gages not included in model comparison)
Adjustable parameters for model calibration	Interior girder stiffness: at abutments near transverse edges (E_{eff}) Exterior girder stiffness: (I_{eff} including contribution of parapet) Continuity at pier: at abutment near center of structure (M_y) Slab stiffness: (E_{eff} of an equivalent homogenous shell element)

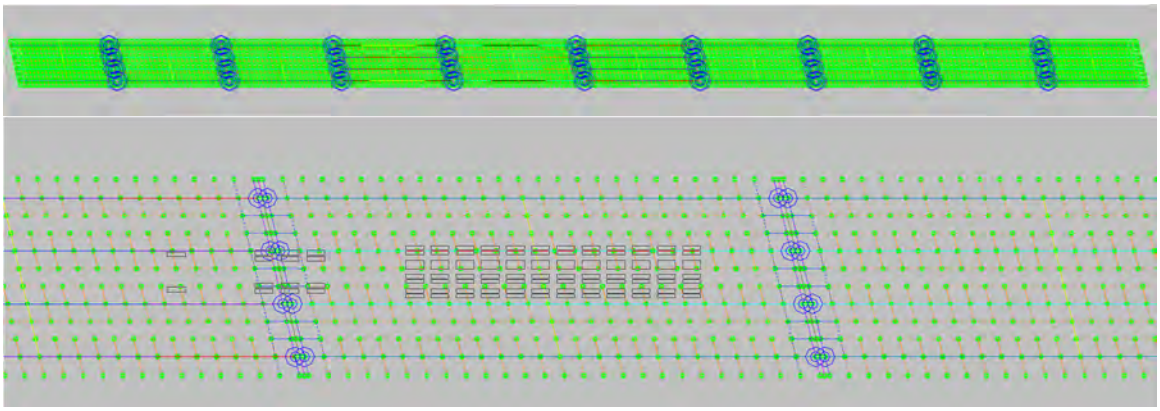

FIGURE 7-43 FEM of superstructure with modeled test truck load.

Following the refinement procedures, the final model produced a 0.9725 correlation with the measured responses, which can be considered an excellent match for a continuous span PS/C girder bridge. The parameters and model accuracy values used in the initial and final bridge models are provided in Table 7-11. Of note, the moment of inertia for the exterior beams increased nearly four times. This increase was a result of the integral parapets that were nearly directly on top of the exterior girders, rather than modeling the parapet as a structural element the exterior girder stiffness was increased to account for the added stiffness of the parapet (Figure 7-47). One additional item of note is the increased stiffness of the slab (deck). A new concrete overlay was recently added to the structural slab resulting in an overall increase in slab stiffness. Once again, this was modeled by increasing eh stiffness of the main structural slab rather than increasing the slab thickness. This makes it easier to remove the stiffness for load rating purposes as the overlay will wear out over time and cannot be counted on for additional stiffness in the long term.

The final model was found to closely match the member strain and beam rotation at all locations. Representative comparison plots are provided in Figure 7-44 through Figure 7-47. Additionally, the model's midspan lateral distribution closely matched that of the actual structure as shown in Figure 7-48.

TABLE 7-11 Model Accuracy and Parameter Values

Modeling Parameter		Initial Model Value	Final Model Value
Slab stiffness	E (kip/in.^{2})	3,200	5,000
PS/C girder modulus	E (kip/in.^{2})	4,750	5,250
Moment of inertia exterior girder	I (in.^{4})	473,700	1,562,000
Slab adjacent to piers (continuity)	E (kip/in.^{2})	3,200	150
Exterior girder stiffness @ piers	I (in.^{4})	473,700	473,700
Model Correlation Parameter		**Initial Model Value**	**Final Model Value**
Correlation coefficient		0.9508	0.9725

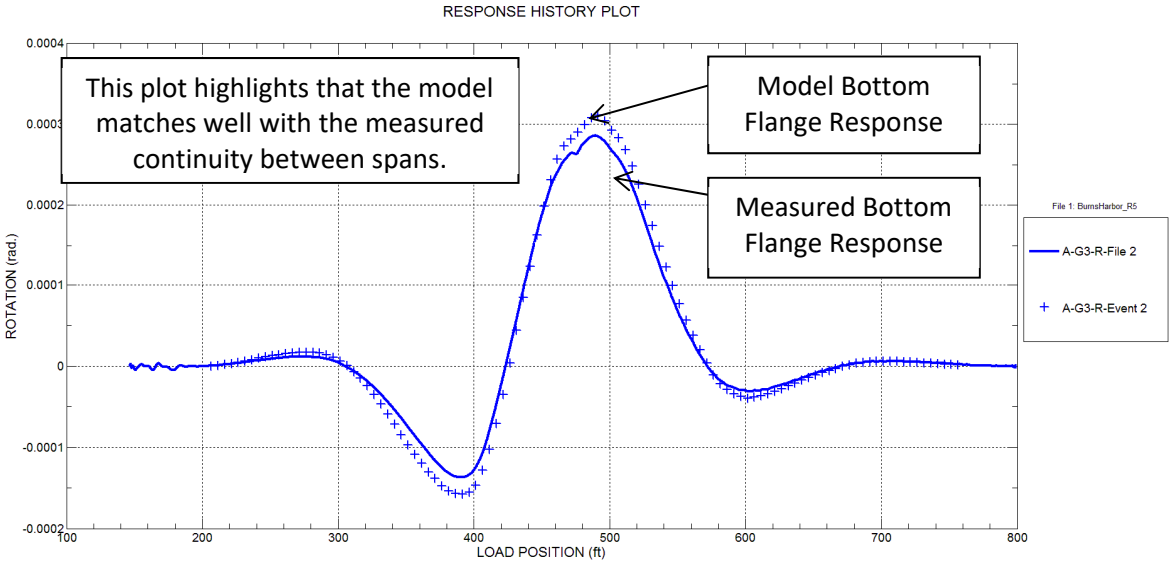

FIGURE 7-44 Beam-end rotation of interior girder G3 at Pier 6, Span F.

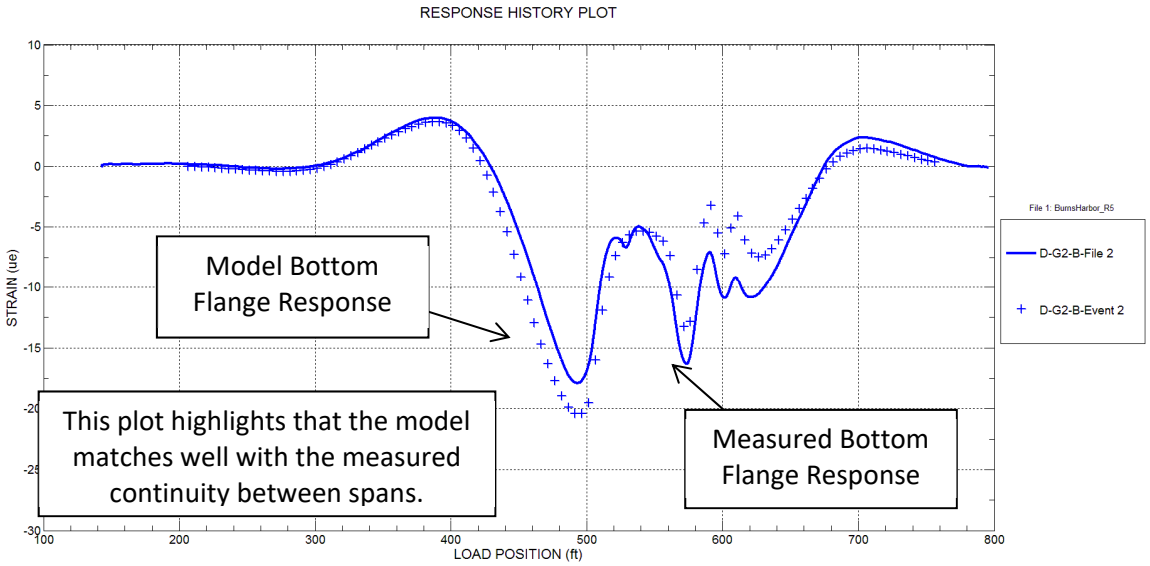

FIGURE 7-45 Bottom flange strain of interior girder G2 at Pier 7, Span G.

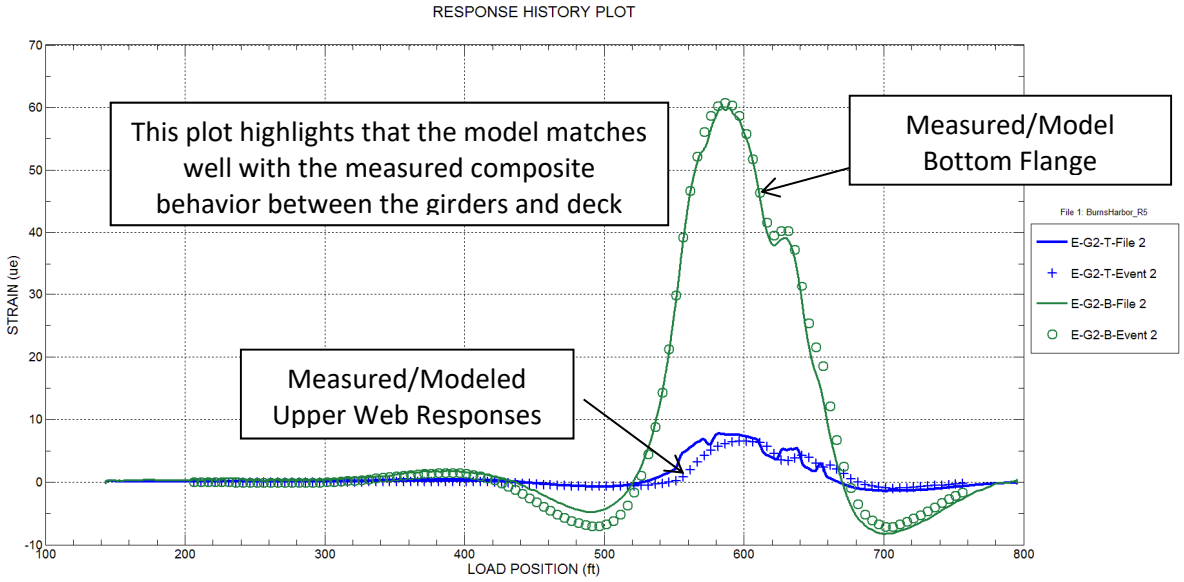

FIGURE 7-46 Bottom flange and upper web strains of interior girder G2 at midspan of Span G.

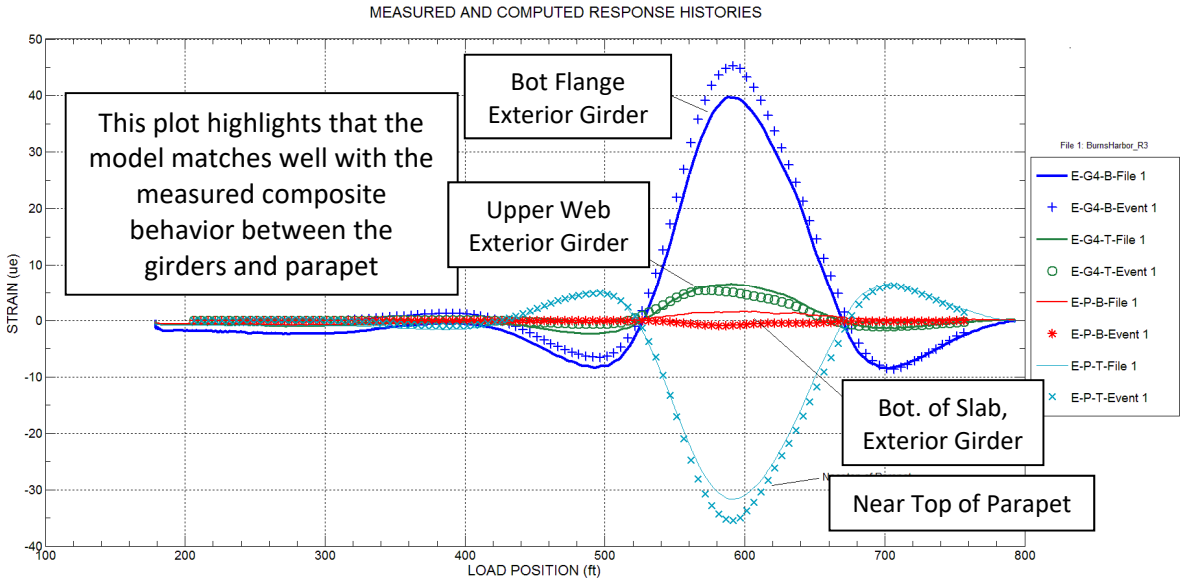

FIGURE 7-47 Exterior girder and parapet strain comparison at G4 at midspan of Span G.

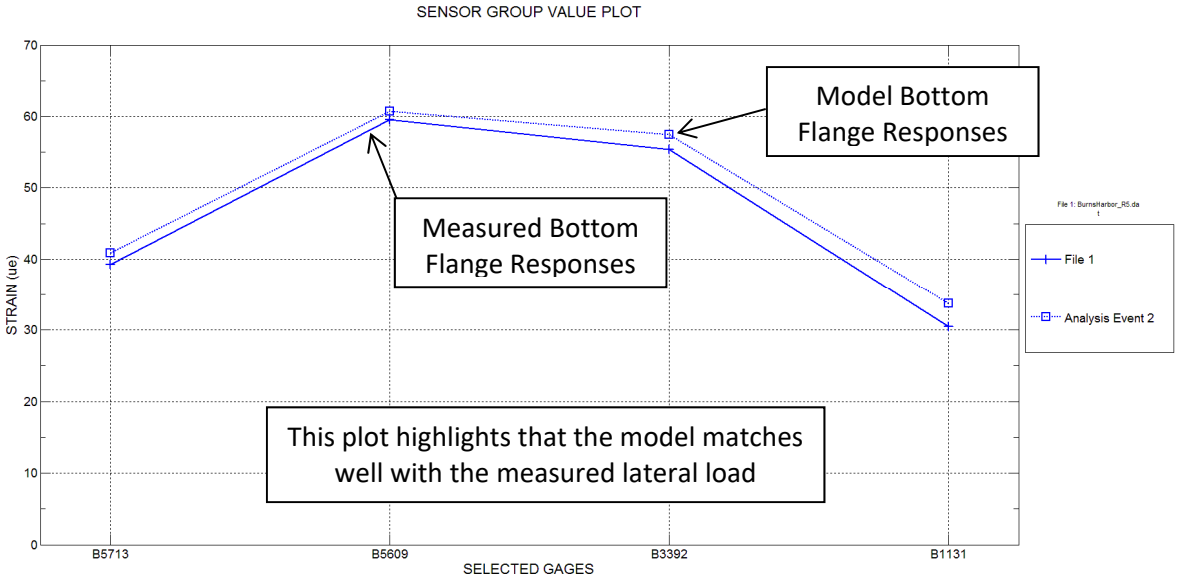

FIGURE 7-48 Midspan lateral strain distribution: Girders 1 through 4 at Span G during maximum moment.

Load Rating Procedures and Results

Load rating was performed on all appropriate bridge elements in accordance with the AASHTO LFR guidelines. Structural responses were obtained from the calibrated model, and member capacities were determined from the design drawings and AASHTO LRFD equations for shear and moment of PS/C beams. The rating methods used closely match typical rating procedures, with the exception that a field-verified FEM analysis was used rather than typical AASHTO distribution factors. This section briefly discusses the methods and findings of the load rating procedures.

All live load responses were computed from the field-verified model, which included the contribution of the parapets in the positive moment regions. Dead load responses were computed from two separate models. A simply supported, noncomposite model was generated for the overall structure self-weight. A composite model without parapet stiffness was used for the superimposed dead load consisting of the parapet and deck overlay.

Load ratings were performed on the final refined model according to the AASHTO *Manual for Condition Evaluation of Bridges* (*198*) (see Table 7-12 for a summary of analysis information and applied load and resistance factors). Given that the permit vehicles will be fully escorted and 18-ft (5.5-m) wide only single-lane loading was applied. A variation of plus or minus 2 ft (0.61 m) on the truck path was considered to account for slight off-center loading. Table 7-12 shows the load configuration for the heaviest permit vehicle. All proposed vehicles have the same trailer axle configuration. All structural dead loads were automatically applied by the modeling program's self-weight function along with an additional 150 lbs/ft^2 (7.2 kN/m^2) for the new wearing surface.

Member capacities were calculated based on the specified design properties; PS/C compressive strength of 5.5 ksi (38 MPa), 270 ksi (1862 MPa) low relaxation prestressing strands, and a yield stress of 60 ksi (414 MPa) for non-prestressed steel. A summary of the girder moment and shear capacities are provided in Table 7-13 through Table 7-15. A summary of capacities and

applied loads are provided in Table 7-16. For simplicity, girder capacities are provided for Span 5 (35 m) and Span 6 (31 m) only as the rating factors for all limit states were controlled by these spans. Controlling load ratings for the heaviest permit load configuration are provided in Table 7-17.

TABLE 7-12 Structure Information and Applied Load and Resistance Factors.

Description	Prestressed bulb-T-girder bridge: 4-beam lines composite with deck (200-mm thick Class C Conc) 10 spans (26.4, 30.0, 30.0, 30.0, 35.0, 31.0, 31.0, 31.0, 31.0, and 26.4 m) 1,524-mm deep bulb-T PS/C girders with 30-mm haunch between girder and slab Bridge designed continuous for live load across interior piers
Sources of information	Structural plans: Inspection report, 1/26/2016 Transport diagram Load test transport diagram Load test data and model calibration
Analysis type	Quasi 3D grid model with 2D footprint of permit load (see figure) Bridge was modeled with accurate span lengths, pier widths, beam spacing and skew angle All 10 spans were modeled to obtain accurate pier loading. Continuity for live load modeled by tension (slab)-compression (btm of girder) couple over pier (continuity calibrated using the response data near the piers)
Load factors	LRFD serviceability: DL factor = 1.0 LL factors = 1.0 LRFD strength I: DC DL factor = 1.25 Superimposed DW DL factor = 1.50 LL factor = 1.30 Impact/dynamic = 0.0
Loads considered	Dead load: Self-weight 150 lbs/ft^3 (23.6 kN/m^3) concrete, including 1.5 in (38 mm) of concrete overlay Girders modeled as simply supported and non-composite for self-weight and slab loading Girders modeled with continuity and composite for overlay and parapet loading Live-load transport: (see figures) Planar grid of point loads moving at 5.0-ft (1.5-m) intervals Girders modeled with continuity and composite with slab, verified with load test data
Controlling rating factors	RF = 1.56 serviceability (tensile stress limit) of PS girders RF = 2.56 strength midspan flexural moment of 35 m span
Restrictions	Transport must travel down centerline of bridge with ± 2 ft (0.6 m) tolerance No other vehicles or equipment shall be on bridge during permit load crossing Transport to travel at 5 mph (8 km/h) to eliminate impact or dynamic response

TABLE 7-13 Girder Serviceability Limit (ASD Flexural Moment Available for Live Load)

Span No.	$Moment_{DC}$ (kip-in.)	$Moment_{DW}$ (kip-in.)	$Stress_{DL\_Total}$ (ksi)	$Stress_{PS\_A\_NC}$ (ksi)	$Stress_{PS\_Ecc\_NC}$ (ksi)	$Stress_{PS\_Allowable}$ (ksi)	Live Load Service Moment Capacity (kip-in.)
5	40,484	1793.6	2.95	1.34	2.47	1.32	25,342.6
6	31,898	1230.5	2.31	1.03	1.99	1.17	22,448.6

TABLE 7-14 Girder Ultimate Moment Capacity

Span No.	Composite PS Depth		Compression Block	Average Prestress Stress	Nominal Moment Capacity
	PS_{Depth_PosC}, in.	c, in.	a, in.	$f_{ps\_comp\_Pos}$, ksi	$M_{ps\_comp\_Pos}$, kip-in.
5	61.97	5.84	4.96	262.88	124,411
6	64.12	4.30	3.65	264.93	95,956

TABLE 7-15 Girder Shear Capacity (Ultimate Strength)

Span No.	Shear Stirrup Area		Effective Shear Depth	Stirrup Spacing	Theta	Beta	Steel Shear Capacity	Concrete Shear Capacity	Nominal Shear Strength	Design Shear Strength
	Av, $in.^2$	Av_min	d_v, in.	S, in.	θ	β	Vs, Simple	Vc, simple	Vn, Simple	φVn, Simple
5	0.62	OK	61.92	6	45	2	383.88	66.80	450.68	405.61
6	0.62	OK	62.72	6	45	2	388.85	67.66	456.51	410.86

Note: Capacities conservatively utilized typical RC assumptions (base-line check).

TABLE 7-16 Summary of Capacities and Applied Loads

Group Name	Mode	RF	Capacity	DC	DW	LL	Location
Span 5 Interior Girder	+My	3.36	124,412	40,484	1,794	16,289	Interior Girder at midspan
	Fz	1.82	451	114	10	105	Interior Girder near support
	Service	1.56	25,343	N/A	N/A	16,289	Interior Girder at midspan
Span 6 Interior Girder	+My	3.15	95,957	31,898	1,231	13,237	Interior Girder at midspan
	Fz	2.17	457	101	9	96	Interior Girder near quarter span
	Service	1.70	22,449	N/A	N/A	13,237	Interior Girder at midspan

TABLE 7-17 Load Rating Results for Heaviest Permit Load Configuration.

Transport Description	Limit State	GVW (kips)	Applied Load Factors			Rating Factor
			DL	LL	Dynamic	Permit
2 wide, 14 line Eastrac Goldhofer	Service	848	1.00	1.00	0.0	**1.56**
	Strength I	848	1.25	1.30	0.0	**2.56**

NOTE: Transport must travel centered on the bridge roadway with a ±2-ft tolerance. No other traffic or equipment can be on the bridge during crossing. Transport must travel 5 mph or slower to eliminate impact or dynamic effects.

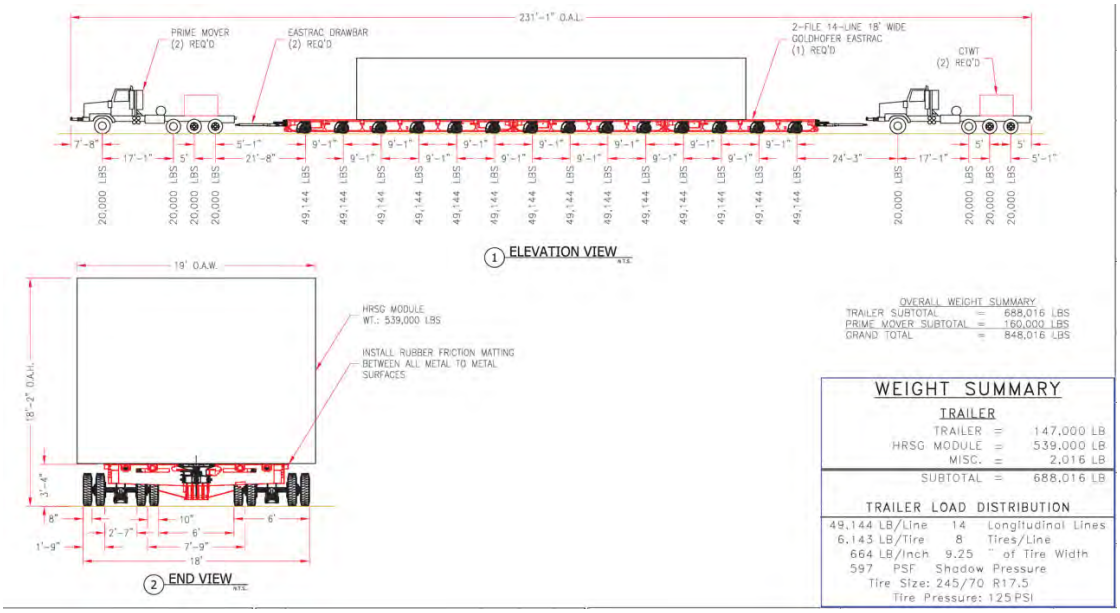

FIGURE 7-49 Proposed permit load rating vehicle configuration.

Example of a Proof Load Test: Introduction

Built in 1968, the Maryland Route 16 over Mill Creek bridge carries two traffic lanes, one in northbound (NB) and one in southbound (SB) direction, with a shoulder on each side. The bridge has one simply supported span with a span length of 50 ft, 0 in. (15.2 m) measured between the centerlines of bearings. The width of the bridge is 45 ft, 6 in. (13.9 m) out-to-out and 42 ft, 0 in. (12.8 m) clear roadway.

The superstructure consists of 11 precast PS/C adjacent box beams with three $1^5/_8$ in. (41 mm) diameter tie rods across all beams located near both ends and midspan. The PS/C box beams have exterior cross-sectional dimensions of 4 ft, 0 in. (1.2 m) wide by 2 ft, 3 in. (686 mm) deep each. The bridge has a concrete overlay of varying thickness (approximately 1⅞ to 3¼ in.; 48 to 83 mm) on top of the box beams.

Previous inspection reports identified multiple types of deterioration in the superstructure, including reflective cracks in the overlay along the longitudinal beam joints, broken prestressing strands, beam spalls, etc. Beam 7 appeared to have experienced most pronounced deterioration including concrete spalls as well as exposed prestressing strands.

Bridge load ratings for the as-inspected condition to account for existing deteriorations were calculated previously using the LARSA Bridge computer software per the AASHTO LFR

method. For the Maryland Type 4 (MD T4) vehicle of 70,000 lbs (311 kN) GVW, the bridge load rating was found to be governed by shear with an Operating Rating Factor (RF_{OPR}) of 0.19. For bending moment, the RF_{OPR} was calculated 1.19 considering a reduction in flexural strength based on a loss of six prestressing strands.

Due to the insufficient load ratings as well as uncertainties in calculating load carrying capacities of the box beams, proof load testing was chosen as a refined method to determine load ratings of the bridge for the MD T4 vehicle in accordance with the AASHTO MBE.

Instrumentation Set-Up

The bridge was instrumented with a total of 24 sensors along the mid-span, including 15 strain transducers of 3 in. (76 mm) gage length and nine displacement transducers, as shown in Figure 7-50. Strain transducers were installed on the soffit of all box beams near their centers with additional gages installed below the webs of select beams (B4, B5, and B7). The joint between Beams 4 and 5 exhibited the most severe longitudinal crack in the wearing surface (Figure 7-51). Beam 7 was in the worst condition of all beams exhibiting many spalls and exposed prestressing strands (Figure 7-52). Displacement transducers were positioned below the centers of all interior beams and mounted on a temporary timber beam support from the ground, which allowed measurement of vertical deflections of the box beams (Figure 7-52). All sensors were connected to a digital data acquisition system to record real-time strain and displacement responses.

Shear was found analytically to govern load ratings of this bridge. However, direct instrumentation for shear was not possible because no access was available to any interior beam webs. The implemented instrumentation plan was able to reflect nonlinear or non-elastic structural response due to any damages or failures in the flexural or shear loading mode.

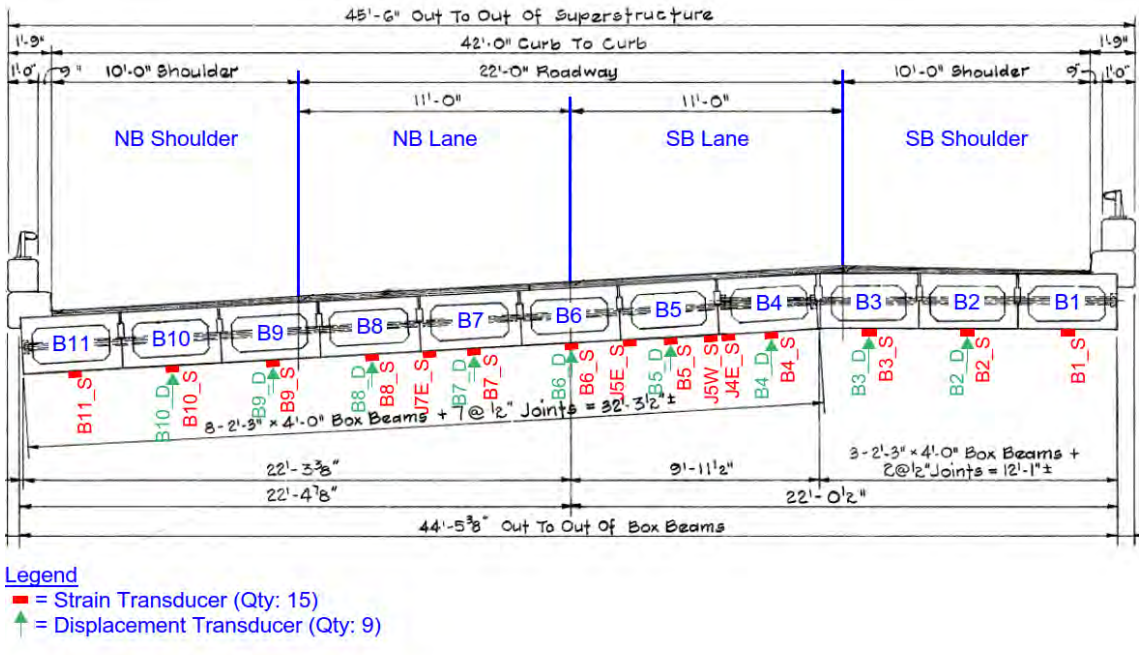

FIGURE 7-50 Instrumentation plan: section view (looking south).

FIGURE 7-51 Cracking of bridge overlay along joints of box beams.

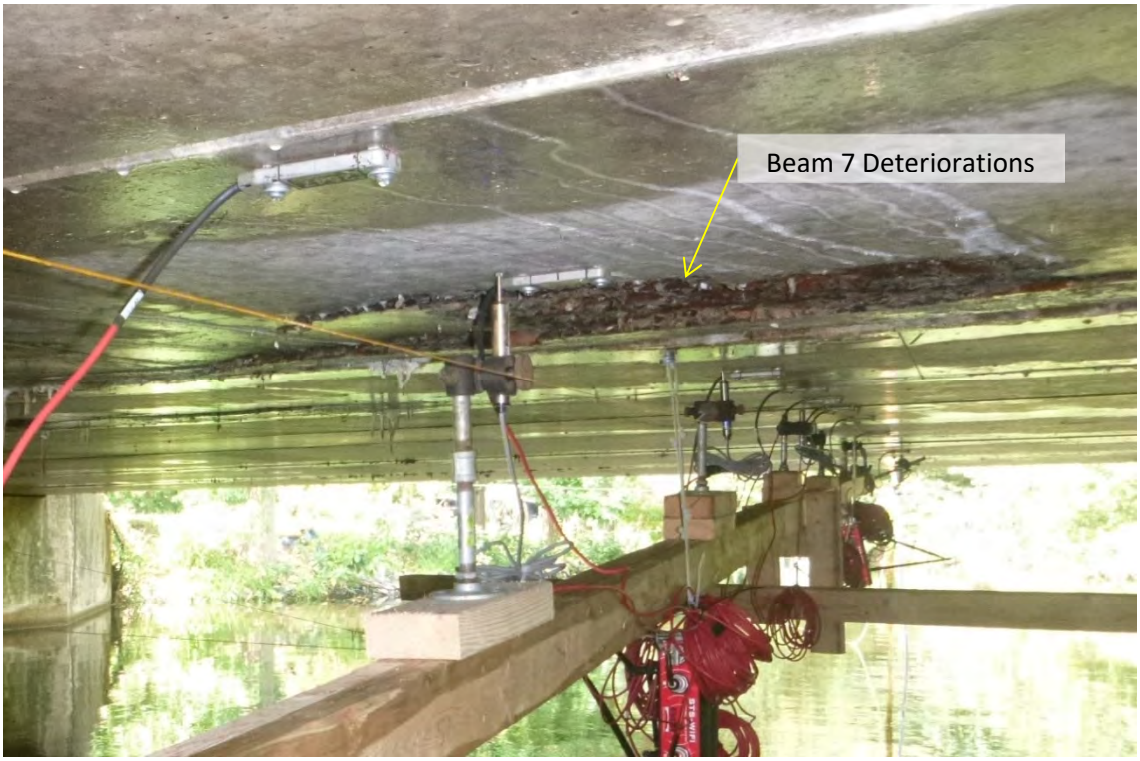

FIGURE 7-52 Sensor set-up and Beam 7 exhibiting spalls and exposed prestressing strands.

Proof Load Testing

A proof load test was performed using two four-axle dump trucks, with axle configurations similar to the MD T4 vehicle. The entire load test was conducted with the test trucks' lift axle lifted for more severe load effects. Based on guidance of the AASHTO MBE, a target proof load for the load test was established to be 98,000 lbs (436 kN) GVW based on a base live load magnification factor of 1.40 (70 kips x 1.40 = 98 kips = 436 kN) without dynamic impact. The live load factor at the operating level of the AASHTO LFR method is 1.3.

The proof load test was conducted and successfully completed at four increasing load levels of the same loading positions. At each load level, one truck was used to cross the bridge at different lateral positions to represent actual live load positions and to check primary load path components. Upon successful completion of the single truck crossings without any signs of distress, both trucks crossing side-by-side were used to load the bridge. The axle weights and configurations of the test trucks at all four load levels are described in Figure 7-53.

A total of 30 test runs were conducted as listed in Table 7-18. Real-time strain and displacement responses were recorded during each test run. At each of the four test load levels, seven test runs were conducted at a crawl speed (5 mph = 8 km/h or less) in different crossing configurations to assess the linear elastic behavior of all beams subject to increasing load. Additionally, Test Runs 15 and 16 were conducted at 40 mph (64 km/h) to investigate the effects of dynamic impact. The bridge was closed to regular traffic intermittently during the load test. After each test run, recorded strain and displacement responses were reviewed for the magnitudes and zero-return. No signs of distress in the bridge were observed at any load level throughout the load test.

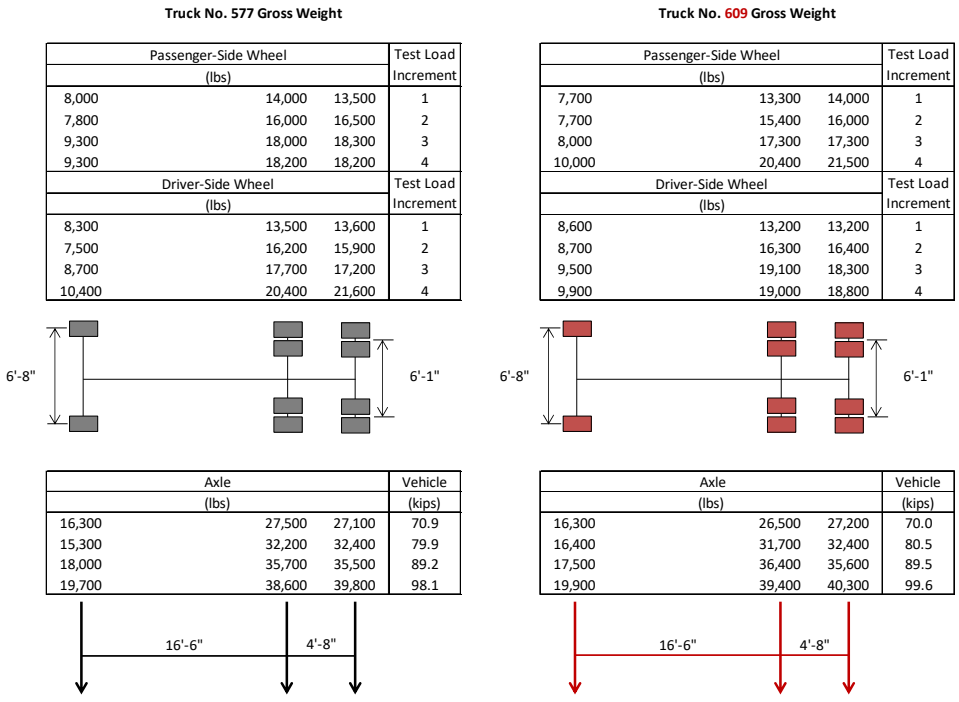

FIGURE 7-53 Measured weight and spacing of test truck axles.

TABLE 7-18 Summary of Test Runs with Test Truck Loading Configurations

Test Run	Start Time	Speed	Test Truck No. (GVW) and Lane Position				Travel Direction	Comments
			SB Shoulder	SB Lane	NB Lane	NB Shoulder		
1	12:50 PM	5 MPH	-	-	-	**577** (70.9k)	NB Fwd	
2	12:52 PM		-	-	**609** (70.0k)	-	NB Fwd	
3	12:54 PM		**577** (70.9k)	-	-	-	SB Fwd	
4	12:55 PM		-	**609** (70.0k)	-	-	SB Fwd	
5	1:00 PM		-	-	**609** (70.0k)	**577** (70.9k)	NB Fwd	Side-by-side
6	1:02 PM		**577** (70.9k)	**609** (70.0k)	-	-	SB Fwd	Side-by-side
7	1:05 PM		-	**609** (70.0k)	**577** (70.9k)	-	NB Fwd	Side-by-side
8	1:44 PM	5 MPH	-	-	-	**577** (79.9k)	NB Fwd	
9	1:45 PM		-	-	**609** (80.5k)	-	NB Fwd	
10	1:46 PM		**577** (79.9k)	-	-	-	SB Fwd	
11	1:47 PM		-	**609** (80.5k)	-	-	SB Fwd	
12	1:49 PM		-	-	**609** (80.5k)	**577** (79.9k)	NB Fwd	Side-by-side
13	1:51 PM		**577** (79.9k)	**609** (80.5k)	-	-	SB Fwd	Side-by-side
14	1:52 PM		-	**609** (80.5k)	**577** (79.9k)	-	NB Fwd	Side-by-side
15	2:00 PM	40 MPH	-	-	**609** (80.5k)	-	NB Fwd	Dynamic Impact
16	2:09 PM		-	**609** (80.5k)	-	-	SB Fwd	Dynamic Impact
17	2:16 PM	5 MPH	-	-	-	**577** (89.2k)	NB Fwd	
18	2:18 PM		**577** (89.2k)	-	-	-	SB Fwd	
19	2:19 PM		-	**577** (89.2k)	-	-	SB Fwd	
20	2:20 PM		-	-	**577** (89.2k)	-	NB Fwd	
21	2:45 PM		-	-	**609** (89.5k)	**577** (89.2k)	NB Fwd	Side-by-side
22	2:46 PM		**577** (89.2k)	**609** (89.5k)	-	-	SB Fwd	Side-by-side
23	2:48 PM		-	**609** (89.5k)	**577** (89.2k)	-	NB Fwd	Side-by-side
24	3:38 PM	5 MPH	-	-	-	**577** (98.1k)	NB Fwd	
25	3:39 PM		**577** (98.1k)	-	-	-	SB Fwd	
26	3:40 PM		-	**577** (98.1k)	-	-	SB Fwd	
27	3:41 PM		-	-	**577** (98.1k)	-	NB Fwd	
28	4:08 PM		-	-	**609** (99.6k)	**577** (98.1k)	NB Fwd	Side-by-side
29	4:10 PM		**577** (98.1k)	**609** (99.6k)	-	-	SB Fwd	Side-by-side
30	4:12 PM		-	**609** (99.6k)	**577** (98.1k)	-	NB Fwd	Side-by-side

Test Results Summary

Test results were plotted in the form of test load versus sensor peak response to investigate the linear-elastic behavior of the adjacent box beams during the proof load test. Figure 7-54 shows the total gross weight of the test truck versus the peak strain and the peak deflection from all sensors for single truck crossings in the SB shoulder (Test Runs 3, 10, 18, and 25) at all four increasing load levels. Similar plots were made for all seven test truck loading configurations including single truck crossings in the NB shoulder, NB lane, SB shoulder, and SB lane, as well

as two-truck side-by-side crossings in the NB shoulder and NB lane, SB shoulder and SB lane, and NB and SB lanes. In these plots, the slope of the line between any two adjacent data points represents the stiffness of the structure in terms of strain or deflection. For an ideal linear-elastic structure, both the strain and deflection responses should increase linearly with a load increase applied in the same pattern. Particular attention should be paid to any noticeable decrease of the slope with the increase of test load, as this may be an indication of nonlinear structural behavior.

In bridge field testing, the lateral position of test vehicles may vary slightly among the test runs intended to be of the same lateral position, resulting in different load distribution among sensors. This phenomenon is practically inevitable as reflected in the results from some sensors as seen in Figure 7-54, where the slope of the line changes between load increments.

It is important to examine the general trend of the load-response lines of all the sensors over all the load steps. A review of all the load-response plots indicated that the slope change happened in different directions at different load steps without a general trend of decreasing slope with increasing load (Figure 7-54). Therefore, this is a result of variation of lateral truck position among the test runs but not due to nonlinear structural behavior.

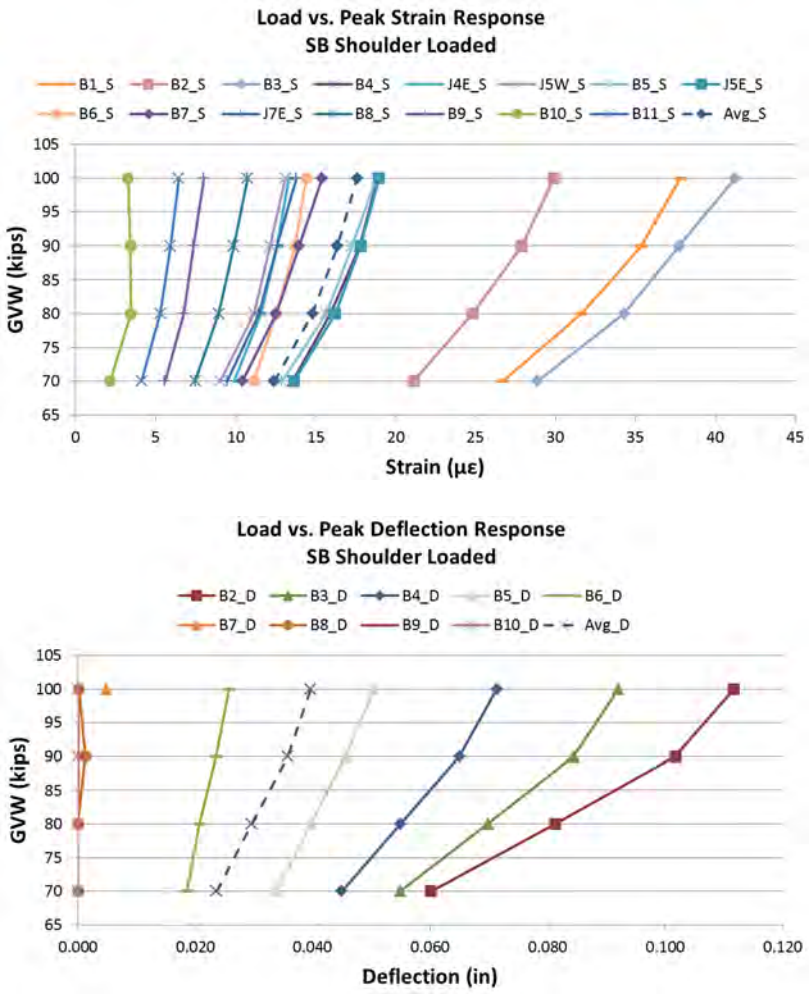

FIGURE 7-54 GVW versus peak strain response (top) and peak deflection response (bottom) for single truck crossing in SB shoulder (Test Runs 3, 10, 18 and 25).

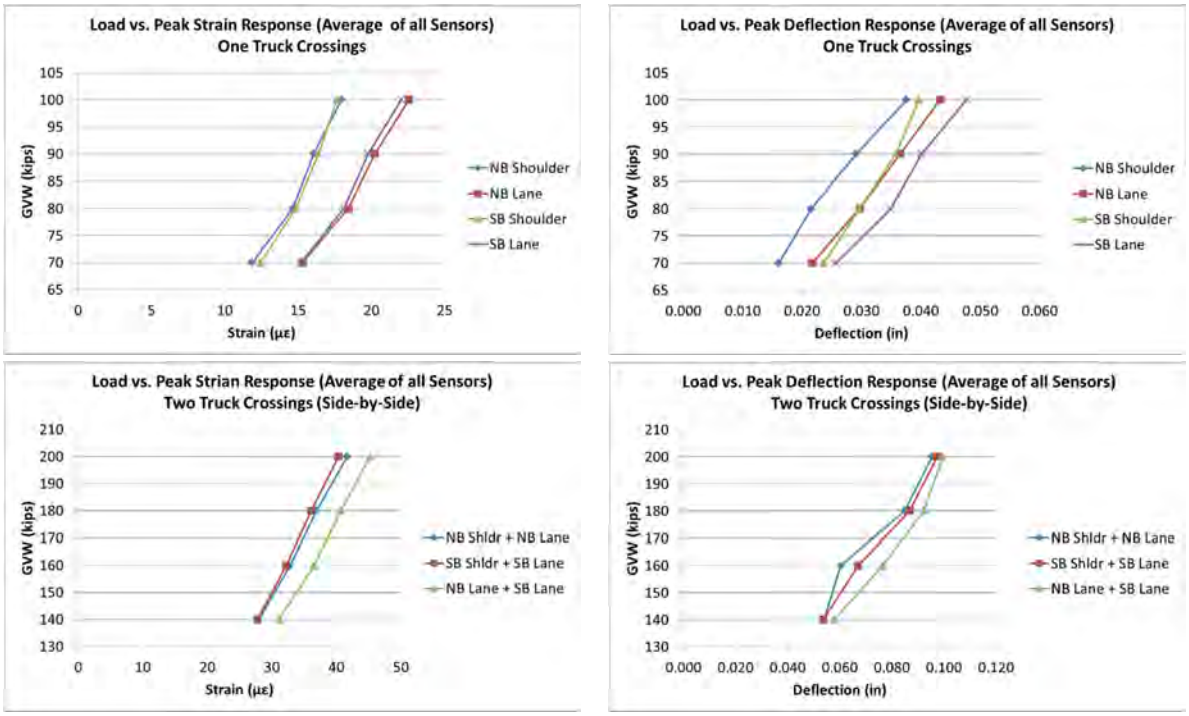

FIGURE 7-55 Load versus average peak response for strain (left) and deflection (right) for one-truck crossings (top) and two-truck crossings side-by-side (bottom).

Figure 7-55 plots the average maximum response of all the box beams with increasing test load for the one-truck and two-truck crossing test runs. The average response better represents the overall structural behavior since the effects of lateral shifting of truck position on different beams tend to cancel each other. From these plots, it is concluded that the bridge performed within the linear elastic range throughout the proof load test.

Key findings from the proof load test results are

- Time history plots from all strain and displacement transducers had smooth and distinctive response to the crossings of the test vehicles. All sensor readings return to 0 after unloading at the end of each test run, further suggesting general elastic behavior of the structure at the test load levels;
- For the one-truck test runs, the maximum measured strain was 50 με (corresponding to 156 psi = 1.08 MPa), occurring at Beam 11 during Test Run 24; the maximum measured deflection was 0.112 in. (2.8 mm) occurring at Beam 2 during Test Run 25; and
- For the two-truck (side-by-side) test runs, the maximum measured strain was 82 με (corresponding to 256 psi = 1.77 MPa), occurring at Beam 8 during Test Run 28; the maximum measured deflection was 0.177 in. (4.5 mm) occurring at Beam 2 during Test Run 29.

Live Load Distribution Factor

Lateral distribution of live load was assessed using the maximum measured tensile strain from the transducers located along the center of each beam. For a certain live load applied to a multi-

beam bridge, the maximum portion of the live load carried by a beam is typically called the LLDF and may be quantified as

$LLDF_{truck} = N(\varepsilon_{max}/\Sigma\varepsilon_i)$ truck load per beam
where, for a certain cross section

ε_{max} = highest measured strain of all beams;
$\Sigma\varepsilon_i$ = summation of measured strains for all beams;
N = number of side-by-side trucks in the test load during measurement; and
$LLDF_{truck}$ = live load distribution factor for truck load per beam.

Based on field measurements, the LLDF determined from the load test is 0.217 truck/beam for one lane loaded and 0.329 truck/beam for two lanes loaded.

For reference information, design provisions were reviewed regarding the LLDF per the AASHTO Standard Specifications and LRFD Bridge Design Specifications. For adjacent box beams, the LLDF depends on the interaction between the beams, which is developed through longitudinal shear keys in combination with transverse ties.

The LRFD Specifications (Article 4.6.2.2.2b) provide LLDFs for two different cases: (1) adjacent boxes sufficiently connected to act as a unit and (2) adjacent boxes connected only enough to prevent relative vertical displacement at their interface. For Case 1, the LLDF for flexure of the 4 ft (1.2 m) wide box beams of Bridge 0500100 is 0.219 truck/box for one lane loaded and 0.295 truck/box for two lanes loaded. For Case 2, the LLDF for flexure is 0.344 truck/box regardless the number of lanes loaded.

The Standard Specifications (Article 3.23.4) have provisions for determining the LLDF only for the more-conservative Case 2 of the LRFD Specifications. Using the formulas provided, the LLDF was calculated to be 0.344 truck/box for three loaded lanes based on the clear roadway width of the bridge.

In an extreme condition when the interaction between adjacent beams is completely lost, the highest amount of live load an individual 4 ft (1.2 m) wide box beam could carry would be one-half the truck load or one wheel line, or LLDF = 0.5 truck/box.

Vehicle Load Dynamic Impact

To investigate the effects of vehicle load dynamic impact, beam responses to a test truck crossing at a dynamic speed (around 40 mph = 64 km/h) was compared with the crossing of the same truck at a crawl speed (less than 5 mph = 8 km/h). The ratio of the peak measured responses from the dynamic crossing to the static crossing from the same sensor is used to represent field measured dynamic impact factor.

Maximum measured strains and displacements due to the same truck traveling in the NB lane (Test Runs 9 versus 15) and the SB lane (Test Runs 11 versus 16) were used to determine vehicle load dynamic impact. Impact factors were calculated for the heaviest loaded beams directly below or near the wheel lines. The maximum impact factor was found to be 1.36 from strain measurements and 1.34 from displacement measurements at Beam 9. Dynamic impact from measurements at all other beams was found no higher than 1.22.

It should be noted that Beam 9 is most likely not directly under truck wheel loads as shown in Figure 7-50. Field measurements indicated that Beam 8 (directly under truck wheel

load) experienced higher responses than Beam 9 in the crawl speed crossing but the two beams experienced nearly the same responses in the high speed crossing. This suggests that the lateral truck position shifted towards the shoulder slightly in Test Run 15 thus measurements from Beam 9 likely overestimated the dynamic impact factor.

In comparison, the live load impact factor is 1.29 per the AASHTO *Standard Specifications* and 1.33 per the LRFD Specifications.

Bridge Load Ratings

Bridge load ratings can be derived from the maximum proof live load concluded by a proof load test in accordance with the AASHTO MBE (72). Using the AASHTO LFR method, a lower-bound Operating Rating Factor (RF_{OPR}) based on the results of a successfully completed proof load test can be calculated as

For two lanes loaded: $RF_{OPR} = (W_P/W_R)(f_V)/(\gamma_{LL}I)$ (7.1)

where

W_R = GVW of rating vehicle MD T4 = 70,000 lbs (311 kN);
W_P = average GVW of two side-by-side trucks at maximum proof load = 98,900 lbs (440 kN);
γ_{LL} = LFR live load factor at the operating level = 1.3;
I = LFR live load impact factor for a 50 ft (15 m) span length = 1.29; and
f_V = vehicle adjustment factor for axle configuration difference between test trucks and rating vehicle = 0.99 for bending; 1.01 for shear, as shown in Table 7-19.

Since the axle configuration (spacings and weight distribution) of the test trucks is not identical to the rating vehicle MD T4, an equivalent weight of MD T4 (W_{eq}) for the same load effect as the test truck at the maximum proven load needs to be determined. Based on results from a structural analysis of the 50 ft (15 m) span box beam, Table 7-19 provides W_{eq} for maximum bending moment (M_{max}) at mid-span and maximum shear force (V_{max}) at support, as well as the vehicle adjustment factor (f_V) for bending and shear.

For two lanes loaded, as shown in Table 7-19, a lower bound bridge load rating was calculated as $RF_{OPR} = 0.84$ using Equation 7.1 and $f_V = 0.99$ based on bending because it results in a lower rating even through a previous rating analysis indicated that shear governed the load rating of this bridge. The LFR live load impact factor of 1.29 was used although load test measurements suggested slightly higher dynamic impact due to lateral shifting of test vehicle position.

For single lane loaded, bridge load rating could be increased by the ratio of maximum measured beam strain due to two trucks side-by-side (82 με) to that due to one truck (50 με). This increase of ratio 1.64 (82/50) is in agreement with the LRFD provisions for multiple presence of live load (Article 3.6.1.1.2), where the Multiple Presence Factor is specified as 1.00 for two lanes loaded and 1.20 for one lane loaded (2 x 1.00/1.20 = 1.67).

Thus, for single lane loaded

$RF_{OPR} = 0.84x1.64 = 1.38$ for MD T4

TABLE 7-19 Load Effects of Rating Vehicle and Maximum Proven Load, Vehicle Adjustment Factor (f_V), and a Lower-Bound Bridge Load Rating

Vehicle	W (lbs)	M_{max} (k-ft)	V_{max} (kips)	M Effects			V Effects		
				W_{eq} (lbs)	f_V	RF_{OPR}	W_{eq} (lbs)	f_V	RF_{OPR}
MD Type 4	70,000	699.11	60.96	98,056	**0.99**	**0.84**	99,752	**1.01**	0.85
Test Truck	98,900	979.31	86.87						

Conclusions

The following are made based on the field test results:

- Decisions on bridge posting for weight restrictions should consider the actual loading condition at the bridge site. If two trucks side-by-side crossing at a dynamic speed can be a realistic event, Bridge 0500100 should be posted for 58,800 lbs (262 kN) GVW for single unit vehicles (0.84 x 70,000=58,800 lbs = 262 kN). Otherwise, the structure has sufficient strength for single lane loading and no posting should be necessary.
- Repairs should be made to the bridge deck overlay to prevent water leakage through the longitudinal beam joints for preserving the durability of the beams. Improved deck surface condition will also reduce dynamic impact of vehicle load.

If any significant change or deterioration occurs, a re-evaluation of the bridge may be required.

SELECTED FURTHER READING OF REPORTED LOAD TESTS

For an overview of load tests reported in the literature, refer to Lantsoght et al. (*199*). Less common types of load tests, such as on timber (*123*, *124*, *200–203*), masonry (*28*, *204–211*), and historical bridges (*26*, *27*, *212*, *213*) are documented in the literature as well, and the reader is encouraged to check the cited references as part of preparations for a similar load test. An overview of all proof load tests that were carried out in the Netherlands over the past decade is given in (*214*). Further illustrative examples can be found in (*215*, *216*).

References

1. Bolle, G., G. Schacht, and S. Marx. Loading Tests of Existing Concrete Structures - Historical Development and Present Practise. *FIB Symposium*, Prague, Czech Republic, 2011, p. 14.
2. Cochet, D., et al. *Load Tests on Highway Bridges and Pedestrian Bridges* (in French). Setra–Service d'Etudes Techniques des Routes et Autoroutes, Bagneux-Cedex, France, 2004.
3. Veneziano, D., D. Galeota, and M. M. Giammatteo. Analysis of Bridge Proof-Load Data I: Model and Statistical Procedures. *Structural Safety*, Vol. 2, No. 2, 1984, pp. 91–104. https://doi.org/10.1016/0167-4730(84)90013-4.
4. Veneziano, D., D. Galeota, and M. M. Giammatteo. Analysis of Bridge Proof-Load Data II. Numerical Results. *Structural Safety*, Vol. 2, No. 3, 1985, pp. 177–198. https://doi.org/10.1016/0167-4730(85)90025-6.
5. Brühwiler, E., T. Vogel, T. Lang, and P. Lüchinger. Swiss Standards for Existing Structures. *Structural Engineering International*, Vol. 22, No. 2, 2012, pp. 275–280. https://doi.org/10.2749/101686612X13291382991209.
6. Taylor, P., T. Hosteng, X. Wang, and B. Phares. *Evaluation and Testing of a Lightweight Fine Aggregate Concrete Bridge Deck in Buchanan County, Iowa*. InTrans Project 12-434; IHRB Project TR-648. Iowa State University, 2016, p. 51.
7. Hernandez, E. S., and J. J. Myers. In-Situ Field Test and Service Response of Missouri Bridge A7957. Proc., European Bridge Conference, Edinburgh, U.K., 2015, p. 10.
8. Au, A., C. Lam, J. Au, and B. Tharmabala. Eliminating Deck Joints Using Debonded Link Slabs: Research and Field Tests in Ontario. *Journal of Bridge Engineering*, Vol. 18, No. 8, 2013, pp. 768–778. https://doi.org/10.1061/(ASCE)BE.1943-5592.0000417.
9. Frangopol, D. M. and S. Kim. Chapter 10: Bridge Health Monitoring. In *Bridge Engineering Handbook, Vol. 5: Construction and Maintenance* (W. F. Chen and L. Duan, eds.) CRC Press/ Taylor & Francis Group, Boca Raton, Fla., 2014, p. 247–268.
10. Hendriks, M. A. N., A. de Boer, and B. Belletti. *Guidelines for Nonlinear Finite Element Analysis of Concrete Structures*. Report RTD:1016-1:2017. Rijkswaterstaat Centre for Infrastructure, 2017.
11. Ferreira, D., J. Bairán, and A. Marí. Efficient 1D Model for Blind Assessment of Existing Bridges: Simulation of a Full-Scale Loading Test and Comparison with Higher Order Continuum Models. *Structure and Infrastructure Engineering*, Vol. 11, No. 10, 2015, pp. 1383–1397. https://doi.org/10.1080/15732479.2014.964734.
12. Puurula, A. M., O. Enochsson, G. Sas, T. Blanksvärd, U. Ohlsson, L. Bernspång, B. Täljsten, and L. Elfgren. Loading to Failure and 3D Nonlinear FE Modelling of a Strengthened RC Bridge. *Structure and Infrastructure Engineering*, Vol. 10, No. 12, 2014, pp. 1606–1619. https://doi.org/10.1080/15732479.2013.836546.
13. Ghodoosi, F., A. Bagchi, and T. Zayed. System-Level Deterioration Model for Reinforced Concrete Bridge Decks. *Journal of Bridge Engineering*, Vol. 20, No. 5, 2014, p. 10.
14. Belletti, B., et al., Developing Standardized Guidelines for Safety Assessment of Shear-Critical RC Beams Based on Nonlinear Finite Element Modeling. Proc., *3rd FIB International Congress*, Washington, D.C., 2010, p. 13.
15. Fanning, P. J., L. Sobczak, T. E. Boothby, and V. Salomoni. Load Testing and Model Simulations for a Stone Arch Bridge. *Bridge Structures (Abingdon)*, Vol. 1, No. 4, 2005, pp. 367–378. https://doi.org/10.1080/15732480500453532.
16. Schacht, G., G. Bolle, and S. Marx. Belastungsversuche—Internationaler Stand des Wissens. *Bautechnik*, Vol. 93, No. 2, 2016, pp. 85–97. https://doi.org/10.1002/bate.201500097.
17. Fu, G., F. P. Pezze III, and S. Alampalli. Diagnostic Load Testing for Bridge Load Rating. *Transportation Research Record 1594*, 1997, pp. 125–133. https://doi.org/10.3141/1594-13.

18. Barker, M. G. Quantifying Field-Test Behavior for Rating Steel Girder Bridges. *Journal of Bridge Engineering*, Vol. 6, No. 4, 2001, pp. 254–261. https://doi.org/10.1061/(ASCE)1084-0702(2001)6:4(254).
19. Koekkoek, R. T., E. O. L. Lantsoght, and D. A. Hordijk. *Proof Loading of the ASR-Affected Viaduct Zijlweg over Highway A59*. Delft University of Technology, Netherlands, 2015, p. 180.
20. Aguilar, C. V., D. V. Jáuregui, C. M. Newtson, B. D. Weldon, and T. M. Cortez. Load Rating a Prestressed Concrete Double T-Beam Bridge Without Plans by Field Testing. *Transportation Research Record: Journal of the Transportation Research Board, No. 2522*, 2015, p. 90–99.
21. Anay, R., T. M. Cortez, D. V. Jáuregui, M. K. ElBatanouny, and P. Ziehl. On-Site Acoustic-Emission Monitoring for Assessment of a Prestressed Concrete Double T-Beam Bridge Without Plans. *Journal of Performance of Constructed Facilities*, Vol. 30, No. 4, 2016, p. 04015062. https://doi.org/10.1061/(ASCE)CF.1943-5509.0000810.
22. Shenton, H. W., M. J. Chajes, and J. Huang. *Load Rating of Bridges Without Plans*. University of Delaware and Widener University, Newark, Del., 2007, p. 66.
23. Puurula, A. M., O. Enochsson, G. Sas, T. Blanksvärd, U. Ohlsson, L. Bernspång, B. Täljsten, A. Carolin, B. Paulsson, and L. Elfgren. Assessment of the Strengthening of an RC Railway Bridge with CFRP Utilizing a Full-Scale Failure Test and Finite-Element Analysis. *Journal of Structural Engineering*, Vol. 141, No. 1, 2015, p. D4014008. https://doi.org/10.1061/(ASCE)ST.1943-541X.0001116.
24. Nilimaa, J., et al. NSM CFRP Strengthening and Failure Loading of a Posttensioned Concrete Bridge. *Journal of Composites for Construction*, 2015, p. 04015076:1-7.
25. Shifferaw, Y., and F. S. Fanous. Field Testing and Finite Element Analysis of Steel Bridge Retrofits for Distortion-Induced Fatigue. *Engineering Structures*, Vol. 49, 2013, pp. 385–395. https://doi.org/10.1016/j.engstruct.2012.11.023.
26. Moen, C. D., E. E. Shapiro, and J. Hart. Structural Analysis and Load Test of a Nineteenth-Century Iron Bowstring Arch-Truss Bridge. *Journal of Bridge Engineering*, Vol. 18, No. 3, 2013, pp. 261–271. https://doi.org/10.1061/(ASCE)BE.1943-5592.0000341.
27. Coletti, D. A. Analytical and Field Investigation of Roma Suspension Bridge. *Journal of Bridge Engineering*, Vol. 7, No. 3, 2002, pp. 156–165. https://doi.org/10.1061/(ASCE)1084-0702(2002)7:3(156).
28. Orbán, Z., and M. Gutermann. Assessment of Masonry Arch Railway Bridges Using Non-Destructive In-Situ Testing Methods. *Engineering Structures*, Vol. 31, No. 10, 2009, pp. 2287–2298. https://doi.org/10.1016/j.engstruct.2009.04.008.
29. Taylor, S. E., et al. Serviceability of Bridge Deck Slabs With Arching Action. *ACI Structural Journal*, Vol. 104, No. 1, 2007, pp. 39–48.
30. Alampalli, S., and O. Hag-Elsafi. Chapter 40. Load Testing of Bridge FRP Applications. In *International Handbook of FRP Composites in Civil Engineering*, CRC Press, 2013.
31. Alampalli, S., and J. Kunin. Rehabilitation and Field Testing of an FRP Bridge Deck on a Truss Bridge. *Composite Structures*, Vol. 57, No. 1, 2002, pp. 373–375. https://doi.org/10.1016/S0263-8223(02)00104-6.
32. Alampalli, S., and J. Kunin. Load Testing of an FRP Bridge Deck on a Truss Bridge. *Applied Composite Materials*, Vol. 10, No. 2, 2003, pp. 85–102. https://doi.org/10.1023/A:1022885728627.
33. Hag-Elsafi, O., S. Alampalli, and J. Kunin. In-Service Evaluation of a Reinforced Concrete T-Beam Bridge FRP Strengthening System. *Composite Structures*, Vol. 64, No. 2, 2004, pp. 179–188. https://doi.org/10.1016/j.compstruct.2003.08.002.
34. Hag-Elsafi, O., R. Lund, and S. Alampalli. Strengthening of a Bridge Pier Capbeam Using Bonded FRP Composite Plates. *Composite Structures*, Vol. 57, No. 1-4, 2002, pp. 393–403. https://doi.org/10.1016/S0263-8223(02)00107-1.
35. Alampalli, S., and R. Lund. Estimating Fatigue Life of Bridge Components Using Measured Strains. *Journal of Bridge Engineering*, Vol. 11, No. 6, 2006, pp. 725–736. https://doi.org/10.1061/(ASCE)1084-0702(2006)11:6(725).

36. Yannotti, A. P., et al. Proof Load Testing and Monitoring of an FRP Composite Bridge. In *Structural Materials Technology: An NDT Conference*, Atlantic City, N.J., 2000, pp. 281–286.
37. Sanayei, M., A. J. Reiff, B. R. Brenner, and G. R. Imbaro. Load Rating of a Fully Instrumented Bridge: Comparison of LRFR Approaches. *Journal of Performance of Constructed Facilities*, Vol. 2016, No. 30, 2016, p. 2. https://doi.org/10.1061/(ASCE)CF.1943-5509.0000752.
38. Sanayei, M., J. E. Phelps, J. D. Sipple, E. S. Bell, and B. R. Brenner. Instrumentation, Nondestructive Testing, and Finite-Element Model Updating for Bridge Evaluation Using Strain Measurements. *Journal of Bridge Engineering*, Vol. 17, No. 1, 2012, pp. 130–138. https://doi.org/10.1061/(ASCE)BE.1943-5592.0000228.
39. Olaszek, P., M. Lagoda, and J. R. Casas. Diagnostic Load Testing and Assessment of Existing Bridges: Examples of Application. *Structure and Infrastructure Engineering*, Vol. 10, No. 6, 2014, pp. 834–842. https://doi.org/10.1080/15732479.2013.772212.
40. Yuefei, L., L. Dagang, and F. Xueping. Reliability Updating and Prediction of Bridge Structures Based on Proof Loads and Monitored Data. *Construction & Building Materials*, Vol. 66, 2014, pp. 795–804. https://doi.org/10.1016/j.conbuildmat.2014.06.025.
41. Hodson, D. J., P. J. Barr, and L. Pockels. Live-Load Test Comparison and Load Ratings of a Posttensioned Box Girder Bridge. *Journal of Performance of Constructed Facilities*, Vol. 27, No. 5, 2013, pp. 585–593. https://doi.org/10.1061/(ASCE)CF.1943-5509.0000356.
42. Casas, J. R., and J. D. Gómez. Load Rating of Highway Bridges by Proof-loading. *KSCE Journal of Civil Engineering*, Vol. 17, No. 3, 2013, pp. 556–567. https://doi.org/10.1007/s12205-013-0007-8.
43. Koekkoek, R., et al. Defining Loading Criteria for Proof Loading of Existing Reinforced Concrete Bridges. Presented at FIB Symposium 2016: Performance-Based Approaches for Concrete Structures, Cape Town, South Africa, 2016.
44. Lantsoght, E. O. L., et al. Development of Stop Criteria for Proof Loading. In IALCCE 2016, Delft, Netherlands, 2016. https://doi.org/10.1201/9781315375175-135.
45. Schacht, G., G. Bolle, M. Curbach, and S. Marx. Experimentelle Bewertung der Schubtragsicherheit von Stahlbetonbauteilen. *Beton- und Stahlbetonbau*, Vol. 111, No. 6, 2016, pp. 343–354. https://doi.org/10.1002/best.201600006.
46. Cremona, C., and B. Poulin. Standard and Advanced Practices in the Assessment of Existing Bridges. *Structure and Infrastructure Engineering*, 2016.
47. Wang, N., et al. Bridge Rating Using System Reliability Assessment Part I: Assessment and Verification by Load Testing. *Journal of Bridge Engineering*, 2010.
48. Wang, N., B. R. Ellingwood, and A.-H. Zureick. Bridge Rating Using System Reliability Assessment Part II: Improvement to Bridge Rating Practices. *Journal of Bridge Engineering*, 2010.
49. Jeffrey, A., S. F. Breña, and S. A. Civjan. *Evaluation of Bridge Performance and Rating through Nondestructive Load Testing*. University of Massachusetts, Amherst, 2009.
50. Harris, D. K., C. N. Brooks, and T. T. M. Ahlborn. Synthesis of Field Performance of Remote Sensing Strategies for Condition Assessment of In-Service Bridges in Michigan. *Journal of Performance of Constructed Facilities*, Vol. 30, No. 5, 2016. https://doi.org/10.1061/(ASCE)CF.1943-5509.0000844.
51. Cai, H., O. Abudayyeh, I. Abdel-Qader, U. Attanayake, J. Barbera, and E. Almaita. Bridge Deck Load Testing Using Sensors and Optical Survey Equipment. *Advances in Civil Engineering*, Vol. 2012, 2012, p. 11. https://doi.org/10.1155/2012/493983.
52. Bentz, E. C., and N. A. Hoult. Bridge Model Updating Using Distributed Sensor Data. *Institute of Civil Engineers—Bridge Engineering*, Vol. 170, No. 1, 2016, p. 74-86.
53. McCormick, N., and J. Lloyd. Digital Image Correlation for the Monitoring and Investigation of Bridges. *Structural Faults and Repair, 13th International Conference and Exhibition*, Edinburgh, U.K., 2010.
54. Matta, F., F. Bastianini, N. Galati, P. Casadei, and A. Nanni. Distributed Strain Measurement in Steel Bridge with Fiber Optic Sensors: Validation Through Diagnostic Load Test. *Journal of*

Performance of Constructed Facilities, Vol. 22, No. 4, 2008, pp. 264–273. https://doi.org/10.1061/(ASCE)0887-3828(2008)22:4(264).
55. Bridge Diagnostics, Inc. *Integrated Approach to Load Testing*, 2012, p. 44.
56. *AASHTO LRFD Bridge Design Specifications* (7th edition with 2015 interim specifications), American Association of State Highway and Transportation Officials, Washington, D.C., 2015.
57. *Manual for Bridge Evaluation*, 2nd ed., American Association of State Highway and Transportation Officials, Washington, D.C., 2011.
58. Manual for Bridge Rating through Load Testing. *NCHRP Research Results Digest*, No. 234, 1998.
59. ACI Committee 437. *Code Requirements for Load Testing of Existing Concrete Structures and Commentary*. ACI 437.2M-13. American Concrete Institute, Farmington Hills, Mich., 2013, p. 24.
60. ACI Committee 342. *Report on Flexural Live Load Distribution Methods for Evaluating Exisiting Bridges*. *ACI 342R-16:* American Concrete Institute, Farmington Hills, Mich., 2016, p. 36.
61. Deutscher Ausschuss für Stahlbeton. *DAfStb-Guideline: Load tests on concrete structures (in German) (DAfStb-Richtlinie: Belastungsversuche an Betonbauwerken)*. Deutscher Ausschuss für Stahlbeton, Berlin, Germany, 2000, p. 7.
62. *Load Testing for Bridge Assessment*. National Roads Authority, Dublin, Ireland, 2014, p. 11.
63. National Steering Committee for the Load Testing of Bridges. *Guidelines for the Supplementary Load Testing of Bridges*, Institute of Civil Engineers, London, 1998, p. 44.
64. PN-S-10040/99. *Bridges. Concrete, reinforced concrete and prestressed structures. Requirements and testing* (in Polish), 1999.
65. Frýba, L., and M. Pirner. Load Tests and Modal Analysis of Bridges. *Engineering Structures*, Vol. 23, No. 1, 2001, pp. 102–109. https://doi.org/10.1016/S0141-0296(00)00026-2.
66. Ministerio de Fomento. *Instrucciones para la Puesta en carga de estructuras (pruebas de carga provisionales)*, 2009, p. 2.
67. Ministerio de Fomento, Direccion General de Carreteras. *Recomendaciones para la realizacion de pruebas de carga de recepcion en puentes de carretera*. Madrid, Spain, 1999, p. 22.
68. Hungarian Chamber of Engineers. *Guidelines for Interventions in Hungary*. Budapest, Hungary, 2013, p. 35 (in Hungarian).
69. SIA. Existing Structures: Bases for Examination and Interventions. SIA 505 269, 2011, p. 26.
70. SIA. Existing Structures: Concrete Structures. SIA 505 269/2, 2011, p. 44.
71. Lantsoght, E., et al. Recommendations for Proof Load Testing of reinforced Concrete Slab Bridges. Proc., 39th IABSE Symposium—Engineering the Future, Vancouver, Canada, 2017. https://doi.org/10.1016/j.engstruct.2017.09.018.
72. *Manual for Bridge Evaluation* (with 2016 interim revisions), 2nd ed. American Association of State Highway and Transportation Officials, Washington, D.C., 2016.
73. Ryan, T. W., et al. *Bridge Inspector's Reference Manual*. Federal Highway Administration, U. S. Department of Transportation, 2012.
74. *NCHRP Synthesis 453: State Bridge Load Posting: Processes and Practices*, 2014, p. 145.
75. Zhou, Y. E., et al. Re-Evaluation of Weight Limits for Six Bridges in Montgomery County Maryland. *IBC 2007*, 2007.
76. Li, Z., J. He, J. Teng, and Y. Wang. Internal Stress Monitoring of In-Service Structural Steel Members with Ultrasonic Method. *Materials (Basel)*, Vol. 9, No. 4, 2016, p. 223. https://doi.org/10.3390/ma9040223.
77. Zhan, Y., C. Liu, X. Kong, and Z. Lin. Experiment and Numerical Simulation for Laser Ultrasonic Measurement of Residual Stress. *Ultrasonics*, Vol. 73, 2017, pp. 271–276. https://doi.org/10.1016/j.ultras.2016.08.013.
78. Samimi, A. A., T. W. Krause, and L. Clapham. Multi-Parameter Evaluation of Magnetic Barkhausen Noise in Carbon Steel. *Journal of Nondestructive Evaluation*, Vol. 35, No. 3, 2016, p. 40. https://doi.org/10.1007/s10921-016-0358-4.

79. Vourna, P., A. Ktena, P. E. Tsakiridis, and E. Hristoforou. A Novel Approach of Accurately Evaluating Residual Stress and Microstructure of Welded Electrical Steels. *NDT & E International*, Vol. 71, 2015, pp. 33–42. https://doi.org/10.1016/j.ndteint.2014.09.011.
80. Russo, F. M., T. J. Wipf, and F. W. Klaiber. Diagnostic Load Tests of a Prestressed Concrete Bridge Damaged by Overheight Vehicle Impact. *Transportation Research Record: Journal of the Transportation Research Board, No. 1696*, 2000, pp. 103–110. https://doi.org/10.3141/1696-50.
81. Moses, F., J. P. Lebet, and R. Bez. Applications of Field Testing to Bridge Evaluation. *Journal of Structural Engineering*, Vol. 120, No. 6, 1994, pp. 1745–1762. https://doi.org/10.1061/(ASCE)0733-9445(1994)120:6(1745).
82. Jáuregui, D. V., A. Licon-Lozano, and K. Kulkarni. Higher Level Evaluation of a Reinforced Concrete Slab Bridge. *Journal of Bridge Engineering*, Vol. 15, No. 2, 2010, pp. 172–182. https://doi.org/10.1061/(ASCE)BE.1943-5592.0000047.
83. Farhey, D. N. Bridge Instrumentation and Monitoring for Structural Diagnostics. *Structural Health Monitoring*, Vol. 4, No. 4, 2005, pp. 301–318. https://doi.org/10.1177/1475921705057966.
84. Brühwiler, E., T. Vogel, T. Lang, and P. Lüchinger. Swiss Standards for Existing Structures. *Structural Engineering International*, Vol. 22, No. 2, 2012, pp. 275–280. https://doi.org/10.2749/101686612X13291382991209.
85. Cochet, D., et al. *Epreuves de chargement des ponts-routes et passerelles pietonnes*. Stra - Service d'Etudes techniques des routes et autoroutes: Bagneux-Cedex, France, 2004.
86. Saraf, V., A. F. Sokolik, and A. S. Nowak. Proof Load Testing of Highway Bridges. *Transportation Research Record 1541*, 1996, pp. 51–57. https://doi.org/10.1177/0361198196154100107.
87. Cai, C. S., and M. Shahawy. Understanding Capacity Rating of Bridges from Load Tests. *Practice Periodical on Structural Design and Construction*, Vol. 8, No. 4, 2003, pp. 209–216. https://doi.org/10.1061/(ASCE)1084-0680(2003)8:4(209).
88. Lin, T. S., and A. S. Nowak. Proof Loading and Structural Reliability. *Reliability Engineering*, Vol. 8, No. 2, 1984, pp. 85–100. https://doi.org/10.1016/0143-8174(84)90057-X.
89. Fu, G. K., and J. G. Tang. Risk-Based Proof-Load Requirements for Bridge Evaluation. *Journal of Structural Engineering*, Vol. 121, No. 3, 1995, pp. 542–556. https://doi.org/10.1061/(ASCE)0733-9445(1995)121:3(542).
90. Nowak, A. S., and T. Tharmabala. Bridge Reliability Evaluation Using Load Tests. *Journal of Structural Engineering*, Vol. 114, No. 10, 1988, pp. 2268–2279. https://doi.org/10.1061/(ASCE)0733-9445(1988)114:10(2268).
91. Brent Hall, W., and M. Tsai. Load Testing, Structural Reliability and Test Evaluation. *Structural Safety*, Vol. 6, No. 2-4, 1989, pp. 285–302. https://doi.org/10.1016/0167-4730(89)90028-3.
92. Rackwitz, R., and K. Schrupp. Quality-Control, Proof Testing and Structural Reliability. *Structural Safety*, Vol. 2, No. 3, 1985, pp. 239–244. https://doi.org/10.1016/0167-4730(85)90030-X.
93. Koekkoek, R., et al. Defining Loading Criteria for Proof Loading of Existing Reinforced Concrete Bridges. *Performance-Based Approaches for Concrete Structures* (H. Beushausen, ed.), Cape Town, South Africa, 2016, p. 10.
94. Fu, G. *Highway Bridge Rating by Nondestructive Proof-Load Testing for Consistent Safety*. New York State Department of Transportation, 1995, p. 78.
95. Fu, G., P. Saridis, and J. Tang. *Proof Testing of Highway Bridges*. New York State Department of Transportation, 1992, p. 44.
96. Fu, G., and J. Tang. Risk-Based Proof-Load Requirements for Bridge Evaluation. *Journal of Structural Engineering*, Vol. 121, No. 3, 1995, pp. 542–556. https://doi.org/10.1061/(ASCE)0733-9445(1995)121:3(542).
97. Paultre, P., O. Chaallal, and J. Proulx. Bridge Dynamics and Dynamic Amplification Factors— A Review of Analytical and Experimental Findings. *Canadian Journal of Civil Engineering*, Vol. 19, No. 2, 1992, pp. 260–278. https://doi.org/10.1139/l92-032.

98. Alipour, M., D. K. Harris, and O. E. Ozbulut. *Vibration Testing for Bridge Load Rating*. Springer International Publishing, Cham, 2016. https://doi.org/10.1007/978-3-319-29751-4_18.
99. Salawu, O. S., and C. Williams. Review of Full-Scale Dynamic Testing of Bridge Structures. *Engineering Structures*, Vol. 17, No. 2, 1995, pp. 113–121. https://doi.org/10.1016/0141-0296(95)92642-L.
100. Yarnold, M. T., and F. L. Moon. Temperature-Based Structural Health Monitoring Baseline for Long-Span Bridges. *Engineering Structures*, Vol. 86, 2015, pp. 157–167. https://doi.org/10.1016/j.engstruct.2014.12.042.
101. Dubbs, N. C., and F. L. Moon. Comparison and Implementation of Multiple Model Structural Identification Methods. *Journal of Structural Engineering*, Vol. 141, No. 11, 2015, p. 04015042. https://doi.org/10.1061/(ASCE)ST.1943-541X.0001284.
102. Mertlich, T. B., M. W. Halling, and P. J. Barr. Dynamic and Static Behavior of a Curved-Girder Bridge with Varying Boundary Conditions. *Journal of Performance of Constructed Facilities*, Vol. 21, No. 3, 2007, pp. 185–192. https://doi.org/10.1061/(ASCE)0887-3828(2007)21:3(185).
103. Hsieh, K. H., M. W. Halling, and P. J. Barr. Overview of Vibrational Structural Health Monitoring with Representative Case Studies. *Journal of Bridge Engineering*, Vol. 11, No. 6, 2006, pp. 707–715. https://doi.org/10.1061/(ASCE)1084-0702(2006)11:6(707).
104. Alampalli, S., G. Fu, and E. W. Dillon. Signal versus Noise in Damage Detection by Experimental Modal Analysis. *Journal of Structural Engineering*, Vol. 123, No. 2, 1997, pp. 237–245. https://doi.org/10.1061/(ASCE)0733-9445(1997)123:2(237).
105. Alampalli, S. Effects of Testing, Analysis, Damage, and Environment on Modal Parameters. *Mechanical Systems and Signal Processing*, Vol. 14, No. 1, 2000, pp. 63–74. https://doi.org/10.1006/mssp.1999.1271.
106. Alampalli, S. Significance of Operating Environment in Condition Monitoring of Large Civil Structures. *Journal of Shock & Vibration*, Vol. 6, No. 5-6, 1999, pp. 247–251. https://doi.org/10.1155/1999/135201.
107. Frangopol, D. M., and D. Saydam, Chapter 9: Structural Performance Indicators for Bridges. *Bridge Engineering Handbook, Vol. 1 Fundamentals* (W. F. Chen and L. Duan, eds.) CRC Press / Taylor & Francis Group: Boca Raton, Fla., 2014, p. 185-205.
108. Frangopol, D. M., K. Y. Lin, and A. C. Estes. Life-Cycle Cost Design of Deteriorating Structures. *Journal of Structural Engineering*, Vol. 123, No. 10, 1997, pp. 1390–1401. https://doi.org/10.1061/(ASCE)0733-9445(1997)123:10(1390).
109. Chen, L., W. Qu, and P. Zhu. Life-Cycle Analysis for Concrete Beams Designed with Cross-Sections of Equal Durability. *Structural Concrete*, Vol. 17, No. 2, 2016, pp. 274–286. https://doi.org/10.1002/suco.201400117.
110. Kim, S., and D. M. Frangopol. Cost-Effective Lifetime Structural Health Monitoring Based on Availability. *Journal of Structural Engineering*, Vol. 137, No. 1, 2011, pp. 22–33. https://doi.org/10.1061/(ASCE)ST.1943-541X.0000280.
111. Kim, S., and D. M. Frangopol. Inspection and Monitoring Planning for RC Structures Based on Minimization of Expected Damage Detection Delay. *Probabilistic Engineering Mechanics*, Vol. 26, No. 2, 2011, pp. 308–320. https://doi.org/10.1016/j.probengmech.2010.08.009.
112. Sabatino, S., D. M. Frangopol, and Y. Dong. Sustainability-Informed Maintenance Optimization of Highway Bridges Considering Multi-Attribute Utility and Risk Attitude. *Engineering Structures*, Vol. 102, 2015, pp. 310–321. https://doi.org/10.1016/j.engstruct.2015.07.030.
113. Sabatino, S., D. M. Frangopol, and Y. Dong. Life-Cycle Utility-Informed Maintenance Planning Based on Lifetime Functions: Optimum Balancing of Cost, Failure Consequences, and Performance Benefit. *Structure and Infrastructure Engineering*, Vol. 12, No. 7, 2016, pp. 830–847. https://doi.org/10.1080/15732479.2015.1064968.
114. Frangopol, D. M., and M. Soliman. Life-Cycle of Structural Systems: Recent Achievements and Future Directions. *Structure and Infrastructure Engineering*, Vol. 12, No. 1, 2016, pp. 1–20. https://doi.org/10.1080/15732479.2014.999794.

115. Hendy, C., and R. Petty. Quantification of Sustainability Principles in Bridge Projects. *Proc., Sixth International Conference on Bridge Maintenance, Safety and Management* (F. Biondini and D. M. Frangopol, eds.) Taylor & Francis Group, Stresa, Lake Maggiore, Italy, 2012, pp. 1793–1800. https://doi.org/10.1201/b12352-263.
116. Mondoro, A., D. M. Frangopol, and L. Liu. Multi-Criteria Robust Optimization Framework for Bridge Adaptation Under Climate Change. *Structural Safety*, Vol. 74, 2018, pp. 14–23. https://doi.org/10.1016/j.strusafe.2018.03.002.
117. Environment Agency. *Carbon Calculator for Construction Activities*, 2016. https://www.ice.org.uk/disciplines-and-resources/best-practice/environment-agency-carbon-calculator-tool.
118. Zinke, T., et al. The Social Dimension of Bridge Sustainability Assessment—Impacts on Users and the Public. *Proc., Sixth International Conference on Bridge Maintenance, Safety and Management* (F. Biondini and D.M. Frangopol, eds.) Taylor & Francis Group, Stresa, Lake Maggiore, Italy, 2012, pp. 1836–1843. https://doi.org/10.1201/b12352-269.
119. Frangopol, D. M., and P. Bocchini. Bridge Network Performance, Maintenance, and Optimisation Under Uncertainty: Accomplishments and Challenges. *Structure and Infrastructure Engineering*, Vol. 8, No. 4, 2012, pp. 341–356. https://doi.org/10.1080/15732479.2011.563089.
120. Ettouney, M., and S. Alampalli. *Infrastructure Health in Civil Engineering*. CRC Press, Boca Raton, Fla., 2012.
121. *Manual on Uniform Traffic Control Devices for Streets and Highways, 2009 Edition with 2012 Revisions*. Federal Highway Administration, U.S. Department of Transportation, 2012, p. 862.
122. Marefat, M. S., E. Ghahremani-Gargary, and S. Ataei. Load Test of a Plain Concrete Arch Railway Bridge of 20-m Span. *Construction & Building Materials*, Vol. 18, No. 9, 2004, pp. 661–667. https://doi.org/10.1016/j.conbuildmat.2004.04.025.
123. Wipf, T. J., M. A. Ritter, and D. L. Wood. Evaluation and Field Load Testing of Timber Railroad Bridge. *Transportation Research Record: Journal of the Transportation Research Board, No. 1696*, 2016, pp. 323–333. https://doi.org/10.3141/1696-34.
124. Gutkowski, R. M., A. M. T. Shigidi, A. V. Tran, and M. L.Peterson. Field Studies of Strengthened Timber Railroad Bridge. *Transportation Research Record: Journal of the Transportation Research Board, No. 1770*, 2001, pp. 139-148. https://doi.org/10.3141/1770-18.
125. Gentry, T. R., J. P. Wacker, K. N. Brohammer, and J. Wells. In Situ Materials and Structural Assessment of Stress-Laminated Deck Bridge Treated with Chromate Copper Arsenate. *Transportation Research Record: Journal of the Transportation Research Board, No. 2028*, 2007, pp. 28–33. https://doi.org/10.3141/2028-04.
126. Concu, G., et al. Combined Non Destructive Testing for concrete compressive strength prediction. *Concrete Repair, Rehabilitation and Retrofitting IV* (F. Dehn et al., eds.), Leipzig, Germany, 2015, pp. 287–290. https://doi.org/10.1201/b18972-40.
127. Cuaron, A. M., D. V. Jáuregui, and B. D. Weldon. A Procedure for Load Rating Reinforced Concrete Slab Bridges Without Plans. Presented at 96th Annual Meeting of the Transportation Research Board, Washington, D.C., 2017.
128. Dilek, U., and E. M. Reis. Evaluation and Load Testing of Posttensioned Concrete Structure Exhibiting Distress. *Journal of Performance of Constructed Facilities*, Vol. 30, No. 1, 2016, pp. 1–10. https://doi.org/10.1061/(ASCE)CF.1943-5509.0000695.
129. Deutscher Ausschuss für Stahlbeton. *DAfStb-Richtlinie: Belastungsversuche an Betonbauwerken*. Deutscher Ausschuss für Stahlbeton, 2000, p. 7.
130. AASHTO. *The Manual for Bridge Evaluation*, 2nd ed. American Association of State Highway and Transportation Officials, Washington, D.C., 2011.
131. Lantsoght, E. O. L., C. van der Veen, D. A. Hordijk, and A. de Boer. Development of Recommendations for Proof Load Testing of Reinforced Concrete Slab Bridges. *Engineering Structures*, Vol. 152, 2017, pp. 202–210. https://doi.org/10.1016/j.engstruct.2017.09.018.

132. Saraf, V. K., A. S. Nowak, and R. Till. Proof Load Testing of Bridges. *Probabilistic Mechanics & Structural Reliability: Proceedings of the Seventh Specialty Conference* (D.M. Frangopol and M.D. Grigoriu, eds.), Worcester, Mass. 1996, pp. 526–529.
133. CEN. *Eurocode 1: Actions on structures - Part 2: Traffic loads on bridges, NEN-EN 1991-2*. Comité Européen de Normalisation, Brussels, Belgium, 2003, p. 168.
134. Lantsoght, E. O. L., Y. Yang, C. van der Veen, A. de Boer, and D. A. Hordijk. Beam Experiments on Acceptance Criteria for Bridge Load Tests. *ACI Structural Journal*, Vol. 114, No. 4, 2017, pp. 1031–1041. https://doi.org/10.14359/51689786.
135. Lantsoght, E. O. L., C. Van der Veen, and D. A. Hordijk. Proposed Stop Criteria for Proof Load Testing of Concrete Bridges and Verification. *IALCCE 2018*, Ghent, Belgium, 2018.
136. Yang, Y., et al. Calibration of the Shear Stop Criteria Based on Crack Kinematics of Reinforced Concrete Beams Without Shear Reinforcement. *FIB Conference 2018*, Melbourne, Australia, 2018.
137. JCSS. *JCSS Probabilistic Model Code - Part 3: Resistance Models*. 2001.
138. Spaethe, G. Die Beeinflussing der Sicherheit eines Tragwerkes durch Probebelastung. *Bauingenieur*, Vol. 69, No. 12, 1994, pp. 459–468.
139. Straub, D. Value of Information Analysis with Structural Reliability Methods. *Structural Safety*, Vol. 49, 2014, pp. 75–85. https://doi.org/10.1016/j.strusafe.2013.08.006.
140. Yang, D. Y., and D. M. Frangopol. Evidence-Based Framework for real-Time Life-Cycle Management of Fatigue-Critical Details of Structures. *Structure and Infrastructure Engineering*, Vol. 14, No. 5, 2018, pp. 509–522. https://doi.org/10.1080/15732479.2017.1399150.
141. Frangopol, D. M., and S. Kim. Chapter 18: Life-Cycle Analysis and Optimization. *Bridge Engineering Handbook, Vol. 5 Construction and Maintenance* (W.F. Chen and L. Duan, eds.), CRC Press / Taylor & Francis Group, Boca Raton, Fla., 2014, pp. 537–566.
142. Frangopol, D. M., J. S. Kong, and E. S. Gharaibeh. Reliability-Based Life-Cycle Management of Highway Bridges. *Journal of Computing in Civil Engineering*, Vol. 15, No. 1, 2001, pp. 27–34. https://doi.org/10.1061/(ASCE)0887-3801(2001)15:1(27).
143. Petcherdchoo, A., L. A. C. Neves, and D. M. Frangopol. Optimizing Lifetime Condition and Reliability of Deteriorating Structures with Emphasis on Bridges. *Journal of Structural Engineering*, Vol. 134, No. 4, 2008, pp. 544–552. https://doi.org/10.1061/(ASCE)0733-9445(2008)134:4(544).
144. Stewart, M. G., D. V. Rosowsky, and D. V. Val. Reliability-Based Bridge Assessment Using Risk-Ranking Decision Analysis. *Structural Safety*, Vol. 23, No. 4, 2001, pp. 397–405. https://doi.org/10.1016/S0167-4730(02)00010-3.
145. Rijkswaterstaat. Richtlijnen Beoordeling Kunstwerken - beoordeling van de constructieve veiligheid van een bestaand kunstwerk bij verbouw, gebruik en afkeur. *RTD 1006:2013.* 2013. p. 117.
146. Koteš, P., and J. Vican. Recommended Reliability Levels for the Evaluation of Existing Bridges According to Eurocodes. *Structural Engineering International*, Vol. 23, No. 4, 2013, pp. 411–417. https://doi.org/10.2749/101686613X13627351081678.
147. Steenbergen, R. D. J. M., and A. C. W. M. Vrouwenvelder. Safety Philosophy for Existing Structures and Partial Factors for Traffic Loads on Bridges. *Heron*, Vol. 55, No. 2, 2010, pp. 123–140.
148. Gokce, H. B., F. N. Catbas, and D. M. Frangopol. Evaluation of Load Rating and System Reliability of Movable Bridge. *Transportation Research Record: Journal of the Transportation Research Board, No. 2251*, 2011, pp. 114–122. https://doi.org/10.3141/2251-12.
149. Sivakumar, B. LRFR Limit States, Reliability Indices and Load Factors. Load and Resistance Factor Rating of Highway Bridges, FHWA LRFR Seminar, 2008.
150. Frangopol, D. M., K. Y. Lin, and A. C. Estes. Reliability of Reinforced Concrete Girders Under Corrosion Attack. *Journal of Structural Engineering*, Vol. 123, No. 3, 1997, pp. 286–297. https://doi.org/10.1061/(ASCE)0733-9445(1997)123:3(286).

151. Vatteri, A. P., K. Balaji Rao, and A. M. Bharathan. Time-Variant Reliability Analysis of RC Bridge Girders Subjected to Corrosion—Shear Limit State. *Structural Concrete*, Vol. 17, No. 2, 2016, pp. 162–174. https://doi.org/10.1002/suco.201500081.
152. Li, C. Q., W. Lawanwisut, and J. J. Zheng. Time-Dependent Reliability Method to Assess the Serviceability of Corrosion-Affected Concrete Structures. *Journal of Structural Engineering*, Vol. 131, No. 11, 2005, pp. 1674–1680. https://doi.org/10.1061/(ASCE)0733-9445(2005)131:11(1674).
153. Enright, M. P., and D. M. Frangopol. Probabilistic Analysis of Resistance Degradation of Reinforced Concrete Bridge Beams Under Corrosion. *Engineering Structures*, Vol. 20, No. 11, 1998, pp. 960–971. https://doi.org/10.1016/S0141-0296(97)00190-9.
154. Stewart, M. G. Spatial Variability of Pitting Corrosion and Its Influence on Structural Fragility and Reliability of RC Beams in Flexure. *Structural Safety*, Vol. 26, No. 4, 2004, pp. 453–470. https://doi.org/10.1016/j.strusafe.2004.03.002.
155. Li, Y., T. Vrouwenvelder, G. H. Wijnants, and J. Walraven. Spatial Variability of Concrete Deterioration and Repair Strategies. *Structural Concrete*, Vol. 5, No. 3, 2004, pp. 121–129. https://doi.org/10.1680/stco.2004.5.3.121.
156. Val, D. V., and R. E. Melchers. Reliability of Deteriorating RC Slab Bridges. *Journal of Structural Engineering*, Vol. 123, No. 12, 1997, pp. 1638–1644. https://doi.org/10.1061/(ASCE)0733-9445(1997)123:12(1638).
157. van Noortwijk, J. M., and H. E. Klatter. The Use of Lifetime Distributions in Bridge Maintenance and Replacement Modeling. *Computers & Structures*, Vol. 82, No. 13–14, 2004, pp. 1091–1099. https://doi.org/10.1016/j.compstruc.2004.03.013.
158. Cheung, M. S., and W. C. Li. Probabilistic Fatigue and Fracture Analyses of Steel Bridges. *Structural Safety*, Vol. 25, No. 3, 2003, pp. 245–262. https://doi.org/10.1016/S0167-4730(02)00067-X.
159. Lukić, M., and C. Cremona. Probabilistic Assessment of Welded Joints Versus Fatigue and Fracture. *Journal of Structural Engineering*, Vol. 127, No. 2, 2001, pp. 211–218. https://doi.org/10.1061/(ASCE)0733-9445(2001)127:2(211).
160. Righiniotis, T. D., and M. K. Chryssanthopoulos. Probabilistic Fatigue Analysis Under Constant Amplitude Loading. *Journal of Constructional Steel Research*, Vol. 59, No. 7, 2003, pp. 867–886. https://doi.org/10.1016/S0143-974X(03)00002-6.
161. Zhu, B. J., and D. M. Frangopol. Incorporation of Structural Health Monitoring Data on Load Effects in the Reliability and Redundancy Assessment of Ship Cross-Sections Using Bayesian Updating. *Structural Health Monitoring-an International Journal*, Vol. 12, No. 4, 2013, pp. 377–392. https://doi.org/10.1177/1475921713495082.
162. Messervey, T. Integration of Structural Health Monitoring into the Design, Assessment, and Management of Civil Infrastructure. *Graduate School in Civil Engineering*, Università di Pavia, Pavia, Italy, 2009, p. 248.
163. Frangopol, D. M. Life-Cycle Performance, Management, and Optimisation of Structural Systems Under Uncertainty: Accomplishments and Challenges. *Structure and Infrastructure Engineering*, Vol. 7, No. 6, 2011, pp. 389–413. https://doi.org/10.1080/15732471003594427.
164. Code Committee 351001. *Assessement of Structural Safety of an Existing Structure at Repair or Unfit for Use: Basic Requirements, NEN 8700:2011* (in Dutch). Civil Center for the Execution of Research and Standard, Dutch Normalisation Institute, Delft, Netherlands, 2011, p. 56.
165. Rijkswaterstaat. *Guidelines Assessment Bridges—Assessment of Structural Safety of an Existing Bridge at Reconstruction, Usage and Disapproval* (in Dutch). RTD 1006:2013 1.1. Utrecht, Netherlands, 2013, p. 117.
166. Estes, A. C., and D. M. Frangopol. Load Rating versus Reliability Analysis. *Journal of Structural Engineering*, Vol. 131, No. 5, 2005, pp. 843–847. https://doi.org/10.1061/(ASCE)0733-9445(2005)131:5(843).

167. Saydam, D., and D. M. Frangopol. Applicability of Simple Expressions for Bridge System Reliability Assessment. *Computers & Structures*, Vol. 114-115, 2013, pp. 59–71. https://doi.org/10.1016/j.compstruc.2012.10.004.
168. Akgül, F., and D. M. Frangopol. Computational Platform for Predicting Lifetime System Reliability Profiles for Different Structure Types in a Network. *Journal of Computing in Civil Engineering*, Vol. 18, No. 2, 2004, pp. 92–104. https://doi.org/10.1061/(ASCE)0887-3801(2004)18:2(92).
169. Imai, K., and D. M. Frangopol. System Reliability of Suspension Bridges. *Structural Safety*, Vol. 24, No. 2, 2002, pp. 219–259. https://doi.org/10.1016/S0167-4730(02)00027-9.
170. Estes, A. C., and D. M. Frangopol. Bridge lifetime System Reliability Under Multiple Limit States. *Journal of Bridge Engineering*, Vol. 6, No. 6, 2001, pp. 523–528. https://doi.org/10.1061/(ASCE)1084-0702(2001)6:6(523).
171. Estes, A. C., and D. M. Frangopol. Repair Optimization of Highway Bridges Using System Reliability Approach. *Journal of Structural Engineering*, Vol. 125, No. 7, 1999, pp. 766–775. https://doi.org/10.1061/(ASCE)0733-9445(1999)125:7(766).
172. Frangopol, D. M., and A. C. Estes. Lifetime Bridge Maintenance Strategies Based on System Reliability. *Structural Engineering International*, Vol. 7, No. 3, 1997, pp. 193–198. https://doi.org/10.2749/101686697780494662.
173. Hendawi, S., and D. M. Frangopol. System Reliability and Redundancy in Structural Design and Evaluation. *Structural Safety*, Vol. 16, No. 1, 1994, pp. 47–71. https://doi.org/10.1016/0167-4730(94)00027-N.
174. Okasha, N. M., and D. M. Frangopol. Integration of Structural Health Monitoring in a System Performance Based Life-Cycle Bridge Management Framework. *Structure and Infrastructure Engineering*, Vol. 8, No. 11, 2012, pp. 999–1016.
175. Decò, A., and D. M. Frangopol. Risk Assessment of Highway Bridges Under Multiple Hazards. *Journal of Risk Research*, Vol. 14, No. 9, 2011, pp. 1057–1089. https://doi.org/10.1080/13669877.2011.571789.
176. Kong, J. S., and D. M. Frangopol. Probabilistic Optimization Of Aging Structures Considering Maintenance and Failure Costs. *Journal of Structural Engineering*, Vol. 131, No. 4, 2005, pp. 600–616. https://doi.org/10.1061/(ASCE)0733-9445(2005)131:4(600).
177. Yang, D. Y., and D. M. Frangopol. Risk-Informed Bridge Ranking at Project and Network Levels. *Journal of Infrastructure Systems*, Vol. 24, No. 3, 2018, p. 04018018. https://doi.org/10.1061/(ASCE)IS.1943-555X.0000430.
178. Barone, G., and D. M. Frangopol. Reliability, Risk and Lifetime Distributions as Performance Indicators for Life-Cycle Maintenance of Deteriorating Structures. *Reliability Engineering & System Safety*, Vol. 123, 2014, pp. 21–37. https://doi.org/10.1016/j.ress.2013.09.013.
179. Zhu, B., and D. M. Frangopol. Reliability, Redundancy and Risk as Performance Indicators of Structural Systems During Their Life-Cycle. *Engineering Structures*, Vol. 41, 2012, pp. 34–49. https://doi.org/10.1016/j.engstruct.2012.03.029.
180. Kim, S., and D. M. Frangopol. Decision Making for Probabilistic Fatigue Inspection Planning Based on Multi-Objective Optimization. *International Journal of Fatigue*, Vol. 111, 2018, pp. 356–368. https://doi.org/10.1016/j.ijfatigue.2018.01.027.
181. Yang, D. Y., and D. M. Frangopol. Life-Cycle Management of Deteriorating Civil Infrastructure Considering Resilience to Lifetime Hazards: A General Approach Based on Renewal-Reward Processes. *Reliability Engineering & System Safety*, Vol. 183, 2019, pp. 197–212. https://doi.org/10.1016/j.ress.2018.11.016.
182. Biondini, F., and D. M. Frangopol. Life-Cycle Performance of Deteriorating Structural Systems under Uncertainty. [Review]. *Journal of Structural Engineering*, Vol. 142, No. 9, 2016, p. F4016001. https://doi.org/10.1061/(ASCE)ST.1943-541X.0001544.
183. Ang, A.-S., and D. De Leon. Modeling and Analysis of Uncertainties for Risk-Informed Decisions in Infrastructures Engineering. *Structure and Infrastructure Engineering*, Vol. 1, No. 1, 2005, pp. 19–31. https://doi.org/10.1080/15732470412331289350.

184. Frangopol, D. M., Y. Dong, and S. Sabatino. Bridge Life-Cycle Performance and Cost: Analysis, Prediction, Optimisation and Decision-Making. *Structure and Infrastructure Engineering*, Vol. 13, No. 10, 2017, pp. 1239–1257. https://doi.org/10.1080/15732479.2016.1267772.
185. Kim, S., and D. M. Frangopol. Efficient Multi-Objective Optimisation of Probabilistic Service Life Management. *Structure and Infrastructure Engineering*, Vol. 13, No. 1, 2017, pp. 147–159. https://doi.org/10.1080/15732479.2016.1198405.
186. Kong, J. S., and D. M. Frangopol. Life-Cycle Reliability-Based Maintenance Cost Optimization of Deteriorating Structures With Emphasis on Bridges. *Journal of Structural Engineering*, Vol. 129, No. 6, 2003, pp. 818–828. https://doi.org/10.1061/(ASCE)0733-9445(2003)129:6(818).
187. Yang, D. Y., and D. M. Frangopol. Probabilistic Optimization Framework for Inspection/Repair Planning of Fatigue-Critical Details Using Dynamic Bayesian Networks. *Computers & Structures*, Vol. 198, 2018, pp. 40–50. https://doi.org/10.1016/j.compstruc.2018.01.006.
188. Lantsoght, E. O. L., et al. Towards Standardization of Proof Load Testing: Pilot Test on Viaduct Zijlweg. *Structure and Infrastructure Engineering*, 2017, p. 16.
189. Siemes, T., N. Han, and J. Visser. Unexpectedly Low Tensile Strength in Concrete Structures. *Heron*, Vol. 47, No. 2, 2002, pp. 111–124.
190. den Uijl, J. A. *Dwarskrachtdraagvermogen van bestaand plaatviaduct*, 2004.
191. den Uijl, J. A., and N. Kaptijn. Structural Consequences of ASR: An Example on Shear Capacity. *Heron*, Vol. 47, No. 2, 2002, pp. 1–13.
192. Rafla, K. Empirische Formeln zur Berechnung der Schubtragfahigkeit von Stahlbetonbalken. *Strasse Brucke Tunnel*, Vol. 23, No. 12, 1971, pp. 311–320.
193. Ahmed, T., E. Burley, and S. Rigden. The Static and Fatigue Strength of Reinforced Concrete Beams Affected by Alkali-Silica Reaction. *ACI Materials Journal*, Vol. 95, No. 4, 1998, pp. 376–388.
194. Lantsoght, E. O. L., A. de Boer, and C. van der Veen. Distribution of Peak Shear Stress in Finite Element Models of Reinforced Concrete Slabs. *Engineering Structures*, Vol. 148, 2017, pp. 571–583. https://doi.org/10.1016/j.engstruct.2017.07.005.
195. Yang, Y., D. Hordijk, and A. De Boer. Acoustic Emission Study on 50 Year Old Reinforced Concrete Beams Under Bending And Shear Tests. *IAES-23, IIIAE 2016 KYOTO & ICAE-8*, Kyoto, Japan, 2016.
196. Chiewanichakorn, M., A. J. Aref, and S. Alampalli. Dynamic and Fatigue Response of a Truss Bridge With Fiber Reinforced Polymer Deck. *International Journal of Fatigue*, Vol. 29, No. 8, 2007, pp. 1475–1489. https://doi.org/10.1016/j.ijfatigue.2006.10.031.
197. AASHTO. *Standard Specifications for Highway Bridges*, 15th ed., American Association for Highway and Transportation Officials, Washington, D.C., 1994.
198. AASHTO. *Manual for Condition Evaluation of Bridges*, 2nd edition with 2003 interim revisions, American Association for Highway and Transportation Officials, Washington, D.C., 2003.
199. Lantsoght, E. O. L., C. van der Veen, A. de Boer, and D. A. Hordijk. State-of-the-Art on Load Testing of Concrete Bridges. *Engineering Structures*, Vol. 150, 2017, pp. 231–241. https://doi.org/10.1016/j.engstruct.2017.07.050.
200. Ritter, M. A., S. Rimal Duwadi, and J. P. Wacker. Field Performance of Stress-Laminated Timber Bridges. *Transportation Research Record: Journal of the Transportation Research Board, No. 1740*, 2000, pp. 96–103. https://doi.org/10.3141/1740-12.
201. Gutkowski, R. M., J. Natterer, and P. A. Favre. Field Load Tests of an Anisotropic-Grid Timber Bridge. *Construction & Building Materials*, Vol. 22, No. 2, 2008, pp. 88–98. https://doi.org/10.1016/j.conbuildmat.2006.05.042.
202. Ekholm, K., R. Kliger, and R. Crocetti. Full-Scale Ultimate-Load Test of a Stress-Laminated-Timber Bridge Deck. *Journal of Bridge Engineering*, Vol. 17, No. 4, 2012, pp. 691–699. https://doi.org/10.1061/(ASCE)BE.1943-5592.0000304.

203. Arangjelovski, T., K. Gramatikov, and M. Docevska. Assessment of Damaged Timber Structures Using Proof Load Test—Experience from Case Studies. *Construction & Building Materials*, Vol. 101, No. Part 2, 2015, pp. 1271–1277. https://doi.org/10.1016/j.conbuildmat.2015.07.010.
204. Gutermann, M., V. Slowik, and K. Steffens. Experimental Safety Evaluation of Concrete and Masonry Bridges. *Insight - Non-Destructive Testing and Condition Monitoring*, Vol. 45, No. 12, 2003, p. 805-808. https://doi.org/10.1784/insi.45.12.805.52972.
205. Brencich, A., and D. Sabia. Experimental Identification of a Multi-Span Masonry Bridge: The Tanaro Bridge. *Construction & Building Materials*, Vol. 22, No. 10, 2008, pp. 2087–2099. https://doi.org/10.1016/j.conbuildmat.2007.07.031.
206. Casas, J. R. Reliability-Based Assessment of Masonry Arch Bridges. *Construction & Building Materials*, Vol. 25, No. 4, 2011, pp. 1621–1631. https://doi.org/10.1016/j.conbuildmat.2010.10.011.
207. Bretschneider, N., L. Fiedler, G. Kapphahn, and V. Slowik. Technische Möglichkeiten der Probebelastung von Massivbrücken. *Bautechnik*, Vol. 89, No. 2, 2012, pp. 102–110. https://doi.org/10.1002/bate.201100010.
208. Domede, N., A. Sellier, and T. Stablon. Structural Analysis of a Multi-Span Railway Masonry Bridge Combining In Situ Observations, Laboratory Tests and Damage Modeling. *Engineering Structures*, Vol. 56, 2013, pp. 837–849. https://doi.org/10.1016/j.engstruct.2013.05.052.
209. Carr, A. J., D. V. Jáuregui, B. Riveiro, P. Arias, and J. Armesto. Structural Evaluation of Historic Masonry Arch Bridges Based on First Hinge Formation. *Construction & Building Materials*, Vol. 47, 2013, pp. 569–578. https://doi.org/10.1016/j.conbuildmat.2013.05.084.
210. Modena, C., G.Tecchio, and F.d. Porto. Masonry Arch Bridges in the Italian Railway Engineering Experience: State of Condition, Static Reliability, Seismic Verification and Retrofit Strategies. *Maintenance, Monitoring, Safety, Risk and Resilience of Bridges and Bridge Networks* (Bittencourt, Frangopol, and Beck, eds.) Foz do Iguacu, Brazil, 2016, pp. 106–122.
211. Ataei, S., M. Jahangiri Alikamar, and V. Kazemiashtiani. Evaluation of Axle Load Increasing on a Monumental Masonry Arch Bridge Based on Field Load Testing. *Construction & Building Materials*, Vol. 116, 2016, pp. 413–421. https://doi.org/10.1016/j.conbuildmat.2016.04.126.
212. Gentile, C., and N. Gallino. Condition Assessment and Dynamic System Identification of a Historic Suspension Footbridge. *Structural Control and Health Monitoring*, Vol. 15, No. 3, 2008, pp. 369–388. https://doi.org/10.1002/stc.251.
213. Gentile, C., and A. Saisi. Ambient Vibration Testing and Condition Assessment of the Paderno Iron Arch Bridge (1889). *Construction & Building Materials*, Vol. 25, No. 9, 2011, pp. 3709–3720. https://doi.org/10.1016/j.conbuildmat.2011.04.019.
214. Lantsoght, E. O. L., C. van der Veen, A. de Boer, and D. A. Hordijk. Proof Load Testing of Reinforced Concrete Slab Bridges in the Netherlands. *Structural Concrete*, Vol. 18, No. 4, 2017, pp. 597–606. https://doi.org/10.1002/suco.201600171.
215. Lantsoght, E. O. L. (ed.). Load Testing of Bridges: Proof Load Testing and the Future of Load Testing. *Structures and Infrastructures*, Vol. 13, CRC Press, Boca Raton, Fla., 2019, p. 406.
216. Lantsoght, E. O. L. (ed.). Load Testing of Bridges: Current Practice and Diagnostic Load Testing. *Structures and Infrastructures*, Vol. 12, 2019, CRC Press, Boca Raton, Fla., 2019, p. 380.

The National Academies of
SCIENCES • ENGINEERING • MEDICINE

The **National Academy of Sciences** was established in 1863 by an Act of Congress, signed by President Lincoln, as a private, non-governmental institution to advise the nation on issues related to science and technology. Members are elected by their peers for outstanding contributions to research. Dr. Marcia McNutt is president.

The **National Academy of Engineering** was established in 1964 under the charter of the National Academy of Sciences to bring the practices of engineering to advising the nation. Members are elected by their peers for extraordinary contributions to engineering. Dr. John L. Anderson is president.

The **National Academy of Medicine** (formerly the Institute of Medicine) was established in 1970 under the charter of the National Academy of Sciences to advise the nation on medical and health issues. Members are elected by their peers for distinguished contributions to medicine and health. Dr. Victor J. Dzau is president.

The three Academies work together as the **National Academies of Sciences, Engineering, and Medicine** to provide independent, objective analysis and advice to the nation and conduct other activities to solve complex problems and inform public policy decisions. The National Academies also encourage education and research, recognize outstanding contributions to knowledge, and increase public understanding in matters of science, engineering, and medicine.

Learn more about the National Academies of Sciences, Engineering, and Medicine at **www.national-academies.org**.

The **Transportation Research Board** is one of seven major programs of the National Academies of Sciences, Engineering, and Medicine. The mission of the Transportation Research Board is to increase the benefits that transportation contributes to society by providing leadership in transportation innovation and progress through research and information exchange, conducted within a setting that is objective, interdisciplinary, and multimodal. The Board's varied committees, task forces, and panels annually engage about 7,000 engineers, scientists, and other transportation researchers and practitioners from the public and private sectors and academia, all of whom contribute their expertise in the public interest. The program is supported by state transportation departments, federal agencies including the component administrations of the U.S. Department of Transportation, and other organizations and individuals interested in the development of transportation.

Learn more about the Transportation Research Board at **www.TRB.org**.

TRB

TRANSPORTATION RESEARCH BOARD
500 Fifth Street, NW
Washington, DC 20001